Polypropylene Modified by Polydimethylsiloxane in Catalytic Cross Metathesis Reactions

by

Yan Rong Wu

A thesis
presented to the University of Waterloo
in fulfillment of the
thesis requirement for the degree of
Master of Applied Science
in
Chemical Engineering

Waterloo, Ontario, Canada, 2010

I hereby declare that I am the sole author of this thesis. This is a true copy of the thesis, including any required final revisions, as accepted by my examiners.

I understand that my thesis may be made electronically available to the public.

Abstract

In this study, we were particularly interested in looking at the possibility that cross metathesis of olefins in melt phase could be used to produce polydimethylsiloxane (PDMS) modified polypropylene (PP). The intention of this project was also to study and quantify relationships among the main experimental factors in the reaction: temperature, catalyst concentration and molar ratio of PP to PDMS, through a 2-level factorial statistical design.

In order to examine if PP-PDMS copolymers were synthesized in the melt phase, measurement of the chemical, physical and viscoelastic properties of the synthesized copolymers was necessary. Techniques including proton (^{1}H)-nuclear magnetic resonance (NMR), differential scanning calorimetry (DSC), thermal gravimetric analysis (TGA), rheometry and scanning electron microscopy (SEM), were all used to characterize the synthesized copolymers. ^{1}H NMR measurements confirmed the presence of PDMS in the copolymers. They also provided a quantitative measurement of PP to PDMS molar ratio in copolymers by determining the integration of PP PDMS repeating unit signals in NMR spectra. Compared to virgin PP, a lower melting enthalpy of the PP phase in the copolymer was observed from DSC results. This implied that the PDMS component influenced the thermal behavior of the PP crystalline phase in the copolymers. Moreover, TGA measurements indicated that a higher thermal stability was obtained for PP-PDMS copolymers than that for virgin PP wax and this was expected since PDMS is known for its

excellent stability at high temperature. Rheological analysis showed that the presence of PDMS in the copolymers gave lower complex viscosities and loss moduli, but higher storage moduli than those for virgin PP. Furthermore, the morphology of copolymers was examined by SEM and elemental analysis at the surface using an energy dispersive X-ray (EDX) analyzer on the SEM. It was found that micrographs of copolymers showed round domains on the surface, which were not observed in virgin PP wax and those round segments were confirmed to contain silicon. Torque values obtained from the batch mixer for modification reactions and the remaining weight % of copolymers at 350°C were used to conduct statistical analysis, through which models to describe the relationships between experimental factors and these physical responses were determined.

Acknowledgements

I would like to thank my supervisors, Professor Tzoganakis and Professor McManus for their kind guidance and support throughout my graduate studies. I am really appreciated to have these two wonderful supervisors.

My sincere thanks to my friends and colleagues: Dr. Shuihan Zhu, Mercy Bulsari, Mohammad M., Michelle, Muhammad, Parshant, Matt and Norwin, in Professor Tzoganakis and McManus labs who shared their knowledge and help to make this experience special.

Special thanks to Professor Alex Penlidis for his kindness and encouragement, to Janet Venne and Ralph Dickhout for sharing their professional knowledge on NMR and thermal analyses.

I am greatly honored to have Professor Richard R. Schrock autograph on my thesis.

Dedication

I would like to dedicate this thesis to my parents, thanks for their support and understanding throughout my studies.

Thanks to Firmin Moingeon’s support, it is a very special journey with you along the side.

Table of Contents

List of Figures

List of Tables

Chapter 1 Introduction and Objectives

1.1 Introduction

Polyolefins are commodity plastics found in a wide range of applications varying from household items such as containers, appliances and grocery bags, to high technology products such as automotive parts, medical items and electronics. Polyolefin homopolymers include polyethylene (PE), polypropylene (PP), polybutylene (PB) and higher polyolefins. PP has one of the largest production volumes and is one of the most commonly used commodity polymers in the world due to its good thermal and mechanical properties, low cost, excellent chemical resistance and easy processability. Another positive factor for PP that is receiving a high degree of interest from researchers is that it can be chemically modified to exhibit a greater variety of properties, which are significant for developing the applications of PP in other highly profitable areas such as aerospace. Previous work has looked at different techniques to modify PP; these include controlled degradation [1], functionalization [2], crosslinking [3] and branching [4].

In this study, the synthesis of siloxane modified polypropylene copolymers was of particular interest. Polyorganosiloxanes have a number of outstanding properties including thermal stability, ultraviolet and flame resistance, chemical stability, biocompatibility, water repellency, electrical insulation and low glass transition temperature. Polydimethylsiloxane (PDMS), the main example of a polyorganosiloxane, consists of an inherently flexible siloxane backbone (Si-O) with two methyl groups attached to the silicon atoms on each side of the chain. This unusual combination of inorganic chain with organic side chains gives PDMS some unique properties, such as low surface energy, low glass transition temperature,

high permeability to oxygen and nitrogen and high compressibility [5]. PDMS polymers are widely used as additives in the plastics industry for improving surface appearance, mold filling, mold release, surface lubricity and wear resistance [5]. However, PDMS polymers tend to migrate onto the surface when used in blends with polyolefins due to the high degree of immiscibility between the two components. This major drawback results in undesired contamination, phase separation and diffusion of the polymer chains, which causes a fast deterioration of blend properties such as surface, flow and mold filling properties [6, 7]. Although most polyolefins and PDMS are immiscible and incompatible, blending of these compounds can provide various useful combined properties for specific applications. Yilgor and his co-workers proved that the primary difficulties (immiscibility and incompatibility) can be eliminated by forming chemical bonds between PDMS and polyolefin [8, 9]. This can be achieved by reactions of terminal functionalized PDMS with functional groups on polyolefin to generate graft or block copolymers [6, 10]. For instance, polyolefin-graft-PDMS copolymers can be produced through grafting reactions between PDMS with hydroxyl or amine terminal groups and modified polyolefins. This grafting of polymers can lead to advantages in processing and improvements in a number of properties such as viscosity, surface free energy and reactivity. Another example is formation of PP-PDMS-PP block copolymers by hydrosilylation reactions. PP with terminal double bonds, that are generated by peroxide initiated degradation has been reacted with hydride-terminated PDMS through a catalytic hydrosilyation reaction to synthesize copolymers [11, 12]. Eventually, block copolymers (PP-PDMS-PP) can be obtained in a multistep hydrosilylation synthesis.

Given that vinyl terminated PP resins are readily accessible, another possible way to achieve modification of PP is by carrying out olefin metathesis reactions, since PDMS can also be obtained with terminal olefin groups. This possibility was examined in this work. Specifically, low molecular weight vinylidene terminated PP reacted with monovinyl terminated PDMS in the presence of a commercial metathesis catalyst at temperatures from 165°C to 175°C. It was hoped that this would lead to PP-PDMS block copolymers and changes in various polymer properties might be achieved by using this methodology. The overall objective was that the synthesized copolymers would retain the favorable properties of both PP and PDMS.

1.2 Research Objectives

The intention of this project was to chemically modify polypropylene (PP) homopolymer wax in the melt phase in order to enhance its mechanical, physical and chemical properties. The project was carried out in four steps:

1) Synthesis of polypropylene-polydimethylsiloxane (PP-PDMS) copolymers and validation of the presence of bonded PDMS in purified copolymers
2) Application of a 2^3 factorial design to detect and quantify relationships amongst experimental factors: temperature, catalyst concentration and mole ratio of PP to PDMS

3) Analysis of the physical, chemical and viscoelastic properties of the synthesized copolymers and an investigation of the effects of experimental conditions on the properties of copolymers
4) Statistical analysis of torque and thermal stability responses of copolymers

In the first stage, copolymers were produced via cross metathesis polymerization by employing terminal functionalized PP wax and PDMS the in melt phase. All the experiments were catalyzed by Grubbs second generation catalyst. Nuclear Magnetic Resonance (NMR) was used to determine the chemical nature of the products and to confirm that PP and PDMS were bonded. In order to examine the effects of reaction variables, a factorial design was carried out in the second stage, in which 14 experiments were performed including replicate experiments. In the third stage, thermal properties of the synthesized copolymers were examined by differential scanning calorimetry (DSC) and thermogravimetric analysis (TGA). DSC was applied to determine the physical properties of copolymers such as melting points and melting enthalpies. Thermal stabilities of copolymers and PP wax were measured as a function of temperature via TGA analysis. Moreover, rheological responses and surface morphology of PP and copolymers were also measured and examined. In the last stage, variance analyses of torque values and TGA thermal results were studied and the models used to describe the relationships between the responses and significant experimental factors were also determined.

1.3 Thesis Outline

The research work presented in this thesis examined the synthesis, physical characterization and the potential applications of modified PP.

Chapter 2 gives a general literature review on the modification of PP and other background information relevant to the thesis work. In addition, metathesis polymerization serving to chemically modify PP using PDMS is reviewed.

In Chapter 3, information about materials used and experimental procedures for the production of PP-PDMS copolymers are introduced. Chapter 3 also includes the characterization methods used to examine the properties of PP-PDMS copolymers and experimental procedures for each characterization technique.

Chapter 4 presents all the experimental results. Copolymer characterization results from NMR, DSC, TGA, rheometry and SEM analyses are all discussed.

The conclusions of this research project are summarized in Chapter 5. In addition, recommendations for future work on this topic are presented in this chapter.

Chapter 2 Literature Review

2.1 Introduction

As mentioned before, the overall focus of this research is on the viability of chemical modifications of PP, which may lead to broader potential applications for PP in higher profitable areas. Therefore, it is necessary to thoroughly review the relevant concepts and methods to modify PP. In the first section of this chapter, properties and applications of PP are reviewed. Section 2.3 gives an introductory discussion of controlled degradation and melt-phase hydrosilylation of PP. A brief discussion of metathesis polymerization techniques used to synthesize PP-PDMS copolymers in this project is provided in Section 2.4, followed by a general discussion of the possible challenges that one could encounter in this project.

2.2 Properties of Polypropylene

Polypropylene (PP) is a crystalline thermoplastic polyolefin, compatible with many processing techniques and is used in a wide variety of commercial applications. It is one of the fastest growing classes of commodity thermoplastics, with a market share growth of 6 to 7 % per year because of its low cost and favorable properties [13]. It has the highest melting temperature (160-170 °C) of all commodity thermoplastic polyolefins and is more rigid than the other low cost thermoplastics due to its high strength-to-weight ratio [14, 15]. PP also has excellent chemical resistance including resistance to most organic solvents because of its crystalline character. It is only soluble at elevated temperatures in appropriate

solvents, but softening may occur due to the permeation of chlorinated solvents and hydrocarbons at lower temperature [15]. Its good fatigue resistance makes it widely used in "living hinge applications", such as those on flip-top bottles, which are made from PP. Furthermore, its chemical inertness, lack of additives and toughness makes it a material of choice of food containers. It is available in a wide range of molecular weights and can be easily recycled and processed by many methods, including injection molding, extrusion, cast film and thermoforming [15].

Conventionally, PP is prepared by polymerizing propylene in the presence of Ziegler-Natta or metallocene catalysts which lead to highly sterospecific polymerizations. Propylene is added to the main polymer chain in a particular orientation such as head-to-tail, tail-to-tail, or head-to-head. It may also add to one of the methyl groups attached to alternating carbon atoms (pendant methyl groups), which could result in branching. As shown in Figure 2-1, polypropylene can be isotactic, syndiotactic and atactic depending on the orientation of the pendant methyl sequence.

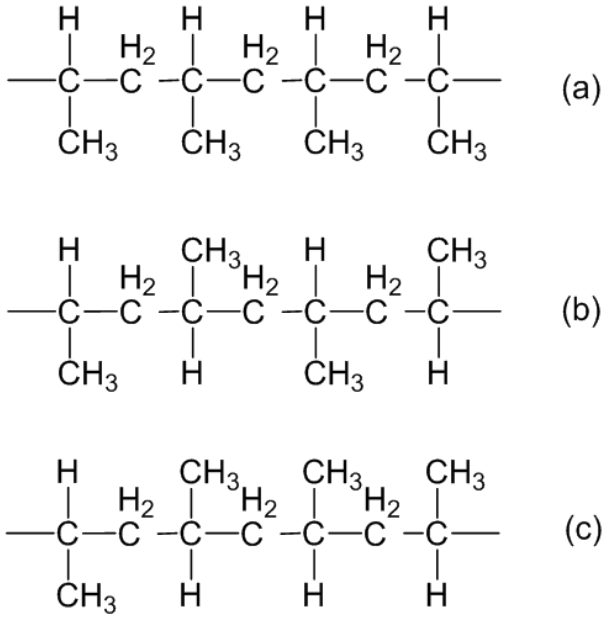

Figure 2-1: Schematic scheme of (a) isotactic, (b) syndiotactic and (c) atactic isomerism in polypropylene

Isotactic PP is the most common commercialized PP; with pendant methyl groups in this form always being on the same side of the polymer chain as seen in Figure 2-1 (a). Syndiotactic PP results from consistent insertion of the monomer in the opposite side of the previous monomer unit. It is not as commercially significant as isotactic PP. In atactic PP, monomer inserted inconsistently and methyl groups have a random orientation with respect to the polymer backbone. Moreover, it is known that crystallinity of materials is largely dependent on the degree of stereoregularity. Therefore, due to its regular repeating arrangement, isotactic PP has the highest degree of crystallinity, which results in good mechanical and thermal properties such as stiffness and tensile strength [15]. Although syndiotactic PP is less stiff than isotactic, it possesses better clarity and greater impact strength [15]. Atactic PP has low crystallinity due to its irregular structure and is mainly used for adhesives and roofing tars [15]. It is noted that amounts of isotactic, syndiotactic or atactic segments are significantly influenced by the polymerization system and used catalysts.

In general, regular tacticity of PP gives a stiffer and rigid polymer chain than other polyolefins such as polyethylene (PE). Hence, PP generally has higher tensile, flexural and compressive strength than PE. In addition, PP synthesized by Zeigler-Natta catalyst systems, which are multi-site catalysts containing several reactive sites, can result in a broad range of molecular weights (MW) from 220,000 to 700,000 [13, 14]. Because molecular weight is directly related to the toughness of PP, higher MWs provide greater toughness, impact resistance and elongation [15]. On the other hand, PP resins from metallocene catalysts give greater puncture resistance, higher impact strength, and better optical properties than Zielger-Natta polypropylene. However, conventional polymerization

methods for PP production do not allow for incorporation of a wide range of functional comonomers into PP resins because the catalysts used have high sensitivity to non-hydrocarbon functional groups. To generate materials with a broader range of properties, modifications to functionalize polyolefins have gained great interest in recent years.

2.3 Polypropylene Modification

Although PP plays an important role in the growing commercial applications because of its low cost and versatile properties, its use is limited in several technologically important fields of applications due to its low impact strength, incompatibility with other synthetic polymers, extremely low adhesion to metal or glass, and lack of functionality [2]. The need for a functional and engineered PP is becoming more and more commercially important. Of all the modification methods, chemical modification of polymers is most important. For instance, chemical modification may be done to increase intermolecular interactions and lead to crosslinking of the polymer backbones through grafting or copolymerizations. It can also be done to modify the surface chemistry of polymers by surface coating, surface degradation, surface hydrolysis and radiation-induced methods [2].

For example, copolymerization of vinylidene terminated polypropylene with acrylate monomers or maleic anhydride can give modified PP, which is able to react with terminal functionalized PDMS [6]. In the field of chemical modification, oxidation is of the most practical interest because it initiates a degradation mechanism in unprotected polyolefins and leads to a rapid deterioration of the mechanical properties [15]. PP can be oxidized in air

at elevated temperature (thermal oxidation) and under exposure to ultraviolet light at room temperatures (photo-oxidation) [14]. Moreover, modification of PP by halogenations (e.g. chlorination and chlorosulfonation) is also possible. The crystalline phase in PP reacts much slower than its amorphous phase; therefore, chlorine will be mainly confined to the non-crystalline phase. It has been shown that chlrosulfonated PP made by reaction of PP with Cl_2 and SO_2, with 6-10% chlorine and 1-3% sulfur, can be vulcanized with metal oxides [15]. However, none of these chemical modifications has provided enough practical importance to reach commercialization.

2.3.1 Controlled Degradation of PP

Of all types of modification, controlled degradation of PP is of great practical significance. This control is accomplished in a post-reactor stage by means of reactive extrusion. Using this method, the molecular weight distribution (MWD) of PP can be modified easily and economically in an extruder, which reduces the high-molecular weight fraction of commodity PP resins and leads to the production of PP with controlled rheological (CR) properties and a significantly narrower MWD [1]. Therefore, polypropylene produced this way is referred to as Controlled Rheology Polypropylene (CRPP) [1]. As a material, CRPP is known to have much higher melt flow rate (MFR), lower molecular weight, narrower MWD and reduced viscosity compared to the parent PP without noticeable changes in the mechanical properties [1, 16-19].

The production of CRPP is well established in industry and is carried out by a peroxide-promoted degradation reaction, where free radical initiators are used to induce chain scission reactions [20]. Several models have been developed for the peroxide-initiated degradation of PP and the accepted peroxide-initiated degradation mechanism is shown in Figure 2-2 [21, 22].

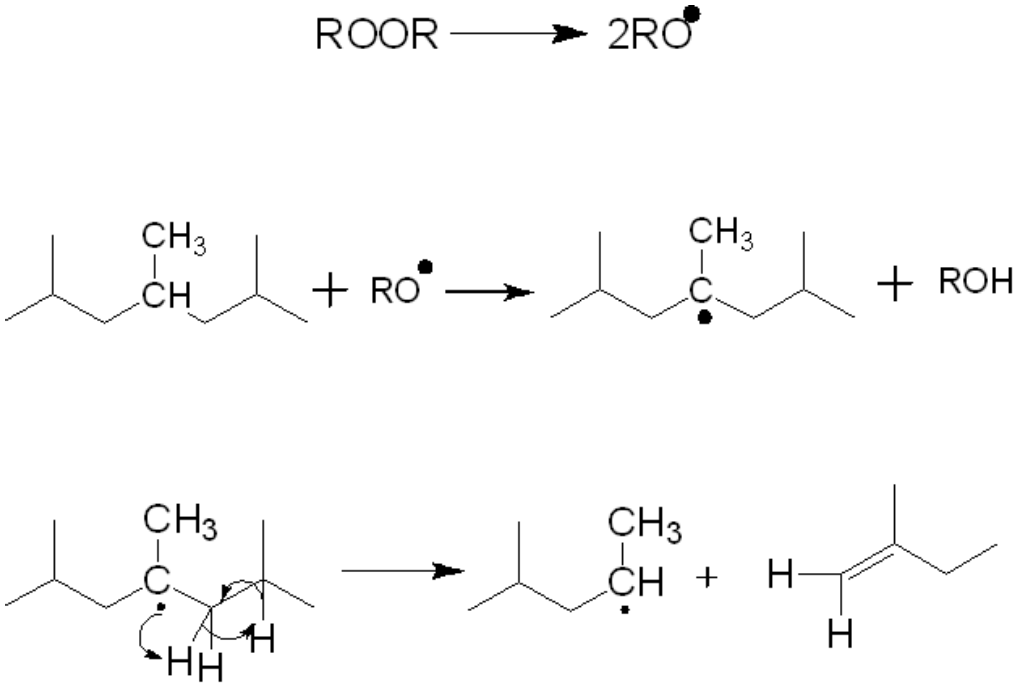

Figure 2-2: Peroxide-initiated degradation mechanism of PP [22]

In the first step, a peroxide radical is formed through thermal decomposition of an organic peroxide. Subsequently, radical attack and hydrogen abstraction by alkoxy radical (RO·) leads to the production of a polymer radical. Eventually, formation of a new polyolefin is obtained through β- scission of the polymer radical.

Although mono- and di-functional peroxide initiators have dominated the production of CRPP, the performance of a new tetra-functional peroxide initiator in the degradation of PP was evaluated in a recent study [22]. It indicated that the di-functional peroxide was more effective to reduce molecular weight at higher processing temperatures (230°C) [22]. However, the tetra-functional initiator was more effective at lower temperatures (200°C) [22]. Furthermore, higher molecular weight could be achieved from the tetra-functional initiator at high processing temperature and low levels of peroxide concentration [22].

2.3.2 Hydrosilylation of PP through Reactive Mixing

The hydrosilylation reaction (Figure 2-3), is an addition reaction of organic and inorganic silicon hydrides to multiple bonds such as carbon-carbon, carbon-nitrogen or carbon-oxygen [12]. Hydrosilylation was first reported by Sommer [23] in 1947 in the reaction between trichlorosilane and 1-octene, in the presence of acetyl peroxide [24]. However, the major scientific and technological breakthrough that made the reaction more useful for general application came in 1957, when Speier reported hexachloroplatinic acid (H_2PtCl_6) as a very efficient catalyst for hydrosilylation. This discovery meant that hydrosilylation became an important reaction in organosilicon chemistry because it gave an additional

method to produce silicon carbon bonds (Si-C) [24]. Since then, the reaction has been studied extensively and it is well-documented that hydrosilylation can be catalyzed radically, ionically, or by transition metal complexes of metals such as rhodium (Rh), platinum (Pt) or palladium (Pd) [25].

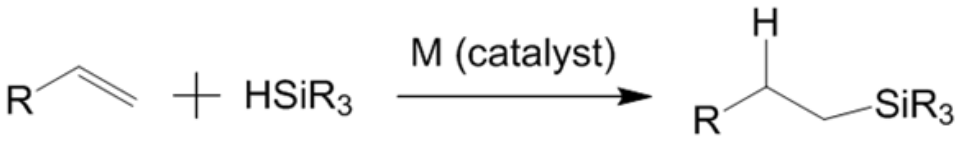

Figure 2-3: Hydrosilylation of an olefin

For a long time, it was believed that the reaction mechanism for platinum catalyzed (Speier's catalyst) hydrosilylation was a homogeneous type [24, 26]. This mechanism was formulated based on fundamental steps of organometallic chemistry, which included oxidative addition of a silane group to a metal-olefin complex to give a hydrido-silyl complex. In the second stage, the olefin substrate was coordinated with the formed complex, which then undergoes migratory insertion, and eventually gives the formation of alkyl-silyl species [27] . However, some of the reaction observations could not be explained by this mechanism. In 1986, Lewis [28, 29] proposed a reaction mechanism based on the formation of platinum colloids as the active catalyst (see Figure 2-4). It had been known that an active catalyst is formed when Si-H bond is broken by a low valence platinum

catalyst. Oxygen is then adsorbed on the catalyst surface and used to prevent irreversible colloid agglomeration by reducing the activity of the colloid particles. The newly formed transition complex has an electrophilic character and oxygen acts as a co-catalyst to activate the complex by withdrawing electrons. In the next stage, formation of an intermediate compound Pt-R_3SiH is obtained followed by the nucleophilic attack from the olefin to generate the desired product organosilane [24, 30]. One disadvantage related to this mechanism is that oxygen may react with PP chains leading to degradation and undesirable oxidative products [31].

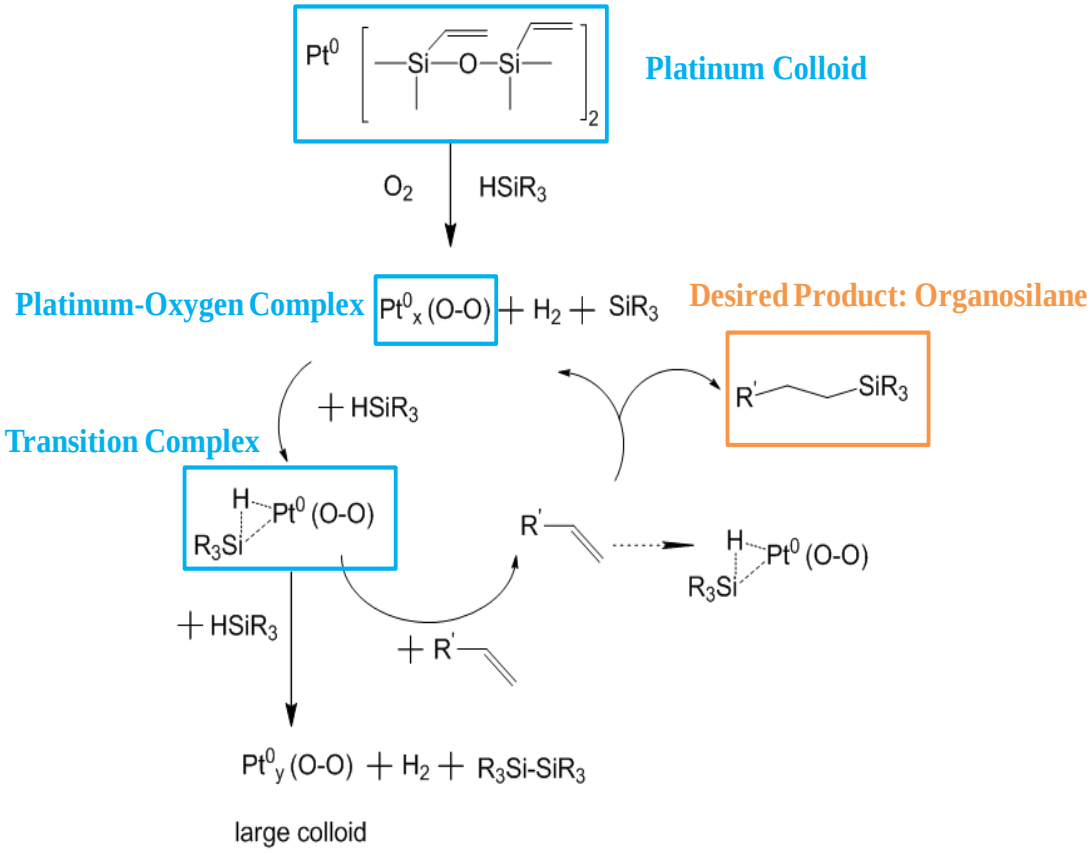

Figure 2-4: Hydrosilylation mechanism proposed by Lewis [8]

Platinum-catalyzed hydrosilylation is preferred because of its tolerance to various functional groups. Using this catalyst, functional groups like acetals, amides, amines, oxirane ether, nitriles, ketone, ether, sulfide, sulfone, phosphate or carborane groups do not interfere in the hydrosilylation reactions [32, 33]. Since some of these functional groups are of great interest in practical applications, utility of hydrosilylation to functionalize polymers was further investigated [32-34]. However, the reactions have almost exclusively been studied in solution, which provides good temperature control, good homogenization and mild experimental conditions. For instance, hydrosilyaltion of polybutadiene, containing vinyl and internal C=C bonds, has been carried out in the presence of $RhCl(PPh_3)_3$. At 110°C, the catalyst was highly selective toward catalyzing the hydrosilylation of vinyl C=C bonds of the polymers. Nevertheless, for large scale commercial processes, hydrosilylation of polymers in solution is a labor- and energy- consuming process because polymers have to be dissolved for reaction, and then precipitated and subsequently dried for final purification. Solvents also have to be disposed off or recycled by distillation; therefore, the utility of hydrosilylation process is seriously limited for polymers with low solubility.

In order to avoid the disadvantages of solution processes, Tzoganakis and Malz found a desirable method to carry out the reaction in a polymer melt phase through reactive extrusion [30]. Carrying out the reaction in an extruder saves considerable amounts of time, labor and energy, since the polymer is functionalized and processed in one stage. As mentioned before, peroxide degradation of PP can produce CRPP with improved rheological properties, but it also leads to vinylidene groups at the terminal site of the polymer chain (Figure 2-2). Therefore, these vinylidene groups can be selectively

functionalized by using hydrosilylation reactions. Two different pathways are available to accomplish the functionalization.

One is the radically induced hydrosilylation (Figure 2-5). A peroxide initiator is used to abstract the hydrogen of the Si-H bond and induce Si radicals (as shown in steps 1 and 2), which attack the vinylidene group on PP to form an alkyl radical in the third step. Initially, a peroxy radical is formed, and this then reacts with the silane to form a Si radical. According to Farmer's rule [24, 26], the Si radical will attack the double bond carbon atom bearing the most hydrogen atoms (see step 3), so that the radical can be placed at the carbon atom bearing the most substituents, which stabilizes the radical. In the next step, the newly formed carbon radical abstracts a hydrogen atom from the hydrosilane bond and leads to the formation of a saturated organosilane and another new Si radical. As a result, this newly formed Si radical will attack another carbon carbon double bond in PP to continue the cycle.

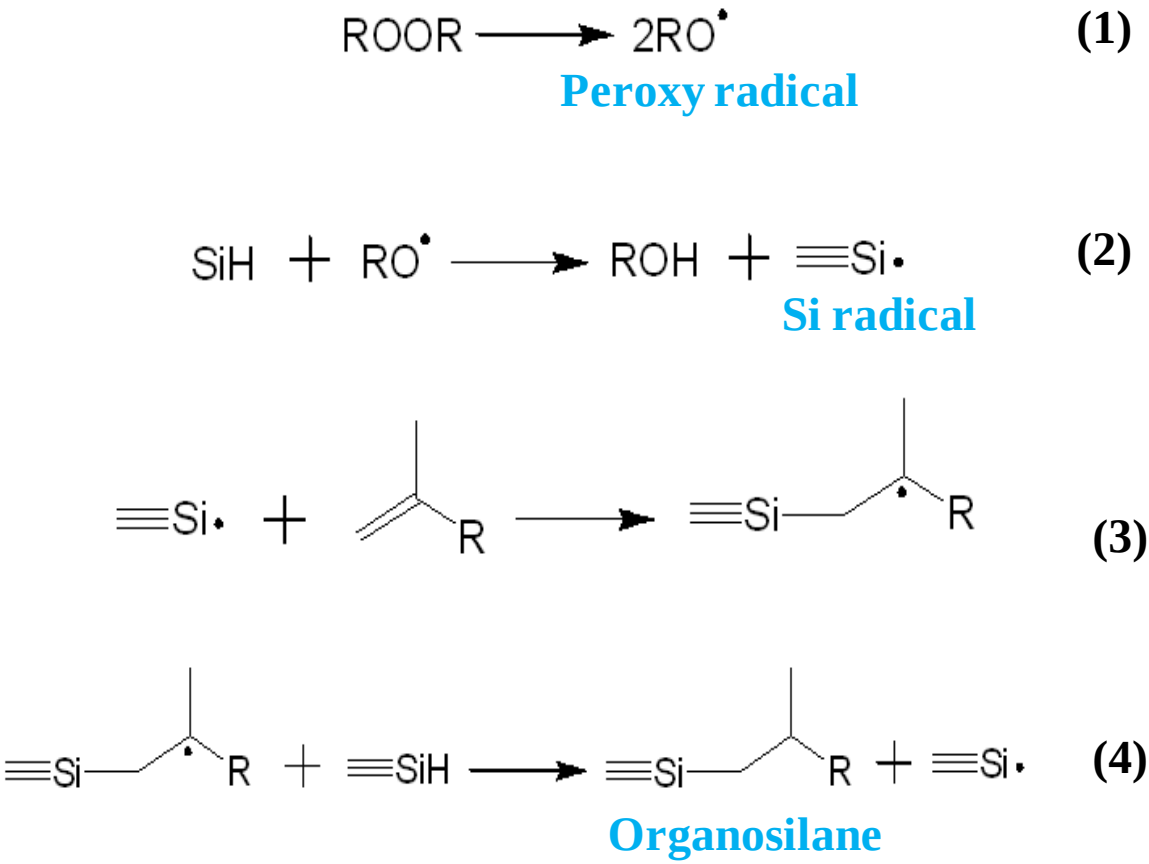

Figure 2-5: Radically induced hydrosilylation reaction mechanism [35]

The other pathway to achieve the desired functionalization is platinum catalyzed hydrosilylation with platinum olefin complexes. Since Speier's discovery of a high efficiency catalyst (H_2PtCl_6), hundreds of platinum catalysts based on chloroplatinic acids as a precursor and other d^8Pt (II) and d^{10}Pt (0) complexes have been reported [24]. Karstedt's catalyst, platinum (0)-divinyltetramethyldisiloxane (as seen in Figure 2-6), which is one of them, was used in Tzoganakis and Malz studies to catalyze terminal double bonds in PP through hydrosilylation. The reaction mechanism is shown in Figure 2-7. The catalytic species was a colloid formed by the reduction of the catalyst as proposed by Lewis in Figure 2-4 [8], and a peroxide cocatalyst is added in the system to maintain the activity of catalyst. The breakthrough in Tzoganakis and Malz [1, 12] was that they proved the feasibility of the hydrosilylation of vinyl terminated PP using Karstedt's catalyst in the melt phase. By carrying out the reaction in a twin screw extruder, functionalization and processing of PP was performed in one stage. Therefore, less labor, time and energy were needed since intermittent solidifying and remelting steps required in a solution process, were unnecessary [30]. The success of this process was an indicator that catalytic reactions are feasible in this harsh experimental condition (high temperature, 165°C - 175°C) and that the mixing capabilities of the extruder can overcome unfavorable phase interactions.

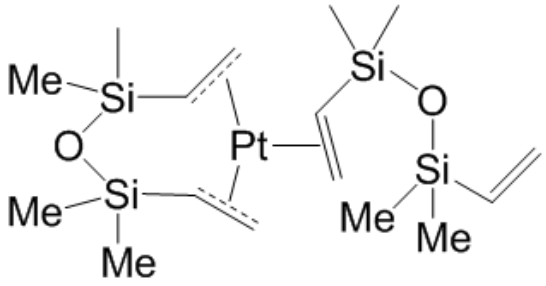

Figure 2-6: Karstedt's catalyst molecular structure [27]

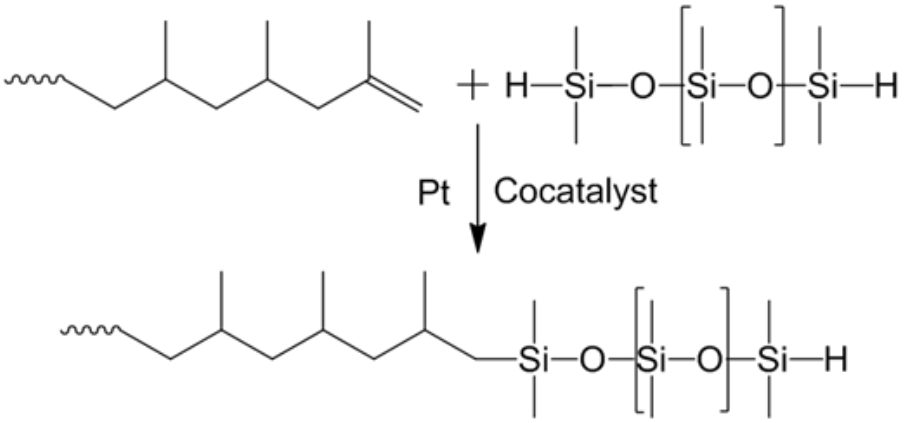

Figure 2-7: Platinum hydrosilylation mechanism

2.4 Metathesis Polymerization

Hydrosilylation is not the only method to form organosilicon polymers by polymers modifications. Metathesis polymerization may also be used to chemically modify PP and introduce siloxane groups into PP to form PP-PDMS copolymers. Olefin metathesis is a metal catalyzed reaction in which transformation occurs between two types of carbon-carbon double bonds and subsequent rearrangement via cleavage and reassembly. Two successful commercially available classes of catalysts used for olefin metathesis are: Shrock catalysts, which are molybdenum- or tungsten-based metal carbenes, and Grubbs catalysts that consist of ruthenium-based systems [36]. Olefin metathesis provides a way to form new carbon-carbon bonds that are often difficult or impossible to prepare by other synthetic routes. Traditional methods require harsh conditions that are not compatible with many other functional groups. Hence, in order to use them, more steps are required to protect and de-protect these functional groups resulting in lengthier syntheses and lower yields.

Under the general heading of olefin metathesis, there are several classes of olefin metathesis (as seen in Figure 2-8), including ring-closing metathesis (RCM), ring-opening metathesis (ROM), cross metathesis (CM) and acyclic diene metathesis polymerization (ADMET). Some significant achievements for these processes include generation of functionalized polymers by the use of ROM or ADMET, transformation of acyclic diene substrates into complex cyclic compounds through RCM or formation of unsymmetrical olefins in CM [37]. As seen in Figure 2-8, the driving force for RCM, ADMET and CM is the

elimination of volatile ethylene molecules; in contrast, release of ring strain drives the ROM reaction forward.

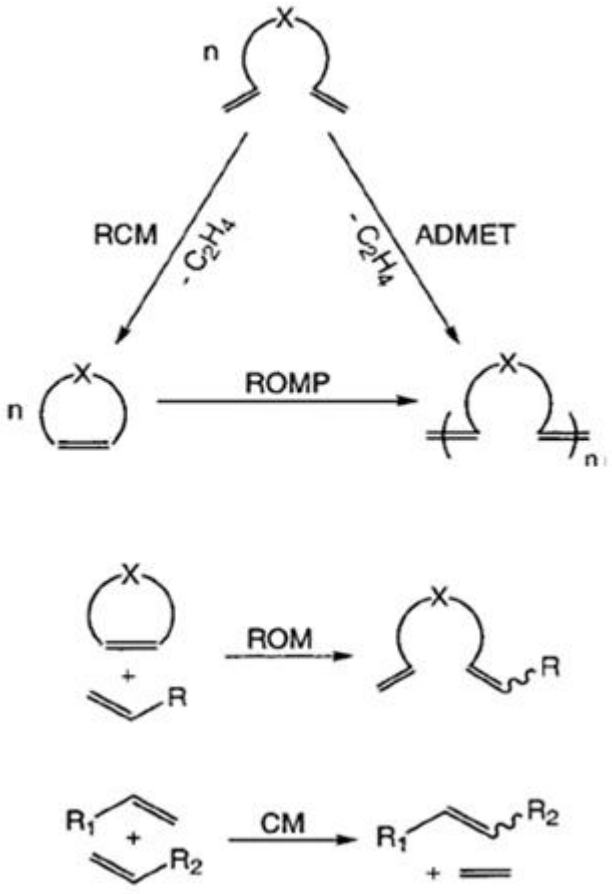

Figure 2-8: Classes of olefin metathesis reactions [37]

Olefin metathesis was a well known reaction method for a long time and new substances were synthesized industrially in this way without understanding the reaction mechanism and chemical nature of the catalytic intermediate. In the 1970s, Chauvin and his student Jean –Louis Hérrison proposed that the true catalyst center for the metathesis reaction was a metal alkylide or metal carbene species, in which the metal is bound to a carbon atom by a double bond [38]. Chauvin also introduced a new mechanism that was entirely different from the previously proposed ones. He suggested that a metal carbene acts as a catalyst in the reaction and this allows the exchange of alkylidenes between two alkene molecules and hence, two entirely new alkenes are produced. Figure 2-9 and 2-10 show the general metathesis of alkenes catalyzed by a metal carbene and the reaction mechanism, respectively.

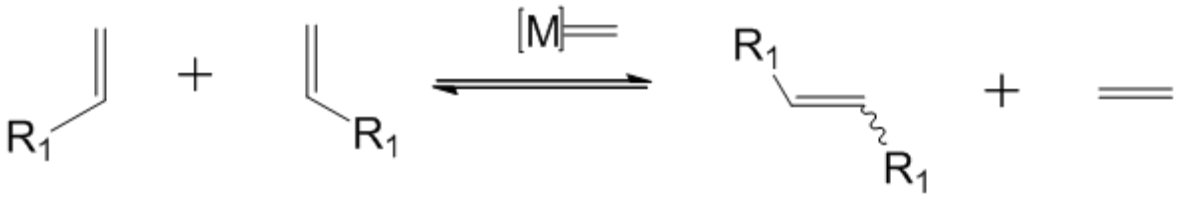

Figure 2-9: Metathesis of alkenes catalyzed by a metal carbene [39]

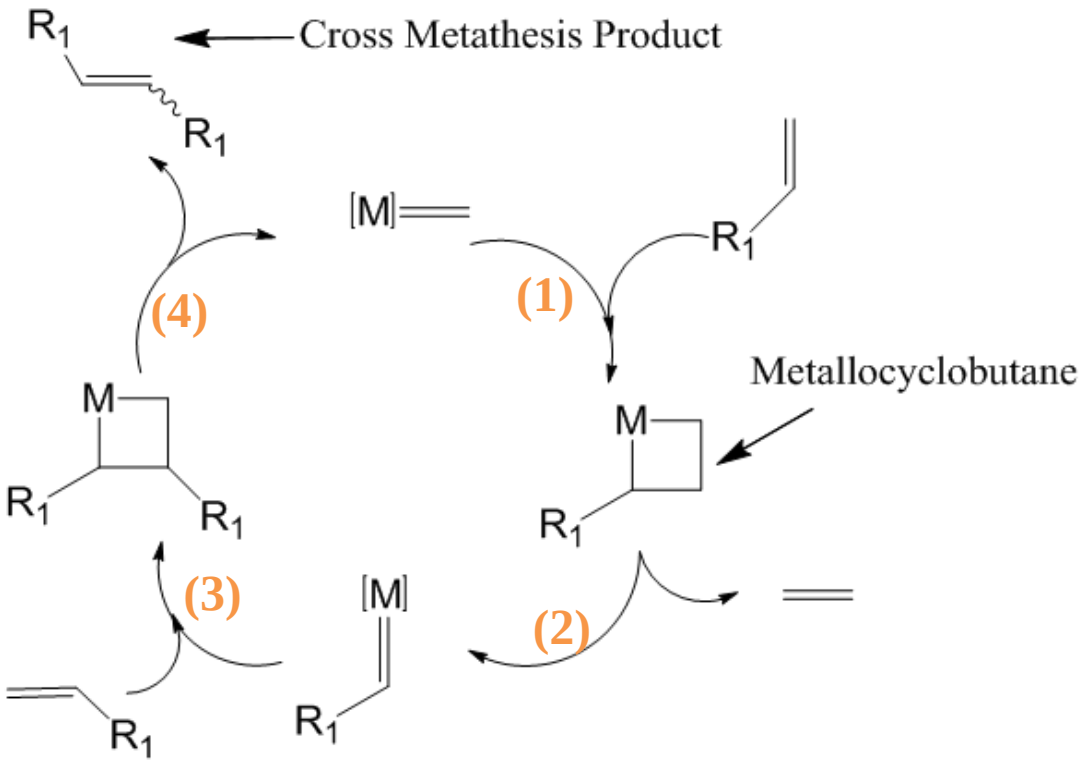

Figure 2-10: Reaction mechanism of alkene metathesis catalyzed by a metal carbene [39]

In the first stage of the reaction, one alkene combines with a metal carbene to form a four-membered ring molecule, called metallocyclobutane, which is subsequently broken into a new ethylene molecule and a new metal carbene in the second step. The newly formed metal carbene reacts with a second alkene in the same fashion (step 3) and produces another metallocyclobutane that will release the cross-metathesis product and regenerate a metal carbine (see step 4). This metal carbene is then ready to act like a catalyst in another metathesis reaction. The catalytic cycle is a thermodynamically controlled process and the reaction is driven forward due to the release of ethylene molecules in open systems.

2.4.1 Cross Metathesis Polymerization

Olefin cross metathesis (CM) involving reaction of two terminal alkenes (Figure 2-8 and Figure 2-9), has recently become a powerful and convenient synthetic method in organic and polymer chemistry, because it allows researchers to synthesize functionalized and higher olefins from simple alkene precursors. However, compared to the other classes of olefin metathesis, CM has not been widely used in industrial areas because of its unpredictable reaction selectivity and streroselectivity, which are challenges to incorporating CM into a synthesis plan [40]. Grubbs proposed that the most convenient way to determine olefin reactivity in CM was to examine their ability to homodimerize [40]. Homodimerization occurs when one monomer reacts with itself, instead of other olefins in CM as seen in Figure 2-11.

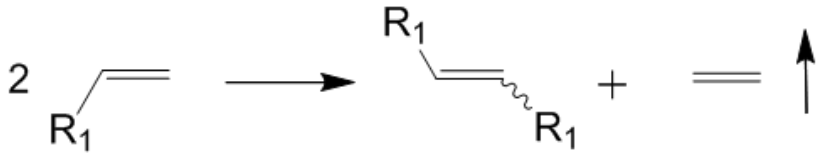

Figure 2-11: Homodimerization in cross metathesis [40]

Based on looking at an olefin's ability to homodimerize relative to other olefins, Grubbs et al. [40] published a general model that can be used to predict selectivity of limiting types of olefin in CM reactions. This was done by investigating several classes of olefins divided into four distinct olefin types. For example, CM is non-selective when two olefins used in the reaction both undergo a rapid homodimerization and their homodimers can participate in CM [40]. Hence, a statistical mixture of cross metathesis products and side products such as homodimers is obtained in this type of reaction (Figure 2-12). To achieve 90% yield with respect to the limiting olefin desired cross metathesis product, the molar ratio of the two olefin reagents used in the reaction must be more than 10:1 (Figure 2-12). Therefore, non-selective product mixtures are obtained when two olefins of the same type are used in CM.

R_1	:	R_2	CM Product Selectivity Relative to R_2
1	:	1	50%
2	:	1	66%
4	:	1	80%
10	:	1	91%

Figure 2-12: Olefin CM statistical mixture of products for limiting types of olefin [40]

In general, CM is an efficient and tolerant method to make carbon-carbon double bonds. It was used in this project to form PP- PDMS copolymers and the reaction mechanism is shown in Figure 2-13. According to the category published by Grubbs [34] , terminal olefins can undergo rapid homodimerization processes and produce homodimers. Since both reagents PP and PDMS were vinyl terminated olefins, a mixture of statistical products may be formed. However, statistical studies published from Grubbs were all based on well mixed systems. In this project, reaction conditions are quite different from the ones described in Grubbs model and non-homogeneous systems may also result due to the immiscibility between PP and PDMS components. Moreover, initial molar ratio of PP to PDMS was set at 100:1, 150:1 and 200:1, which meant that PP has more chances to react with itself instead of PDMS during the polymerization process.

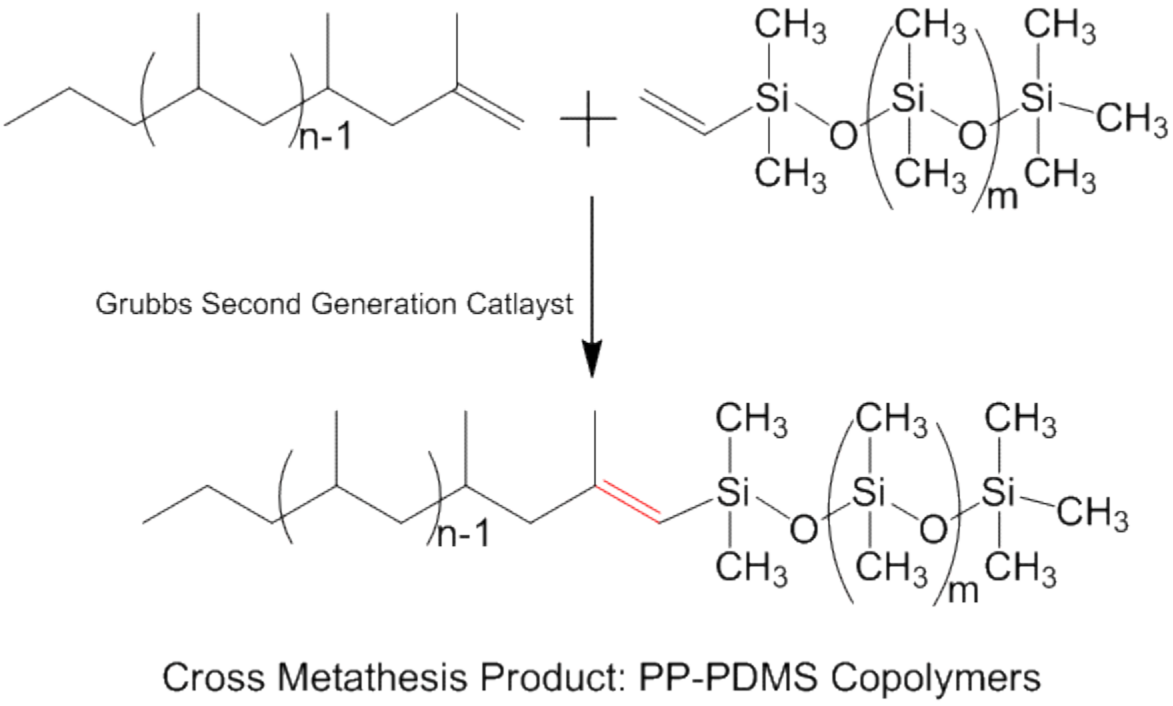

Figure 2-13: Cross metathesis reaction scheme of PP and PDMS

2.4.2 Catalyst Selection

From the mid – 1950s to early 1980s, all metathesis reactions were accomplished using undefined homogeneous or heterogeneous catalyst systems, which were combinations of transition metal salts along with main group alkylating agents. Some of the common examples are MoO_3/SiO_2, WCl_6/Bu_4Sn, $WOCl_4/EtAlCl_2$ and Re_2O_7/Al_2O_3 [37]. The utility of these catalysts was limited due to their sensitivity to air and moisture and they were also relatively short-lived in the reaction environment. These problems motivated extensive research work to produce catalysts with well defined structure, stability and tolerance to functional groups. In addition, catalysts have to be selective, to only react with C=C double bonds and be inert towards the other functional groups in the molecules.

As illustrated before, Chauvin's mechanism involves interconversion of a metal carbene and an olefin. The discovery of this mechanism had a profound influence on the development of well defined metathesis catalysts, since it provided a way to understand their activity. Of the scientists researching the topic, Robert H. Grubbs and Richard R. Schrock have perhaps made the greatest contributions in this area and as such were awarded the Nobel Prize in chemistry 2005 for their work, as was Chauvin.

Schrock started research on alkylidiene complexes by studying complexes based on different metals such as tantalum, tungsten and molybdenum [41]. One of molybdenum catalysts (Figure 2-14) discovered by Schrock and co-workers, was the first of many homogeneous catalysts to become widely used for metathesis. This catalyst was reported to have a high reactivity with a well defined structure, which allowed it to react with both

terminal and internal carbon-carbon double bonds and to perform ROMP of norbornenes and norbornadienes [41-44]. It was also effective for RCM for the formation of five-to seven-membered carbocycles and heterocycles [41, 42, 44, 45]. With this discovery, metathesis could replace a number of traditional organic synthetic methods and thus gained increasing awareness in synthetic chemistry. Nevertheless, molybdenum catalysts such as the one in Figure 2-14, are of limited use in many particular applications because they are extremely sensitive to oxygen and moisture [39, 42]. Therefore, an extremely inert atmosphere and rigorously purified, dried and degassed solvents, and dried equipment are required to handle these catalysts.

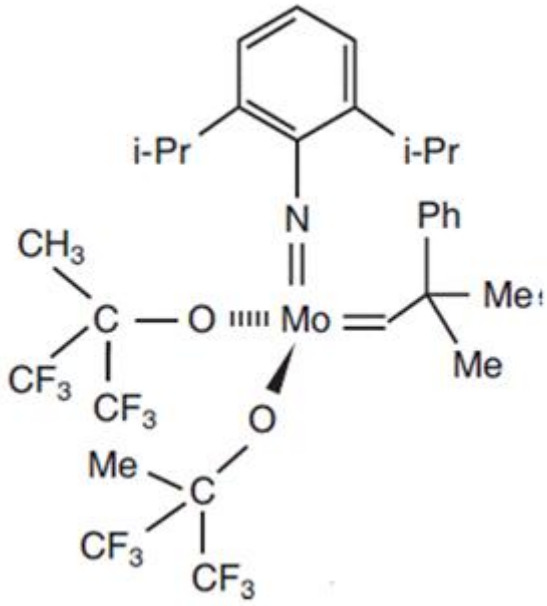

Figure 2-14: Shrock's molybdenum catalyst, *i*-Pr = isopropyl and Ph = Phenyl [39, 41]

In contrast to the Schrock catalysts, the catalysts originally developed by Grubbs consisted of a variety of ruthenium-based systems with general formula $(L)_2(X_2)Ru=CHR$, in which L, X and R represent ligands, halogen and alkyl groups, respectively. The first generation of Grubbs′ catalyst was developed in 1992 (Figure 2-15 a). It is significantly stable in air, it also demonstrated higher selectivity and tolerance to a larger range of functional groups, but has lower reactivity than Schrock's catalysts [46]. In addition, Grubbs′ catalysts also show the ability to initiate metathesis in the presence of alcohols, water and carboxylic acids [33]. This allows for their use with more substrates and the capability to undergo cross metathesis reactions in different environments. Practical utility of this is shown by the recent development of a hydrogenated nitrile rubber (HNR) with low weight average molecular weight (30,000 – 250,000) and importantly, a relatively low Mooney viscosity, which was successfully produced through degradation of nitrile rubber by cross metathesis reactions with olefins, using Grubbs first or second generation catalyst, and subsequent hydrogenation [47].

Although the first generation catalyst has been commercialized and is the most used metathesis catalyst by organic chemists, catalysts with improved properties were still needed to enhance the life-time of the catalyst in RCP. Extensive mechanistic studies have concluded that dissociation of one of the phosphines to generate a reactive ruthenium intermediate was the first step in CM reaction. To accelerate the metathesis activity and the dissociation rate, Grubbs and co-workers have developed a second generation catalyst (Figure 2-15 b) by replacing one of the phosphine ligands in first generation complexes with much larger and more electron donating N-heterocyclic carbene (NHC) ligands.

Similar results were published by Nolan, Fürstner and Herrmann in 1999 [48-50]. The second generation Grubbs catalysts exhibit dramatically high reactivity with olefinic substrates compared to their first generation catalysts. They can also catalyze the formation of tri-and tetra-substituted olefins in RCM and CM and they are highly reactive for ROM of cyclooctadiene [51, 52].

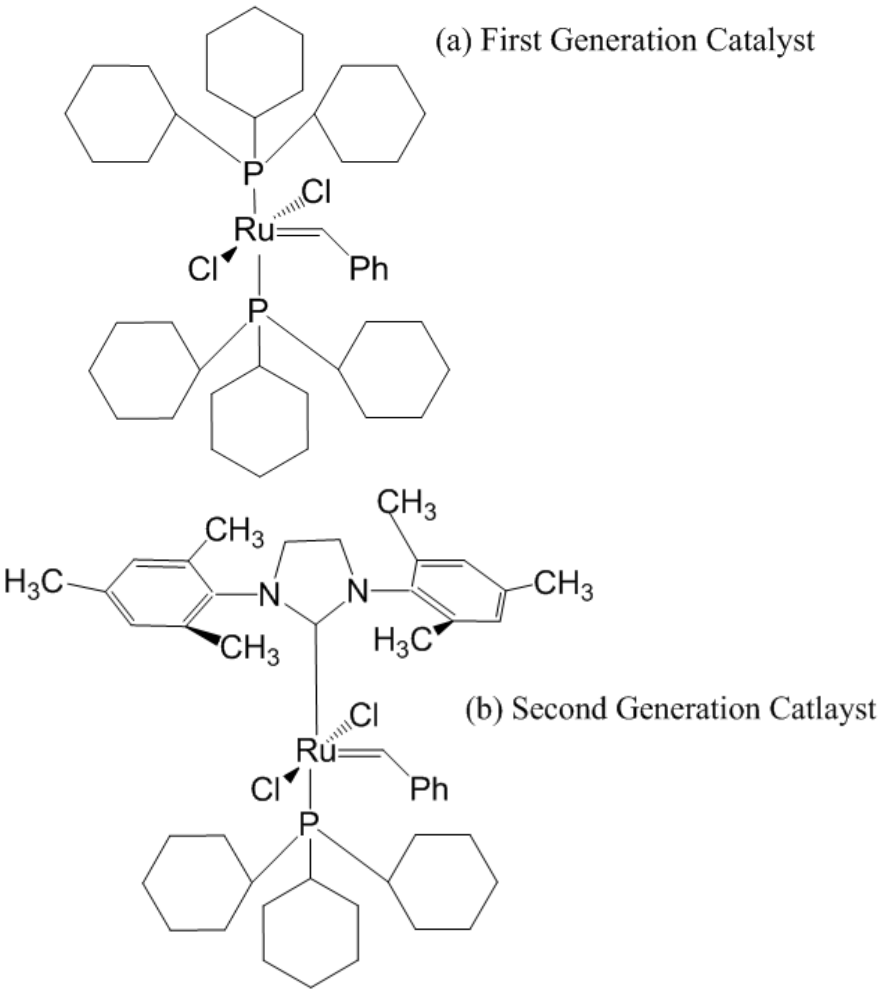

Figure 2-15: Grubbs Catalysts (a) First generation and (b) Second generation [46]

The Grubbs catalysts have been widely used in organic chemistry due to their tolerance of a large range of functional groups. Considering their high reactivity and ease of handling in air, as well as thermal stability, Grubbs second generation catalyst was selected as the catalyst to use in this research project to catalyze the cross metathesis reaction. This was in preference to Grubbs first generation catalyst which was too sensitive to the environment to be used in this research project since the metathesis polymerization was carried out in an exceptionally high temperature relative to standard conditions in organometalilc chemistry.

2.4.3 Challenges of the Project

The purpose of this project, as mentioned in Chapter 1, was to investigate the feasibility of CM of PP and PDMS in the melt phase. By performing the polymer modification reactions in a batch mixer, not only the quantity of products could be scaled up to 200 g, but also more time and energy could be saved by carrying out the functionalization and processing in a single stage. However, one of the challenges in this project was the catalyst activity, which could be significantly reduced due to the high reaction temperature. Since catalyst degradation was a possibility, another challenge related to the batch mixer reaction was the chance of a poor mixing process, since PP and PDMS are essentially incompatible. Therefore, in order for the reaction to be successful, the catalyst had to be stable at temperatures greater than 160°C. In addition, mixing efficiency would have to be rather

higher to ensure that the relatively dilute reactive species would be brought together to react.

Chapter 3 Experimental

3.1 Introduction

In this chapter, a brief description of the experimental procedures is given. The reaction experiments described in this chapter were all carried out in a batch mixer. Materials used in this research are summarized in Section 3.2. The experimental set up for copolymer production in the Haake Mixer and factorial design are explained in Section 3.3. The objective of these experiments was to evaluate the effects of experimental factors on the physical, chemical and rheological properties of the copolymers. For that purpose, a 2-level factorial design with three factors: batch mixer temperature, catalyst amount and molar ratio of PP and PDMS were applied, and details of the experimental set up are discussed in Section 3.4. Instruments used to characterize the copolymers are described in section 3.5. These techniques include: NMR, DSC, TGA, cone and plate rheometer, and SEM. The hot press used to press samples for rheometer analysis is also described in the characterization section.

3.2 Materials

The polyolefin resin used in this study was a vinyl terminated PP, Epolene N-15 wax from Eastman Chemical Co. The siloxane used to chemically modify PP was mono-vinyl terminated PDMS (MCR-V41) purchased from Gelest Inc. The properties of Epolene N-15 wax and PDMS are presented in Table 3-1 and Table 3-2. The catalyst used in this study is Grubbs second generation catalyst, (Benzylidene[1,3-bis(2,4,6-trimethylphenyl)-2-

imidazolidinylidene]dichloro(tricyclohexylphosphine)ruthenium) with molecular weight (MW) MW = 848.97, from Sigma-Aldrich (569747). Chlorobenzene (> 95%) and acetone (99%) solvents used to dissolve and precipitate the polymers respectively were received from Fischer Scientific and Caledon.

Table 3-1: Properties of PP wax (Epolene N-15) [53]

Property	PP wax
Density (g/ml)	0.902
Number Average $\bar{M}_n$ (g/mol)	5000
Weight Average $\bar{M}_w$ (g/mol)	12,000
Ring and Ball Softening Point (°C)	163
Vinylidene Concentration (mol/g polymer)	$8.4*10^{-5}$

Table 3-2: Properties of PDMS (Gelest Inc. MCR-V41)

Property	PDMS
Boiling Point (°C)	>205
Melting Point,(°C)	<-60
Molecular Weight, (g/mol)	60,000-70,000
Viscosity , (cSt)	9000-11,000

3.3 Batch Mixer

A batch mixer is one of the most widely used instruments for polymer processing. It requires a relatively small amount of materials and mixes all of the materials in a single isolated volume where rotating rotors homogenize its contents at a chosen temperature [54]. A batch mixer is usually used as a primary step for testing and verifying, for example, the mixing quality between reagents, the feasibility of polymer–polymer interaction, polymer degradation and crosslinking, etc [54]. A typical schematic structure of a batch mixer is shown in Figure 3-1. It consists of two rotors of certain cross section and a heated chamber of bi-circular cross section. Several experimental parameters for mixing such as the temperature of the mixing chamber and the speed of rotors (rpm) can be controlled. Other parameters may be monitored and recorded with respect to time. The most important ones are temperature of the mixer, and the torque needed to maintain the chosen rpm.

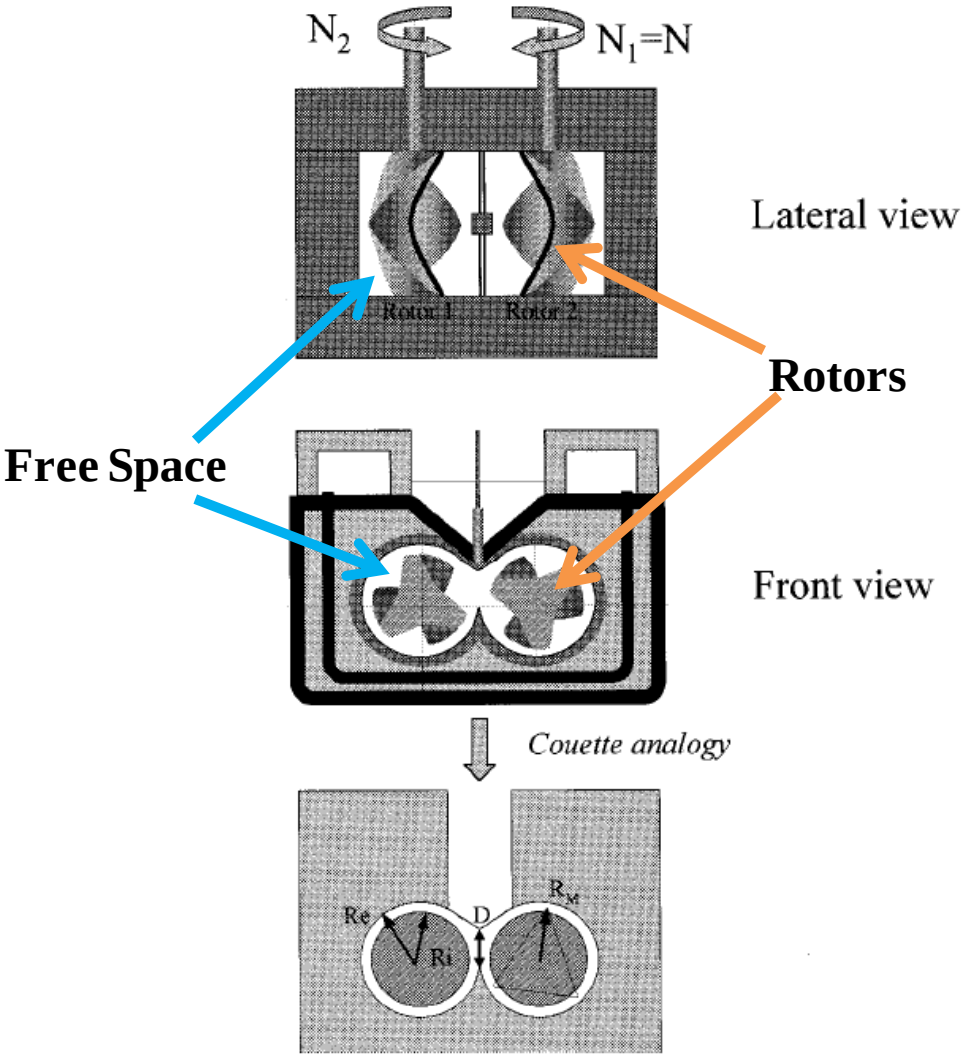

Figure 3-1: Schematic illustration of a batch mixer [54]

When polymer is fed in the heating chamber, it is then fused and milled by rotating blades at a constant rotating speed, and the torque required for this is recorded as a function of time. A typical curve of a torque (Γ) as a function of time (t) is shown in Figure 3-2. This indicates the thermal history of the polymer under mixing and the increase/decrease of torque refers to the occurrence of reactions such as crosslinking or degradation. Polymer is initially introduced in the form of granules or powder in the mixing chamber, resistance occurs between the polymer and rotation blades and results in the increase of torque. When this resistance is overcome, the torque decreases slightly and in a short time reaches steady state. The torque often increases again later because energy is required to completely melt the polymers. Subsequently, the torque decreases and reaches another steady state. This may take up to 3 to 15 min depending on the material and processing conditions such as temperature and rotor speed [54]. The torque will eventually increase or decrease depending on whether crosslinking or degradation phenomena happen [54].

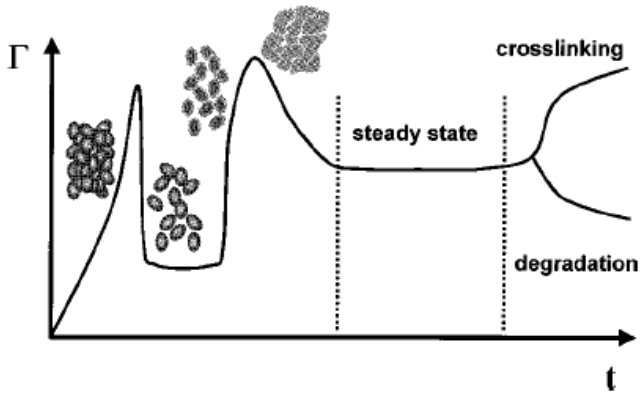

Figure 3-2: Typical batch mixer torque vs. time curve [54]

3.3.1.1 Description of the Haake Mixer

The batch mixer used in this research project was a Haake Rheocord 90 Mixer, model Rheomix 3000. Its mixing chamber has 625 cm^3 capacity without rotors and it can reach to a maximum torque of 300 Nm, 450 °C maximum temperature and 4.15 kW total heating capacity. It is equipped with one melt temperature thermocouple that detects the temperature inside the mixing chamber. A cooling system is also connected with the option of temperature control for the mixer. The mixing chamber, of bi-circular cross section, has 8.3 cm depth and each of the circular cross sections has a 3.4 cm radius. The rotors are connected to a torque meter, which measures the torque data and represents the actual torque exerted on the polymer melt [12]. The rotor speed was fixed at 120 rpm in all the experiments and the temperature, torque and reaction time were instantly recorded during the reaction process.

3.4 Synthesis of PP-PDMS Copolymers

Synthesis of PP-PDMS copolymers involved two major steps. First of all, the metathesis reaction of functionalized PP and PDMS was carried out in a high temperature batch mixer with two Banbury rotors rotating at 120 rpm. The torque, temperature and corresponding time data were recorded.

Epolene N-15 PP was initially charged into the preheated batch mixer at a temperature higher than its melting point. PP was melted in the chamber and when completely homogeneously melted and mixed, a stable torque value was indicated. Subsequently,

PDMS was added into the mixer. Nitrogen (N_2) was passed into the mixer to maintain an inert reaction environment. After 1 or 2 mins, another stable torque was observed, and this inferred that a homogeneous mixing was obtained between PP and PDMS. Then, Grubbs' second generation catalyst was added to the mixer as a powder, after which reaction conditions were maintained for 30 mins. Around 0.5 to 1g samples were taken out every five minutes to monitor the extent of the reaction. After 30 minutes, the rotors were stopped, the batch mixer was opened and then the copolymer mass was removed from the batch mixer and allowed to cool in air.

In the second step, a small quantity of each synthesized copolymer was purified and used for further characterization analysis. The raw copolymers (5 to 10 g) were dissolved in 50 ml boiling mono-chlorobenzene solvent in a round bottom flask (RBF), then precipitated and stirred in 200 ml wash acetone for an hour in order to remove non-bounded PDMS, which is acetone soluble. The purified copolymers were dried in a vacuum oven at 50°C for at least 24 hrs. The weight of sample was measured every 12 hrs and the drying process was not stopped until the weight of each measurement was constant (+/- 3 mg).

3.4.1 Factorial Design of Experiments

A factorial design is a tool for researchers to examine the effects of multiple independent variables and their degree of interactions. Designed experiments are the best way to get the most information for the least effort. They are much more efficient than one-factor-at-a-time measurements whenever more than one factors affecting the process. By choosing the

right fraction of many possible experiments and analyzing the results appropriately, designed experiments may detect and quantify the special relationships between factors and the chosen process responses.

A 2^3 factorial design was used in this project, which meant that three factors, each at two levels, were examined and eight experiments were performed to provide a complete factorial design. The three factors were temperature, catalyst concentration and the molar ratio between double bonds in PP and PDMS; each was studied at high and low levels. In order to perform variance analysis on the physical responses, two sets of replicate runs were performed. One set was designed at the center point experimental condition, called center point runs: CP 1 to CP 3 (as shown in Table 3-3). The experimental conditions for the second replicate set (BM 1 to BM 3) was similar to the CP runs, except the reaction temperature was set 5°C higher than the CP runs. Note that Run 5-2 mentioned below was operated under exactly the same experimental condition as Run 5. Results obtained from Run 5 are not shown in here because the reaction did not occur due to the failed catalyst dispersion in the reaction chamber. Besides the factorial design experiments, another two reactions were carried out. One was the CM polymerization of virgin PP wax itself, without adding PDMS. The other one was to produce a PP and PDMS physical blend, without addition of catalyst. The purpose of performing such reactions was to investigate the differences in properties between these non-desirable products (physical blend and PP homodimers) and PP-PDMS copolymers.

Table 3-3: Data of factorial design experiments

Factor	Temperature (°C)	Catalyst (mg)	PP/PDMS (mole ratio)
Run 1	175	140	200
2	175	140	100
3	175	60	200
4	175	60	100
5	165	140	200
6	165	140	100
7	165	60	200
8	165	60	100
CP 1	170	100	150
CP 2	170	100	150
CP 3	170	100	150
BM 1	175	100	150
BM 2	175	100	150
BM 3	175	100	150

Where CP = Center Point and BM = Batch Mixer

3.5 Characterizations of PP-PDMS Copolymers

3.5.1 Nuclear Magnetic Resonance (NMR)

Nuclear Magnetic Resonance (NMR) spectroscopy is a powerful and theoretically complex analytical tool. It has become the most widely used technique for organic compound characterization because of its versatility. It can be used with a very small sample and it is non-destructive. The NMR spectrum provides a lot of detailed information about the structure of compounds, and some complete structures can be determined using only NMR. Only certain elements may be detected by NMR techniques. Proton (^{1}H) and carbon (^{13}C) NMR are found to be the most useful and commonly used techniques because hydrogen and carbon are the most common components of organic compounds.

In this study, ^{1}H NMR spectroscopy was used to determine the composition and to confirm the formation of PP-PDMS copolymers. For each purified and dried copolymer sample, about 5 to 10 mg samples were dissolved in 0.7 ml deuterated tetrachloroethane (TCE-D2) solvent at room temperature. Spectra were recorded on a Bruker-500 (500 MHz) spectrometer at 120 °C. All samples were heated at 120°C for at least three hours in a heating block before starting the measurements to ensure homogeneous solutions were obtained. In addition, NMR spectra of intermediate samples were also examined under the same analytical conditions.

Besides confirming the presence of silicon groups ($Si(CH_3)_2$) and PP segments in the final products, ^1H NMR was also used to quantify the relative amounts of double bonds in copolymers and the molar ratio between PP and PDMS segments in the copolymers.

3.5.2 Differential Scanning Calorimetry (DSC)

DSC is a thermal method that is used to measure the enthalpic and other thermal responsive changes of a sample. By monitoring the changes in supplied energy, relative to a material, against temperature, the thermal transitions of a polymer such as the glass transition and the heat of fusion or crystallization can be observed. For a semi-crystalline polymer, the shape of the DSC curve also gives an indication with respect to the proportion of crystalline species present. In general, the degree of crystallinity of polymers depends on the molecular weight and structural regularity of the chain [55].

As discussed in Chapter 2, PP and PDMS cross metathesis polymerization and PP homopolymerization may take place simultaneously during the reaction process. These reactions will result in changes of molecular weight and its distribution, chain structure and stereoregularity. These changes should have an effect on the crystallization behavior of the modified PPs. It is expected that the crystallinity level and melting temperature of PP will be reduced by the introduction of amorphous PDMS and non-isotactic sequences into the chains.

Thermal analyses of the purified batch mixer PP/PDMS copolymers were carried out on a TA Instruments equipped with a 2920 differential scanning calorimetric (DSC) cell under

a helium environment. The DSC was weight calibrated and temperature calibrated with mercury and zinc as standards for low and high temperature, respectively. Around 5 to 10 mg of each copolymer and physical blend samples were scanned from -150°C to 200 °C at a heating rate of 10 °C/min. An empty pan was used as a reference. Moreover, thermal transitions of virgin PP and pure PDMS were also examined by heating the PP wax from 25 °C to 200 °C and PDMS from -150 °C to 0 °C, respectively. For all the experiments, the first heating/cooling cycle was used to condition the samples and hence only the data of the second cycle are reported in the results section.

3.5.3 Thermogravimetric Analysis (TGA)

In polymer production, it is important to determine the thermal stability of the material because in this way its useful temperature range without degradation can be measured. TGA is a technique that may be used to determine a material's thermal stability and its fraction of volatile components by monitoring the weight change as a specimen is heated. Thermal degradation of polyolefins occurs at elevated temperature and the resistance to thermal degradation is strongly dependent on the structure of the polymer. For example, polypropylene has less thermal resistance than polyethylene because of the presence of reactive tertiary carbon atoms. Similarly, branched polyethylene has higher thermal degradation rate than linear polyethylene due to the presence of tertiary carbon atoms at chain branches. However, it is found that the thermal degradation rate is relatively independent of molecular weight, and it has been concluded that number and length of

branches are more important than the sizes of the molecules. Thermal degradation of PP can be described as: (a) random chain scission by dissociation of a covalent bond into two macroradicals, preferentially at the tertiary carbon atoms, (b) disproportionation of the macroradicals and the intermolecular/intramolecular transfers preferentially to the tertiary hydrogen atoms, and (c) termination through recombination of two macroradicals. In this project, it was expected that addition of PDMS onto PP can increase the thermal stability of PP.

Thermal degradation analyses of PP and purified copolymers were obtained by using a TA Instruments –TGA 2000. For each sample, two sets of measurements were performed in two dynamic environments: air and nitrogen (N_2). All the experiments were carried out from 40°C to 650°C, at a heating rate of 10°C/min in both air and N_2 environments.

3.5.4 Rheological Properties

Rheology is defined as the science of flow and deformation of materials [56]. It is concerned with the response of materials to deformations and that response could be reversible elastic deformation, irreversible flow or a combination of both [57]. Equations used to study the fundamental relations between flow and deformation, are called constitutive equations, which describe the relationship between force and deformation in materials [56].

3.5.4.1 Viscous Liquid

A liquid is constantly deformed when it is subjected to a tensile or shear stress. The simplest constitutive equation used to express the linear relationship between rate of deformation or shear rate ($\dot{\gamma}$) and applied shear stress (σ) is called Newton's Law of Viscosity (3-1) [56]:

$$\boldsymbol{\sigma = \eta\dot{\gamma}} \tag{3-1}$$

where η is the Newtonian viscosity. According to Newton's Law, viscosity is independent of shear rate and a liquid with flow properties obeying Newton's Law is called a Newtonian liquid. For liquids that are non-Newtonian, shear stress is not proportional to the shear rate and the ratio $\sigma/\dot{\gamma}$ is called the apparent viscosity (η_a), which is not necessarily constant [58]. Shear thinning, the most commonly exhibited phenomenon of non-Newtonian fluids, indicates the decrease of viscosity as the shear rates increase. Some shear thinning fluids are polymer melts such as molten polystyrene and polymer solutions such as paints. In the opposite case where viscosity increases as the shear rate increases, the fluid is called a shear-thickening fluid [57]. Typical shear thickening fluids are clay slurries, certain surfactants and corn starch. Another general class of non-Newtonian fluids is called viscoplastic or "yield stress" fluid. They behave like elastic solids and will not flow when a small shear stress is applied. Once the shear stress exceeds a critical value known as the yield stress (τ_0), the fluid will flow readily [58]. Typical flow behaviors of non-Newtonian

fluids discussed above are illustrated in Figure 3-3. The linear line indicates the Newtonian flow and the rest of them represent different types of non-Newtonian fluids.

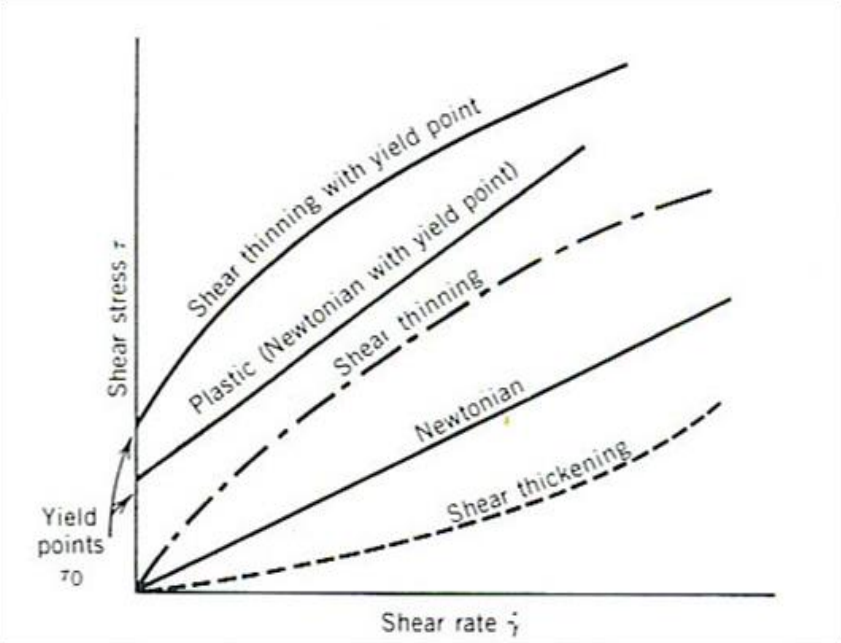

Figure 3-3: Flow behaviors of Newtonian and Non-Newtonian fluids [59].

3.5.4.2 Elastic Solid and Viscoelasticity

Similarly, there is a simple constitutive equation used to describe the relationship between force and deformation for solids:

$$\sigma_E = \varepsilon E \tag{3-2}$$

where σ_E is the tensile stress and is proportional to deformation or strain, ε. The coefficient of proportionality is Young's modulus, E. An ideal elastic or Hookean solid is defined as a material that has deformation proportional to the applied stress according to Hooke's Law, with immediate recovery of the original shape when the stress is released.

Some materials exhibit both solid—like and liquid-like properties and show non-linear dependencies between forces and deformations [56]. Such materials which show a combination of properties of liquids (viscous dissipative losses) and solids (storage of elastic energy) are known as viscoelastic materials [59]. The degree of viscoelasticity is strongly dependent upon the test temperature and the rate at which the polymer is deformed, as well as structural variables such as degree of crystallinity, crosslinking, and molecular mass. The special feature of the viscoelasticity of polymers is that their deformations under stress are time dependent [59]. The simplest and most commonly measured type of this behavior is linear viscoelasticity. In this situation, the polymer molecules are only slightly disturbed from their equilibrium state and the deformation is very small. The linear viscoelastic region of a polymer can be determined by performing a strain sweep, in which viscoelastic properties are measured at a fixed frequency value but

varying the strain. When the viscoelastic properties are constant over a certain range of strain, the limit of linear region is found. The strain sweep of virgin PP wax used in this study, at 162°C, is presented in Figure 3-4, in which viscoelastic properties (storage modulus, G′ and loss modulus, G″) are constant from 10 to 100% of strain. Therefore, the linear viscoelastic region for virgin PP wax was identified.

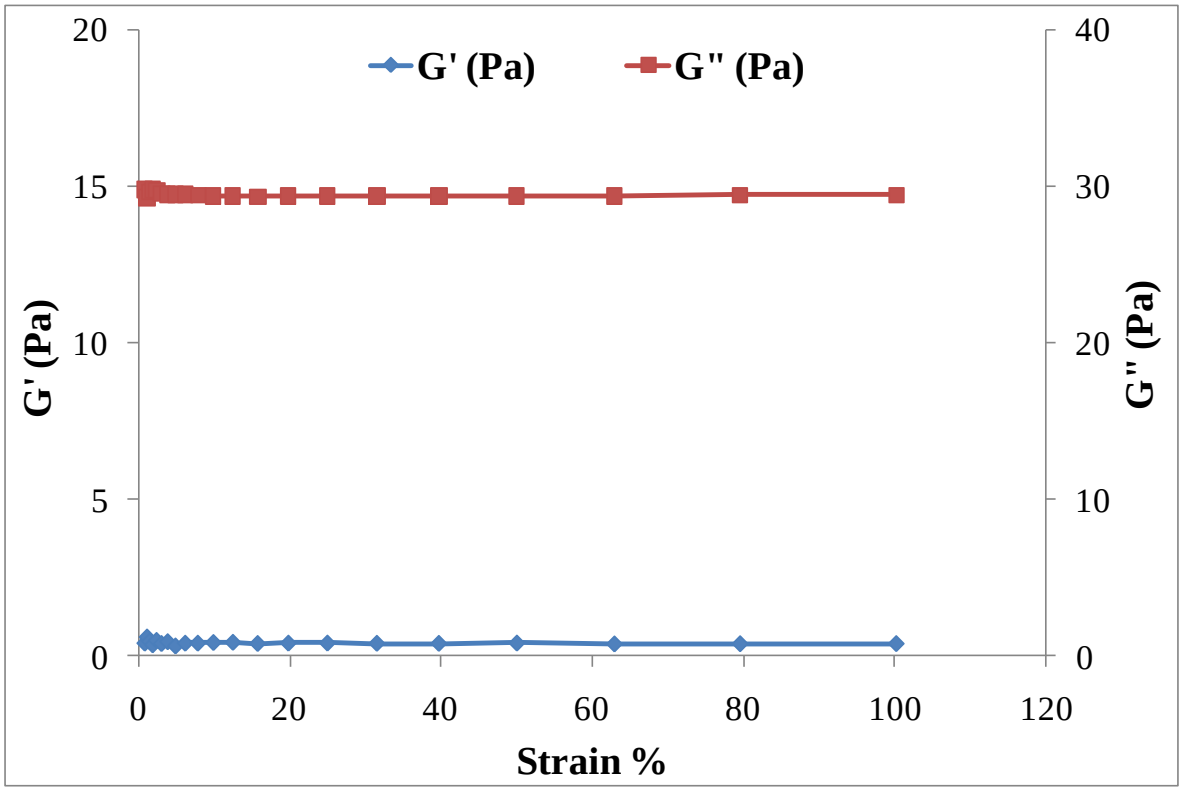

Figure 3-4: Strain test for virgin polypropylene wax (N-15)

3.5.4.3 Oscillatory Shear Experiments

Information on both the elastic and viscous characteristics of the material can be obtained by subjecting a specimen to an oscillatory stress experiment and monitoring the time-dependent deformation. Depending on the material tested, information on polymer degradation, solvent evaporation, dispersion settling, and cure information can be obtained. The oscillation technique involves applying a sinusoidal shear strain wave to a material (a thin disc) and measuring the resulting shear stress:

$$\boldsymbol{\gamma}(\boldsymbol{t}) = \boldsymbol{\gamma_0}\ \mathbf{sin}(\boldsymbol{\omega}\,\boldsymbol{t}) \tag{3-3}$$

$$\boldsymbol{\sigma}(\boldsymbol{t}) = \boldsymbol{\sigma_0}\ \mathbf{sin}(\boldsymbol{\omega t} + \boldsymbol{\delta}) \tag{3-4}$$

where γ_0 is the strain amplitude, $\sigma_0$is the stress amplitude, ω is the frequency and δ is the phase shift between strain and stress. Measuring this time dependent stress response reveals the differences between different materials (Figure 3-5).

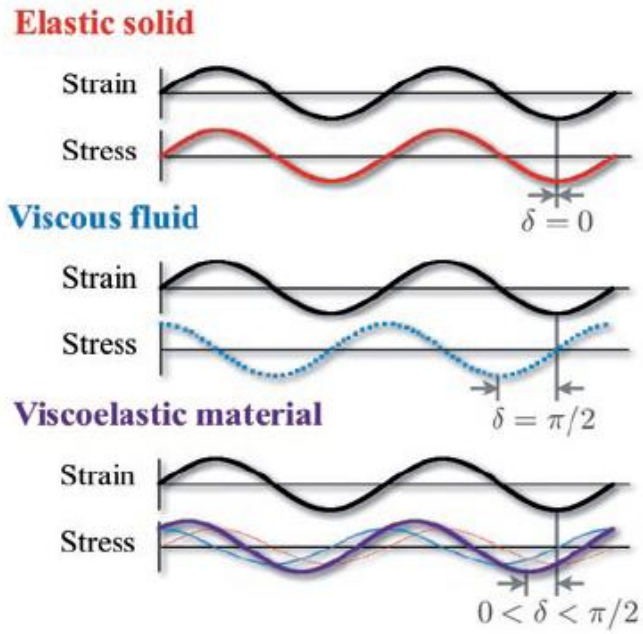

Figure 3-5: Oscillatory measurements of a Hookean (Elastic) solid, a Newtonian (Viscous) fluid and a viscoelastic material [60]

If a sinusoidal stress (σ) is placed on an elastic (Hookean) solid, a sinusoidal displacement (strain, γ) will result, which is in phase with the applied stress; 0 ° phase shift angle is observed because an elastic solid retains all the deformation energy applied to it. Conversely, a Newtonian (viscous) fluid dissipates all the applied energy and has a phase shift angle of 90° (Figure 3-5). For viscoelastic materials, the phase shift angle (δ) will be in between 0° and 90°, revealing the extent of solid-like and liquid-like behavior. The

viscoelastic behavior of the samples at ω is characterized by the loss modulus (G'') and storage modulus (G') (Equations (3-5) and (3-6)), in which G″ represents the liquid-like and G' represents the solid-like component contributions to the measured stress response.

$$\boldsymbol{G'' = \sigma_0 \sin(\delta / \gamma_0)} \quad (3\text{-}5)$$

$$\boldsymbol{G' = \sigma_0 \cos(\delta / \gamma_0)} \quad (3\text{-}6)$$

3.5.4.4 Cone and Plate Rheometer

A rheometer is an instrument that measures both stress and deformation on a material. A cone and plate rheometer is a type of shear rheometer with drag flow in which shear is generated between a moving truncated cone and a fixed flat plate [56]. The geometry is such that cone and plate are arranged to be parallel, in principle, with the tip of the cone on the top of the plate as seen Figure 3-6 (a). However, to avoid contact between the cone and plate and to prevent damage to either of them, the cone is truncated, which means that the tip is blunt as shown in Figure 3-6 (b). This small truncated region also makes the gap-setting procedure between cone and plate easier to carry out and any error introduced by the truncation is negligible [59].

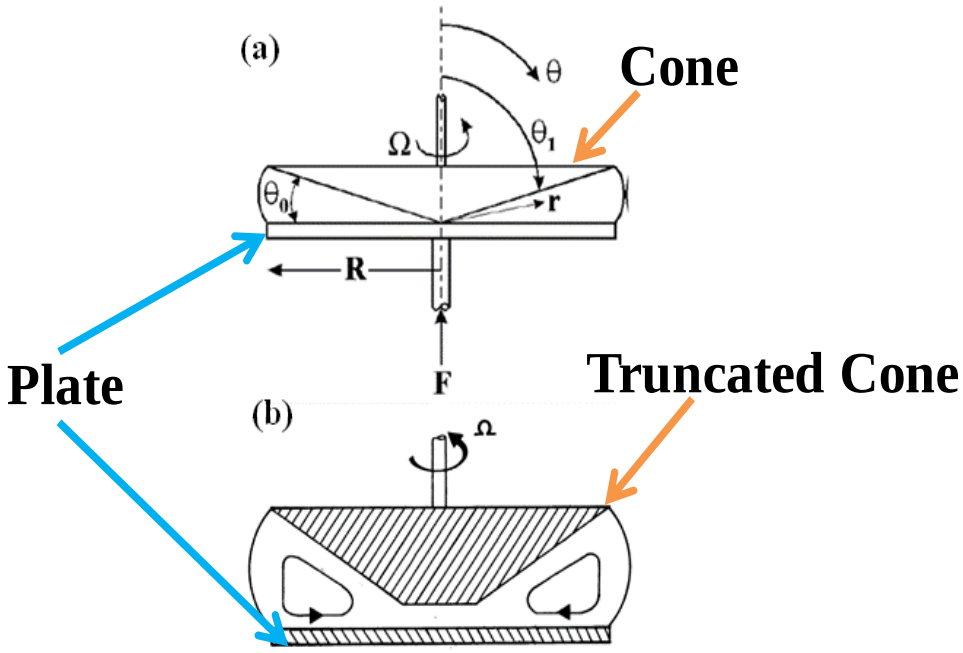

Figure 3-6: Shear flow geometry of (a) cone and plate in principle and (b) truncated cone and plate [59]

The disk radius R, is essentially a few centimeters and the cone angle θ_0 is generally smaller than 5° so that an approximately uniform shear rate can be generated through the sample when the cone is rotated. It is important to select the appropriate geometry and diameter when preparing the samples for cone and plate rheometry. It is known that a greater angle causes a lower shear rate factor and hence, a large angle is suited to low strain or shear rate measurements, whereas a smaller angle is suited to high shear rate measurements [61]. On the other hand, the smaller the diameter of the cone, the larger the shear stress. This means that the higher the modulus or viscosity of the sample, the smaller the diameter that should be used. Normally, 4° is the largest available angle for the cone and plate rheometer because assumptions in the theory used to calculate the material properties do not hold for larger angles [61].

In a cone and plate rheometer, the cone rotates while the plate is stationary. All oscillatory shear experiments were performed on a TA Instruments (AR 2000) rheometer (Figure 3-7) with a cone and plate geometry (40 mm diameter). Experiments were carried out at 162°C, with a 26 μm gap in between the cone and the plate. However, it is known that the true behavior of a material can only be observed if the system is in at steady state. Therefore, prior to performing the oscillatory frequency sweep, an oscillatory time sweep was carried out at 162°C (10 Hz, 10% strain) for 30 min to determine if a sample has time dependent rheological properties. The region of linear viscoelasticity for each sample was determined from a strain sweep from 1 to 100% strain, at 1Hz. Based on strain sweep results, strain amplitude was controlled at 10% and 15%, respectively, for all samples in order to determine the dynamic rheological properties: G′, G″ and viscosity, in frequency

sweeps over the range of 1 to 100 Hz, at 162°C. The surrounding insulation jacket was used to maintain an inert atmosphere over samples by purging at 5 ml/min with N_2 to prevent sample degradation. A hot press was used to prepare samples as disks (diameter = 25 mm, thickness = 1mm) at 162°C. Detailed experimental results are discussed in Chapter 4.

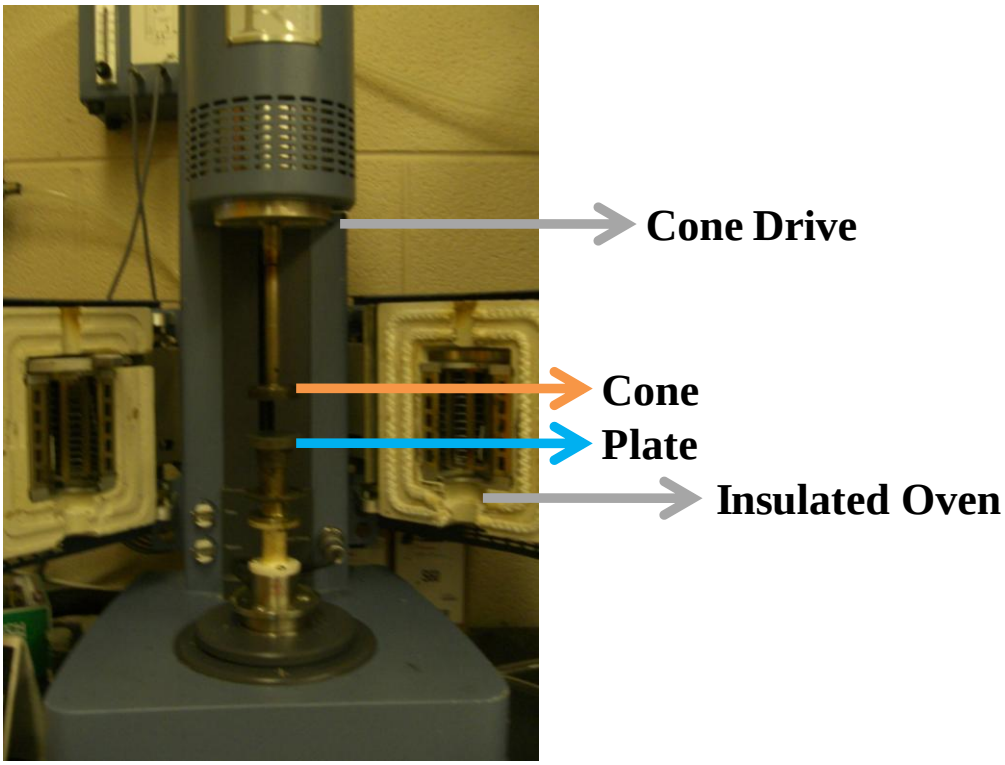

Figure 3-7: TA (AR 2000) cone and plate rheometer

3.5.5 Scanning Electron Microscopy (SEM)

SEM is a technique that has been used in a wide range of applications including medical, materials and semiconductor industries. It has also been used to study the surface analysis of rubber bonding and the chemical composition of polymer blends [62]. The basic principle of SEM is to scan the specimen with a very fine focused beam of high-energy electrons. SEM examination of polymers provides information such as external morphology, chemical composition and crystalline structure.

In this project, morphologies of virgin PP and copolymers obtained from Runs 6 and 8 were observed by a GEMINI 1530 scanning electron microscope using a secondary electron detector with accelerated voltage at 5 kV. Samples were prepared as films through a hot press and then they were inserted into liquid nitrogen for 1 minute and broken. However, polymers are non-conductive materials and they tend to build up charge when scanned by the electron beam, and this can cause image artifacts and scanning faults. Therefore, prior to SEM examinations, a thin layer of gold was coated on top of each sample's surface to prevent the accumulation of static electric charge during the electron irradiation. From SEM, we can not only obtain the morphology of copolymers, but also determine the chemical composition of samples that could be assessed by applying SEM-EDX (electron dispersive X-ray microscopy).

Chapter 4 Results and Discussion

4.1 Introduction

This chapter will present a discussion of the properties studied for the PP-PDMS copolymer products. In Section 4.2.1, chemical structure determination and mass ratio of PP and PDMS in copolymers obtained from NMR analysis are discussed. Thermal properties of all copolymers determined from DSC and TGA are compared to virgin PP wax and pure PDMS in Section 4.2.2. In addition, rheological characteristics obtained by a cone and plate rheometer and examinations of copolymers' morphology are provided in Sections 4.2.3 and 4.2.4. In Section 4.2.5, the chapter will end with a discussion of variance analyses for physical responses.

4.2 PP-PDMS Copolymer Characterization

4.2.1 Nuclear Magnetic Resonance Results

^{1}H NMR spectroscopy was used as the primary characterization technique in this study to quantify the chemical interaction between PP and PDMS. This was chosen because PP and PDMS have very distinct ^{1}H NMR signals. Therefore, the proportions of the two components of the reaction products and formation of copolymers were monitored by ^{1}H NMR spectroscopic analysis.

Preparation for NMR samples has been explained in Chapter 3, section 3.5.1. A representative spectrum of virgin PP wax is provided in Figure 4-1.

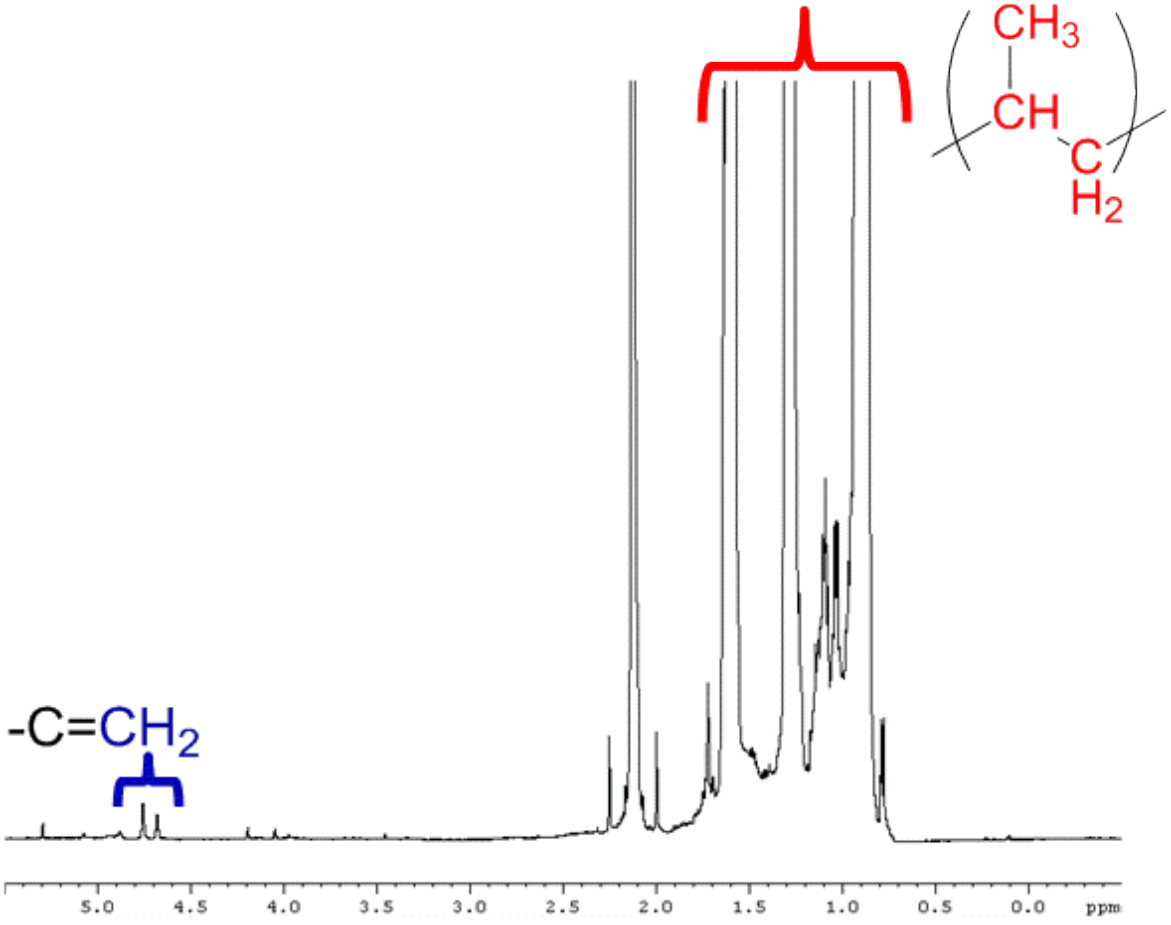

Figure 4-1: ^{1}H NMR spectrum of virgin PP wax (TCE-D2 solvent, 120°C)

The multiple peaks shown from 0.7 to 1.9 ppm corresponded to signals from the 3 types of protons on saturated carbon centers, in the repeating unit of the virgin PP wax as indicated in Figure 4-1. The presence of vinylidene protons was also observed as two small signals at 4.6 and 4.7 ppm.

Integration of the vinylidene signals relative to the saturated ones allows for quantifying the proportion of double bonds in PP and in copolymers. Figure 4-2 shows the ^{1}H-NMR spectrum of PP-PDMS copolymer obtained from Run 2. It is obvious that the signals at both δ = 0.7-1.9 and δ = 4.6-4.7 ppm, attributed to repeating unit- and vinylidene- protons of PP wax phase in the copolymers, respectively, are still apparent. In addition, the sharp peak observed near 0.0 ppm was assigned to the methyl protons attached to silicon atoms. Hence, the formation of chemical bonds between PP and PDMS in purified copolymers was supported by these observations. Spectra from other PP-PDMS copolymer products were qualitatively the same as the spectrum for copolymer from Run 2.

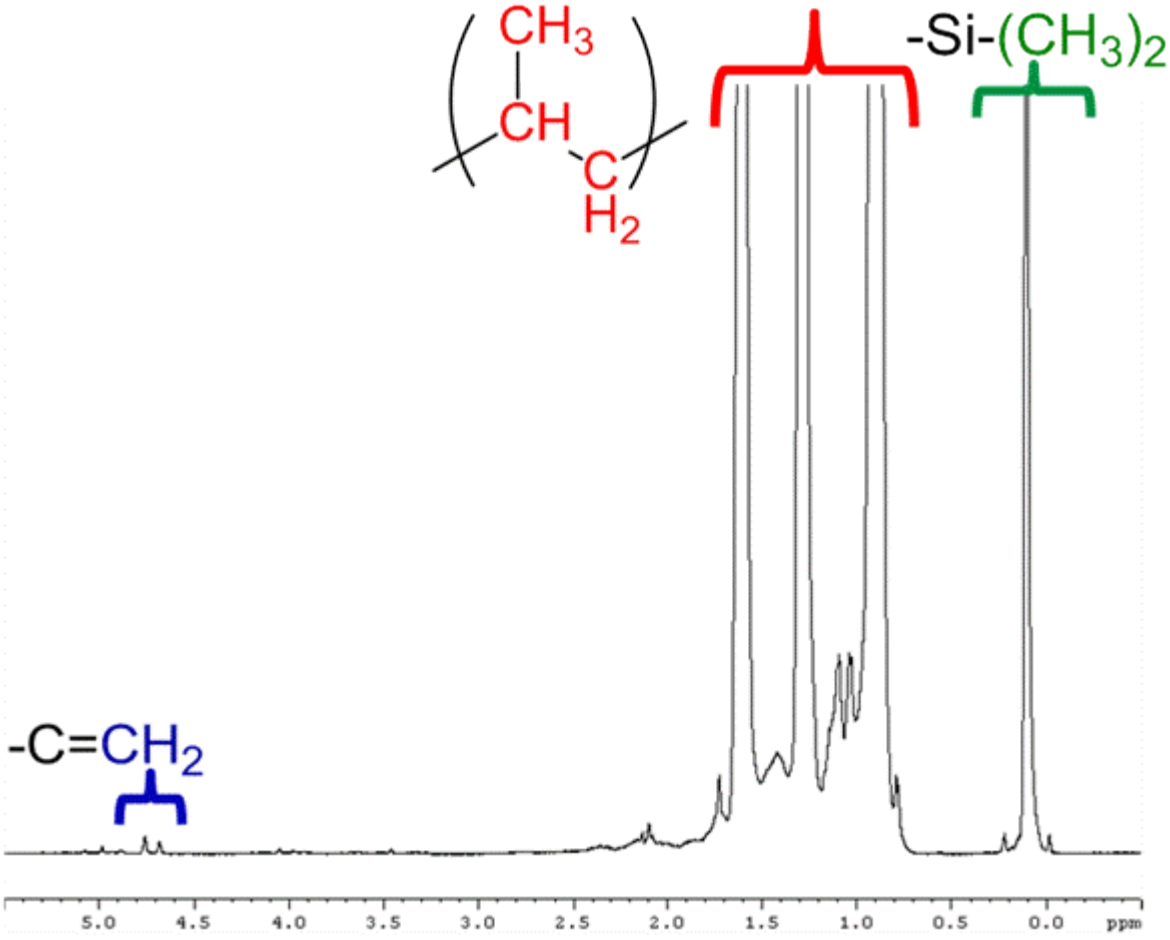

Figure 4-2: ^{1}H NMR spectrum of Run 2 purified copolymer (TCE-D2 solvent, 120°C)

Relative amounts of double bonds in copolymers and the mass ratio between PP and PDMS in copolymers were quantified through ^{1}H NMR analysis as indicated in Table 4-1 and Table 4-2. For all the experiments, there were no significant differences in $\frac{PP}{PDMS}$ mass ratio before and after the reaction. For instance, the $\frac{PP}{PDMS}$ mass ratio for Run #1 before the polymerization was set at 16:1, and it was 13:1 after 30 mins CM reaction (as seen in Table 4-1). This indicated that reagents PP and PDMS were almost completely reacted in melt phase and synthesized PP-PDMS copolymers.

Table 4-1: PP to PDMS mass ratio from analysis of ^{1}H-NMR spectra

Run #	Initial molar ratio	Initial mass ratio	5 min mass ratio	30 min mass ratio
1	200	16	16	13
2	100	8	7	7
3	200	16	12	12
4	100	8	6	7
5-2	200	16	12	13
6	100	8	6	8
7	200	16	13	14
8	100	8	9	8

Table 4-2: PP to Vinylidene mass ratio from analysis of ^{1}H-NMR spectra

Run	Initial mass ratio	5 min mass ratio	30 min mass ratio
1	329	488	408
2	329	348	362
3	329	514	447
4	329	647	357
5-2	329	601	315
6	329	353	334
7	329	1264	350
8	329	468	854

Table 4-2 summarizes the ratio of PP repeating units to vinylidene groups in copolymers. The given average molecular weight ($\bar{M}_n$) of virgin PP wax is 5000 (by GPC), and this implies that the ratio of PP repeating units to vinylidene should be 119:1 if all the chains were vinylidene terminated. However, based on NMR analysis (Figure 4-1), the ratio was determined to be 329:1, which indicates that not all the chains in virgin PP wax have a terminal double bond. A similar ratio ($\frac{PP}{Vinylidene} = 283:1$) was supported by studies from Zhang who determined vinylidene content in PP wax by Fourier Transform Infrared Spectroscopy (FT-IR) [53].

From the data in Table 4-2, it can be seen that the relative amounts of double bonds were smaller in copolymers than in virgin PP as indicated by the increase in mass ratio of PP to vinylidene protons. For instance, PP to vinylidene group mass ratio of 30 mins copolymer sample from Run 2 is 362, which is relatively higher than the initial mass ratio, 329 (sample calculation shown in Appendix). This indicated that around 10% of vinyl double

bonds in virgin PP wax were consumed during CM polymerization, which is far more than would be expected for PP and PDMS reaction. The initial set up for PP to PDMS molar ratio was 100:1 in this experiment, which meant that only 1% of PP double bonds should be consumed to form PP-PDMS copolymers (Figure 4-3 a), since both reagents are mono-vinyl terminated. However, instead of losing 1% of vinylidene groups in virgin PP wax, 10% of them were consumed. This is due to the large amount of PP added in the reactions; the vinylidene groups on PP likely prefer to react with themselves to form PP-PP homodimers instead of reacting with the vinyl groups on PDMS. However, synthesized PP homodimers have no vinyl protons attached on the double bond as shown in Figure 4-3. The amount of vinylidene groups in PP that were consumed in reaction with PDMS could not be quantitatively determined from NMR analysis. This is because the relative low proportion of C=C double bond formed between PP-PDMS is not observed definitely in the NMR spectra of products. This is because the low intensity of the relevant signal is masked by noise.

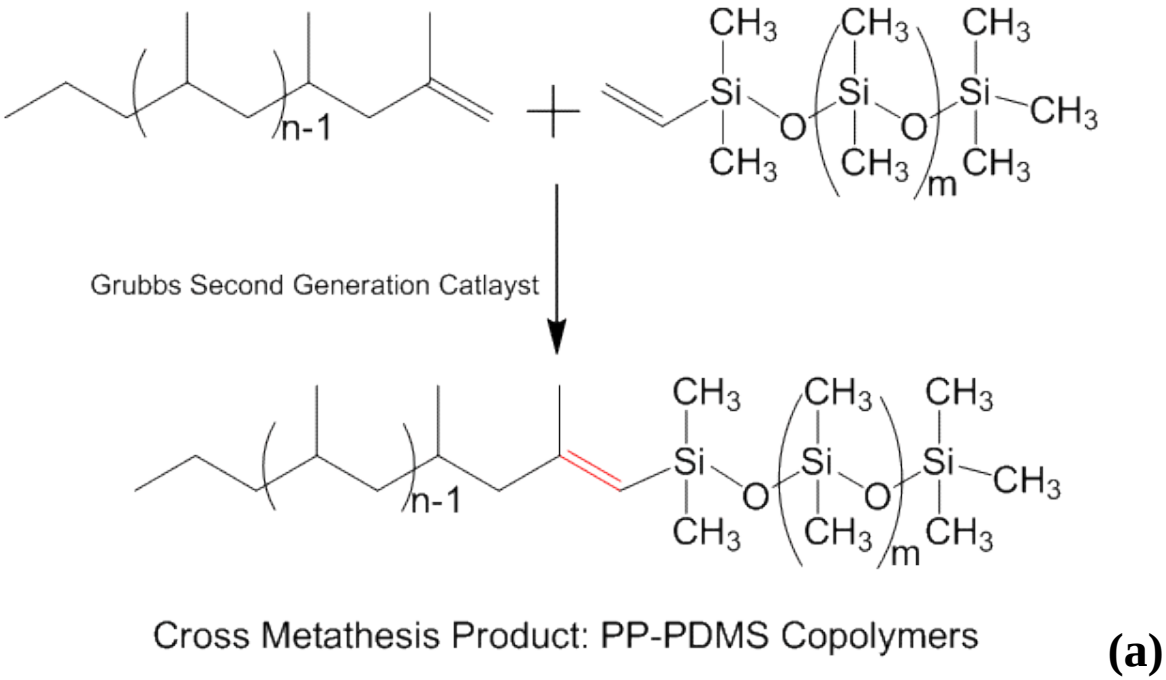

Cross Metathesis Product: PP-PDMS Copolymers

(a)

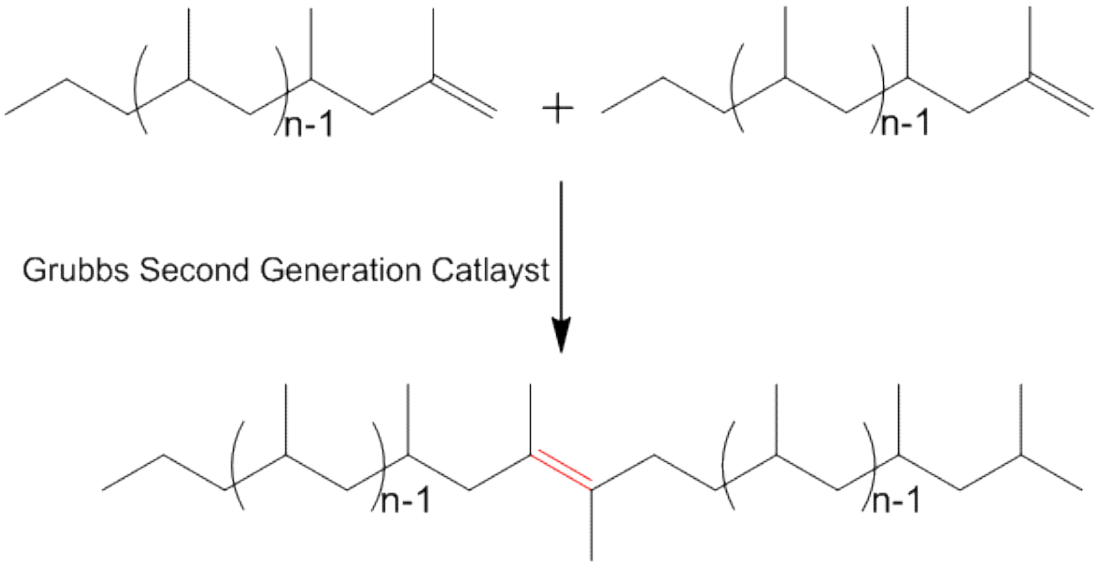

PP-PP Homodimer Product

(b)

Figure 4-3: Cross metathesis reaction scheme of (a) PP-PDMS and (b) PP homodimers formation

In addition, it was found that an intermediate sample (5 min) obtained from Run 7 gave a quite different PP to vinyl group molar ratio compared to the others. This may be due to sample heterogeneity during the NMR analysis and this was indicated visually by the presence of un-dissolved material in the NMR solution even though all the samples had been heated for 3 hours prior to analysis. This would lead to inconsistencies in the quality of spectra, which also have a great effect on the relativity of integrations of small signals from vinylidene protons. This in turn may result in a relatively higher error when calculating ratios of PP repeating units to vinylidene. Also, it should be noted that although the NMR technique provided reasonable results, specific machine parameters used in NMR experiments could also affect the signal to noise ratio and final quantitative analysis.

In addition, NMR samples were very small and if the products were not completely homogeneous, some differences in analyses would be likely observed. Hence, replicate analyses to determine typical measurement uncertainties are recommended in the future.

4.2.2 Thermal Characterization

Because PP and PDMS have different temperature related behaviors, thermal analyses were carried out by differential scanning calorimetry (DSC) and thermogravimetric analysis (TGA).

In DSC measurements, temperature was increased gradually and the heat flow, which was necessary to maintain the desired heating rate, was recorded. The heat flow was plotted as a function of temperature for virgin PP wax, pure PDMS and all the purified copolymer products. An inflection point in the DSC thermogram indicates a glass transition, whereas, a minimum (maximum) indicates an exothermic (endothermic) process, related to melting of crystalline domains [63].

Figure 4-4 shows the DSC profiles of virgin PP and pure PDMS. A double melting peak ($T_{m\text{-}pp1}$, $T_{m\text{-}pp2}$) was observed in the DSC profile of pure PP wax, at 148.7°C and 157.9°C. From the melting curve of pure PDMS, several thermal transitions were evidenced. Initially, a change in the heat capacity baseline, which corresponded to its glass transition, was examined at -126.5°C. As the temperature increased, a cold crystallization exothermic peak (T_c) at -86.0°C and a doublet endothermic peak corresponding to melting points at -46.7°C and -37.6°C were also exhibited.

As was seen in the DSC profile of virgin PP, a clear doublet melting peak at 148.5°C ($T_{m\text{-}pp2}$) and 156.5°C ($T_{m\text{-}PP1}$) was obtained in the melting curve of the purified copolymers (the trace for the product of Run 8 is shown on Figure 4-5). This observation confirmed the presence of the PP crystalline phase in the copolymer. Another section of melting profile

for this copolymer is shown in Figure 4-6, over a temperature range from -140°C to 0°C. Similar features to those in the melting curve of pure PDMS were observed. For example, the weak glass transition (T_{g1}) and melting temperatures ($T_{m\text{-}PDMS1,}$ $T_{m\text{-}PDMS2}$) in the copolymer representing the PDMS phase were comparable with the temperatures seen for pure PDMS. However, the exothermic peak corresponding to cold crystallization of pure PDMS was not detected in Figure 4-6; instead, the copolymer exhibited a glass transition temperature. It was believed that the amorphous PDMS component was homogeneously mixed with crystalline PP, which influenced the thermal transitions of PDMS component in copolymers. Also, because the proportion of PDMS in the copolymer sample was relatively low, and it was therefore expected that the peaks for the PDMS component melting events would be relatively insignificant. Similar DSC results were detected for all the other synthesized copolymers as shown in the Appendix (Figure A-0-2 and Figure A-0-3).

The DSC thermogram for a PP and PDMS physical blend mixture is presented in Figure 4-7. It can be seen that only one glass transition peak was observed at around -80°C, indicating the PDMS component in the physical blend. Disappearance of other thermal transitions of pure PDMS was resulted from the purification process, which washed away the PDMS phase in the physical blend. This also indicated that characteristic properties of PDMS were not retained in the purified physical blend because the amount of PDMS observed here was very low.

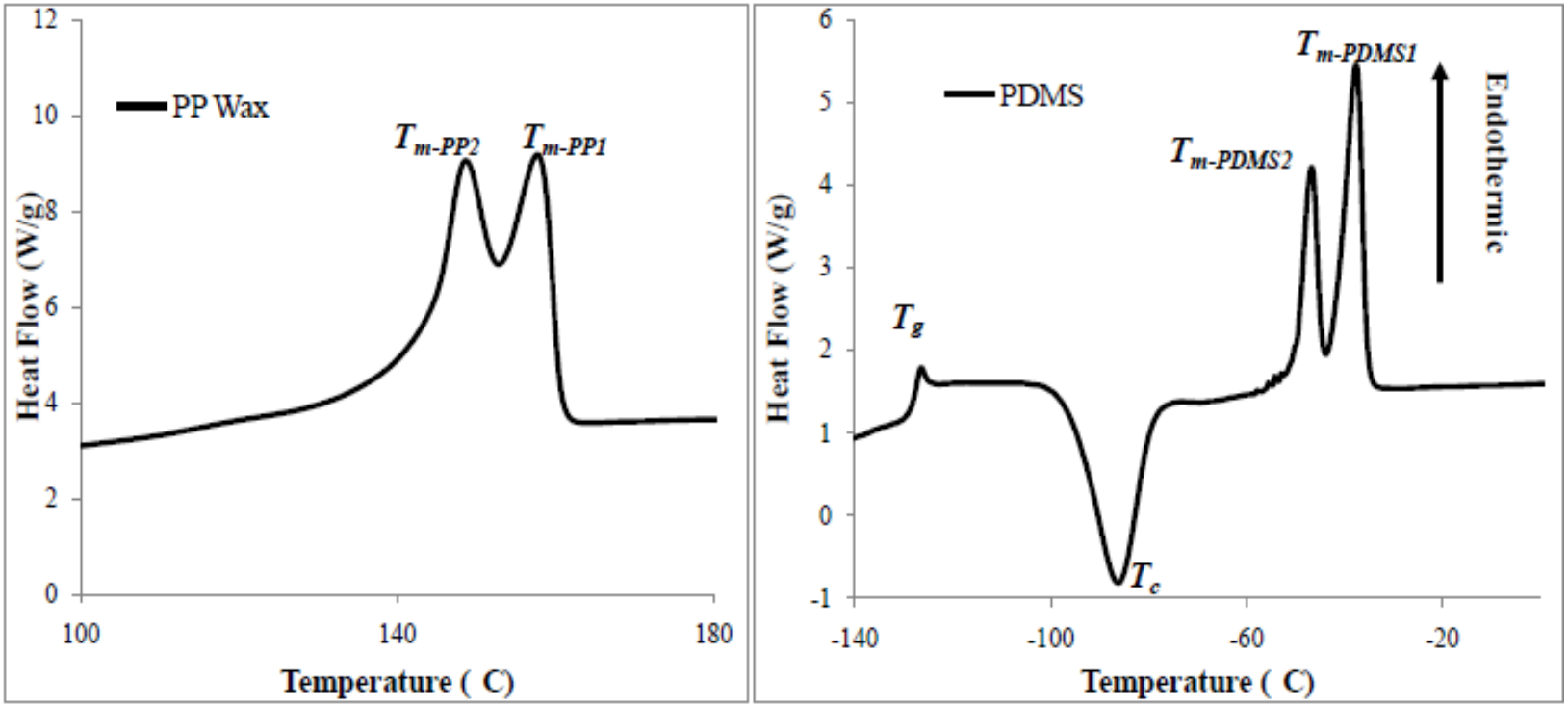

(a) **(b)**

Figure 4-4: DSC thermograms of virgin PP (a) and PDMS (b)

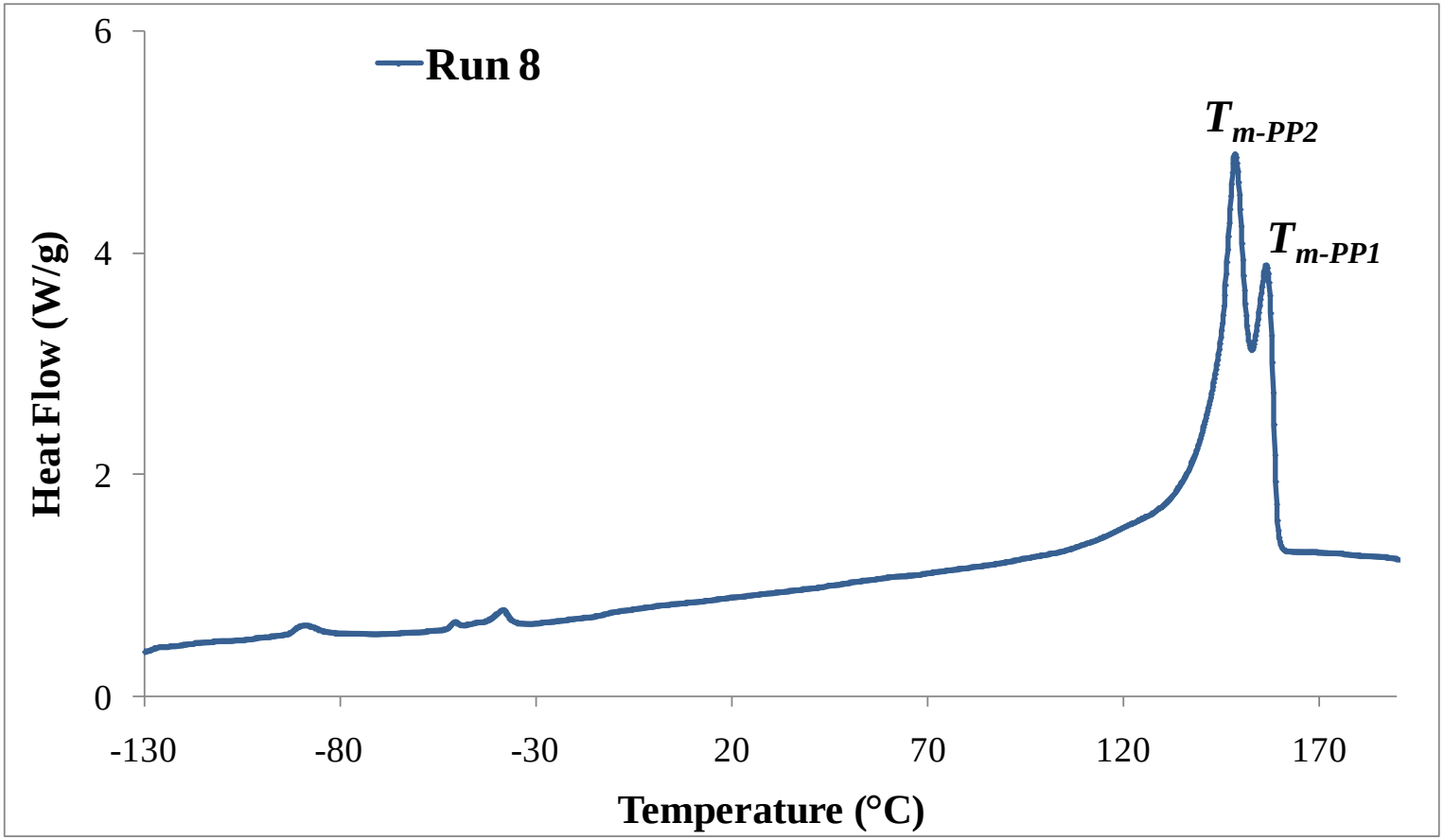

Figure 4-5: DSC thermogram of purified copolymer sample from Run 8, -130°C to 190°C

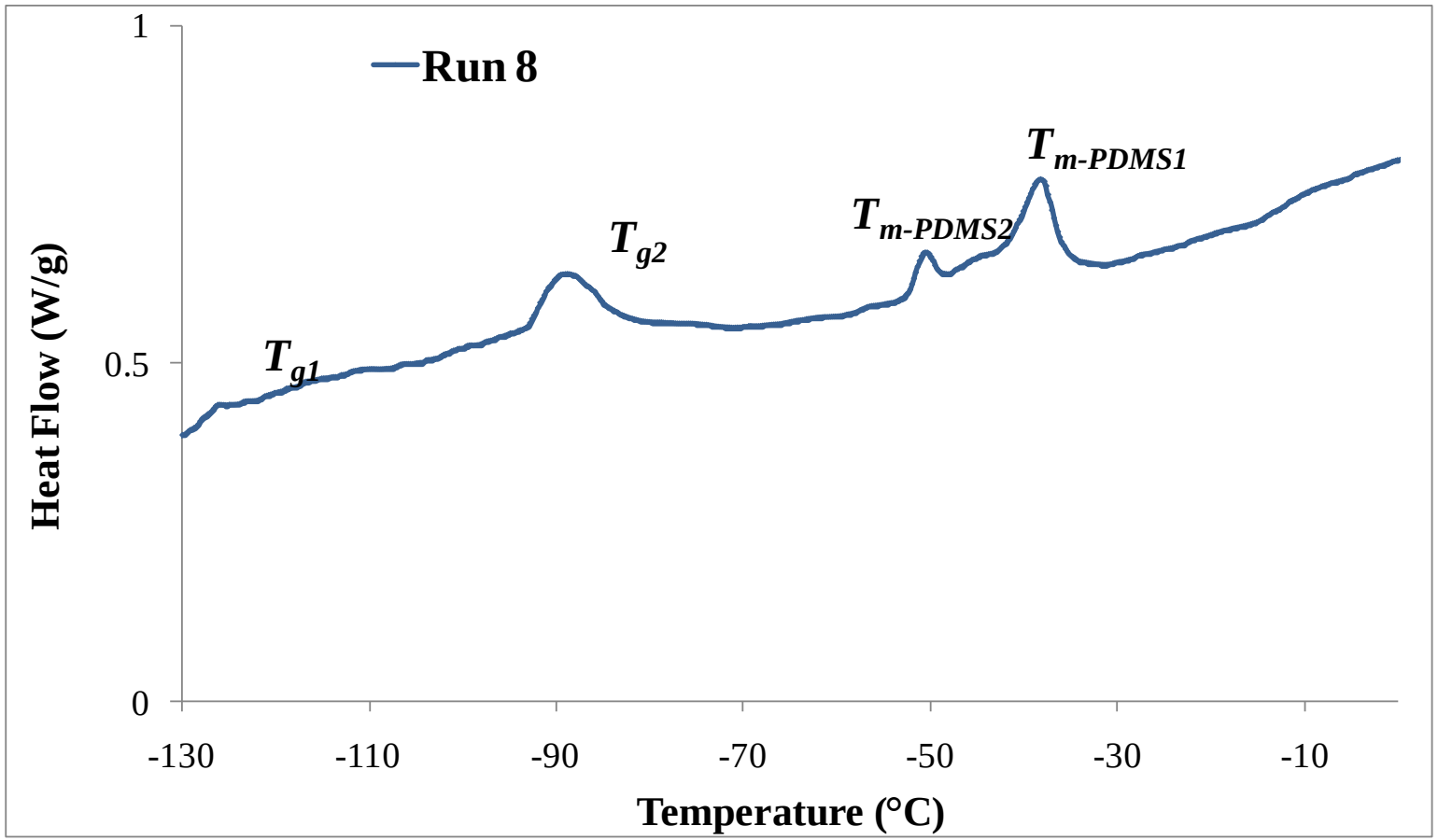

Figure 4-6: DSC thermogram of purified copolymer sample from Run 8, -130°C to 0°C

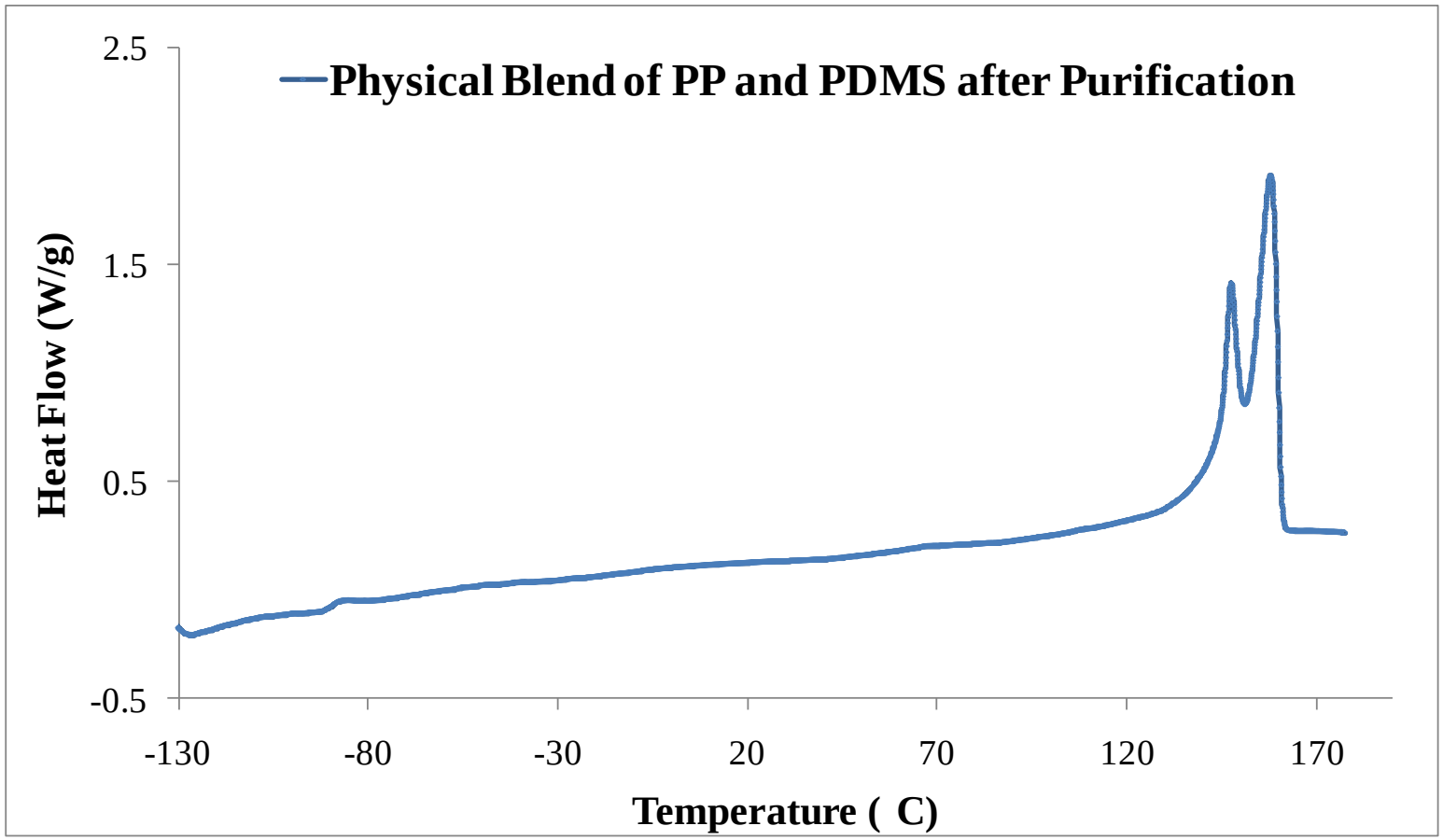

Figure 4-7: DSC thermogram of purified PP and PDMS physical blend sample, -130°C to 190°C

The glass transition (T_g), melting temperatures (T_m) and related heating enthalpies (ΔH) of each copolymer were determined using the TA Instruments-DSC and the data are summarized in Table 4-3 and Table 4-4. Symbols (T_{m-PP1} and T_{m-PP2}) represent the melting points of the PP crystalline phase in copolymers. As expected, the values of T_{m-PP1} and T_{m-PP2} of copolymers were similar to virgin PP in the presence of PDMS. Moreover, it is known that the crystallinity level is related to the measured heating enthalpy. In Table 4-3, heating enthalpies of the copolymers ($\Delta H_{m-PP1,}\, \Delta H_{m-PP2}$) associated with two melting peaks in the range from 145°C to 160°C were generally smaller than the ones of pure PP. This suggested that less heating energy was required to melt the PP-crystalline phase in copolymers than the virgin PP because of the addition of PDMS. As discussed above, most copolymers exhibited two glass transition peaks (T_{g1}, T_{g2}). Nevertheless, due to the small amount of PDMS added into the reaction, glass transition peaks of several copolymers were not clearly observed. It was also found that melting points corresponding to the PDMS-phase in copolymers were almost the same as the ones from pure PDMS.

Interpretations of DSC melting curves and summarized data proved the presence of PDMS in purified copolymers and the feasibility of cross metathesis polymerization in melt phase. They also indicated that the proportion of the PP crystalline phase in copolymers influenced thermal transitions of PDMS component.

Table 4-3: DSC thermal transition data of copolymers and virgin PP in the range from 0°C to 180°C

Sample	T_{m-PP1} (°C)	ΔH_{m-PP1} (J/g)	T_{m-PP2} (°C)	ΔH_{m-PP2} (J/g)
1	157.0	1189.9	147.6	973.6
2	156.8	1067.0	147.2	882.8
3	156.0	1195.9	145.8	851.2
4	156.8	1028.7	148.5	1164.9
5-2	156.8	1282.8	148.8	1319.7
6	157.4	950.8	147.2	766.4
7	155.7	1004.9	146.2	870.2
8	156.8	1646.0	148.8	771.6
CP1	156.4	1307.0	146.2	1023.4
CP2	156.4	1132.6	146.9	918.4
PP	**157.9**	**1546.9**	**148.7**	**1115.5**

Table 4-4: Glass transition temperatures and thermal transition data of copolymers, and pure PDMS in the range between -140°C and 0°C

Sample	T_{g1} (°C)	T_{g2} (°C)	$T_{m-PDMS2}$ (°C)	$T_{m-PDMS1}$ (°C)
1	-126.2	-98.2	-49.7	-37.7
2	-126.2	-110.5	-50.4	-37.9
3	-126.0	-110.8	-46.3	-37.5
4	-127.1	-89.6	-50.1	-37.5
5-2	-126.3	-95.8	-50.8	-38.3
6	-130	-92.7	-50.3	-38.0
7	-126.8	-88.3	-51.2	-38.3
8	-128.0	-91.8	-50.8	-38.2
CP1	-122.6	—	-50.8	-38.0
CP2	—	-115	-50.8	-37.8
PDMS	**-126.5**	**-86.0 (T_c)**	**-46.7**	**-37.6**

Chemical modification of PP with PDMS through cross metathesis polymerization may result in two structural changes. One was the formation of PP-PDMS block copolymers, which should possess higher thermal stability than virgin PP, since PDMS is widely known for its excellent stability at high temperatures. Another structural change could be the synthesis of homodimerized polypropylene. This change may also enhance the thermal stability due to the increase of molecular weight and the reduction of chain mobility.

In TGA, the weight loss of copolymers was measured as a function of temperature from 40 °C to 550 °C under two different environments: air and nitrogen. Figure 4-8 and Figure 4-9 illustrate TGA curves for copolymer Run 8 and virgin PP wax in air and nitrogen, respectively. It has been reported that polypropylene thermally degrades to volatile products in air at temperatures higher than 250°C through a radical chain process [64]. From Figure 4-8, it can be seen that the major proportion of weight loss for both copolymer and PP wax occurred between 200°C and 400°C. Tests made in air showed that significant degradation of copolymer started at 368°C, but that of virgin PP occurred at 309°C. On the other hand, the temperatures for the onset of degradation of the same samples in nitrogen (Figure 4-9) were 423°C and 419°C, respectively. It was known that in nitrogen, thermal degradation is mainly expected with slight or no thermal-oxidation, due to the absence of oxygen. As a result, the degradation for PP and copolymer in nitrogen proceeded in a similar manner and the difference in degradation temperatures is much smaller (4°C) than in air (59°C).

The remaining weight (RW) percentages of copolymers and virgin PP wax at 350°C and 450°C were tabulated in Table 4-5. It was apparent that virgin PP wax lost the most weight at both temperatures, which implied that addition of PDMS onto PP chains leads to better thermal

stability for the copolymer as compared to pure PP wax. Moreover, PP to PDMS high and low molar ratios (200 and 100) are plotted against the average remaining weight % at 350°C (Figure 4-10). It was shown that lower PP to PDMS molar ratio (100), which meant higher PDMS content in the initial set-up, gave greater thermal stability. Therefore, it is expected that the thermal stability of copolymers increases as the concentration of PDMS increases. TGA curves of other copolymers obtained in air and nitrogen are shown in Figure A-0-4 and Figure A-0-5. From obtained graphs and data, it can be concluded that all the synthesized copolymers possess higher thermal stability than virgin PP wax.

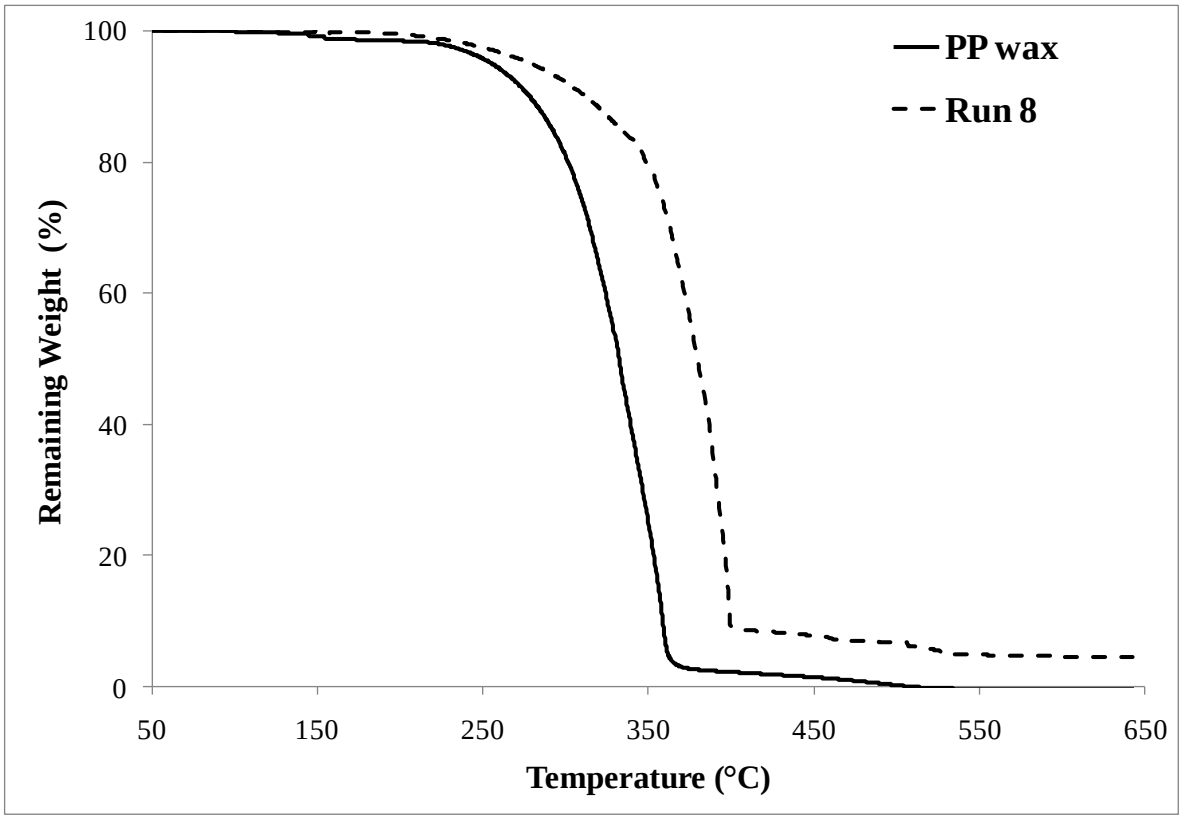

Figure 4-8: TGA curves of virgin PP and Run 8 copolymer, 50°C to 650° in air

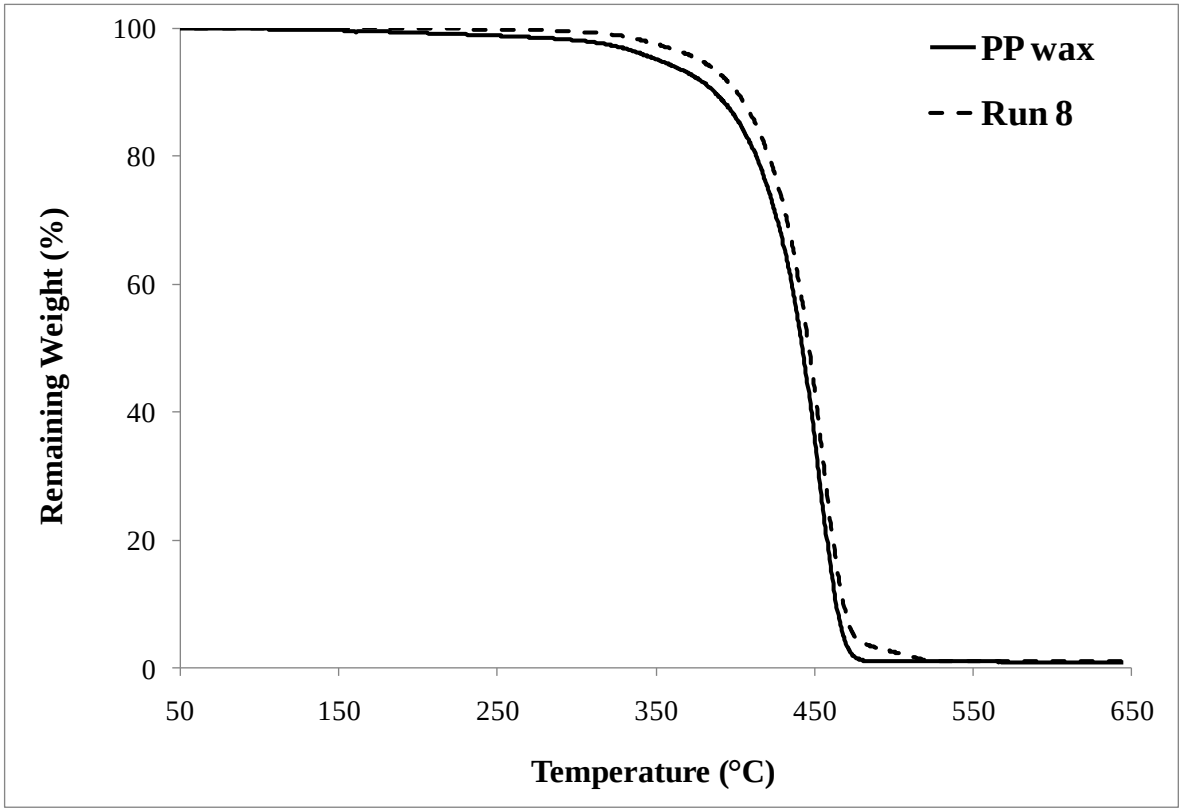

Figure 4-9: TGA curves of virgin PP and copolymer from Run 8, 50°C to 650° in N_2

Table 4-5: Remaining weight (RW) % of virgin PP and copolymers from TGA studies in air

Run #	RW at 350 °C (%)	RW at 450 °C (%)
1	52.41	3.14
2	61.93	8.36
3	40.90	5.50
4	55.96	7.04
5-2	43.06	5.37
6	62.33	7.78
7	61.06	8.09
8	79.16	7.83
CP1	40.37	5.90
CP2	47.10	5.78
PP	**24.49**	**1.49**

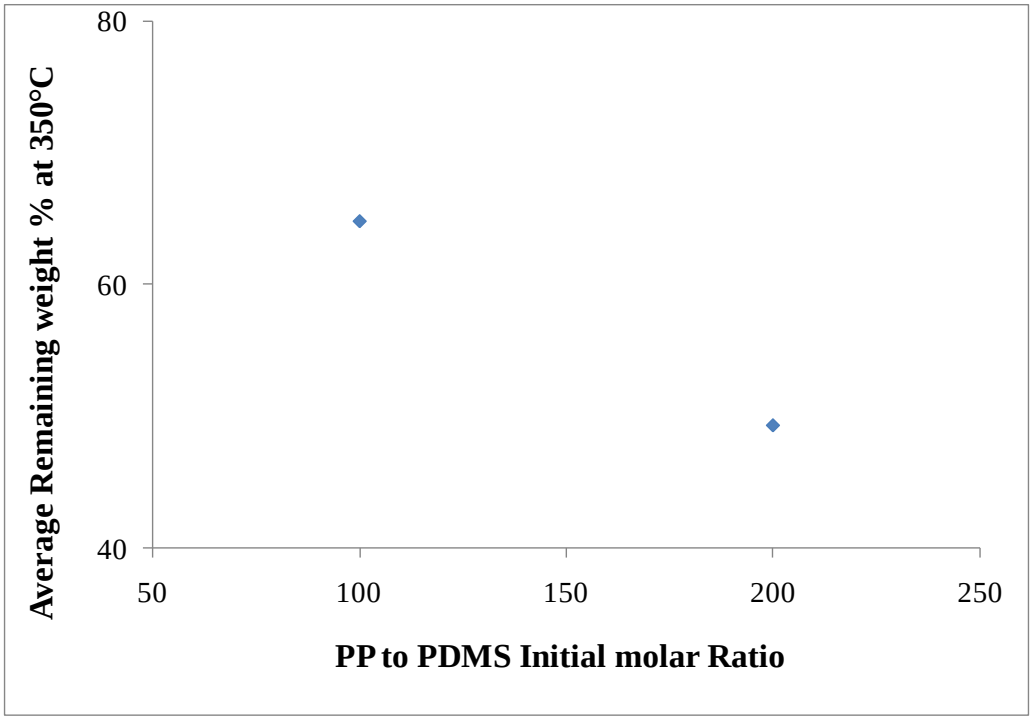

Figure 4-10: Effects of PP/PDMS molar ratio on thermal stability of copolymers

4.2.3 Analysis of Viscoelastic Properties

Since processability of materials is largely dependent on the rheological properties, dynamic mechanical measurements were performed on the product copolymers and virgin PP to study their relative flow behavior in a cone and plate rheometer. By comparing the obtained results, the influence of the PDMS component on the viscoelastic properties of PP was also investigated. All viscoelastic materials exhibit more or less solid-like (elastic) and liquid-like (viscous) properties depending on the rate at which they are deformed. This is because the strained macromolecules of viscoelastic materials tend to pull back to their original conformation when they undergo deformation [59]. The dynamic storage modulus (G') and the dynamic loss modulus (G") represent the amount of energy stored and the amount of energy dissipated respectively [61]. These properties can be measured in rheometer tests.

Experimental procedures for these studies were described in Chapter 3, section 3.4.4. Consecutive tests on the same sample at the chosen temperature (162°C) were repeatable, and this meant that there was negligible degradation of the polymer compounds during the course of all the experiments. The linear viscoelastic range for each sample was determined by a strain sweep from 1 to 100 % of strain at 1Hz. After performing strain tests for all the copolymer products, it was found that both 10% and 15% of strain were within the linear response region. Therefore, viscoelastic properties such as loss modulus (G″), storage modulus (G′) and complex viscosity (η*) for each sample were all measured using the cone and plate rheometer at 162 °C, from two sets of frequency sweeps at 10% and 15% strain.

Figure 4-11 presents the rheological responses for typical frequency sweeps of storage modulus (G') and loss modulus (G") against angular frequency, ranging from 6 to 625 rad/s. The samples used for these scans were virgin PP wax, and purified copolymers from Run 7 and 8. It was clear that slopes of loss moduli (G") curves for all the samples were much greater than those of storage moduli (G'). The values obtained from G″ curves were larger than G′ over the entire range of frequency. This indicated that the viscous component was dominant over the elastic counterpart for both copolymers and virgin PP wax. Qualitatively, the same trends were observed for all the copolymers. Moreover, as expected, it was found that as storage modulus values increased, loss modulus values decreased over the whole frequency range.

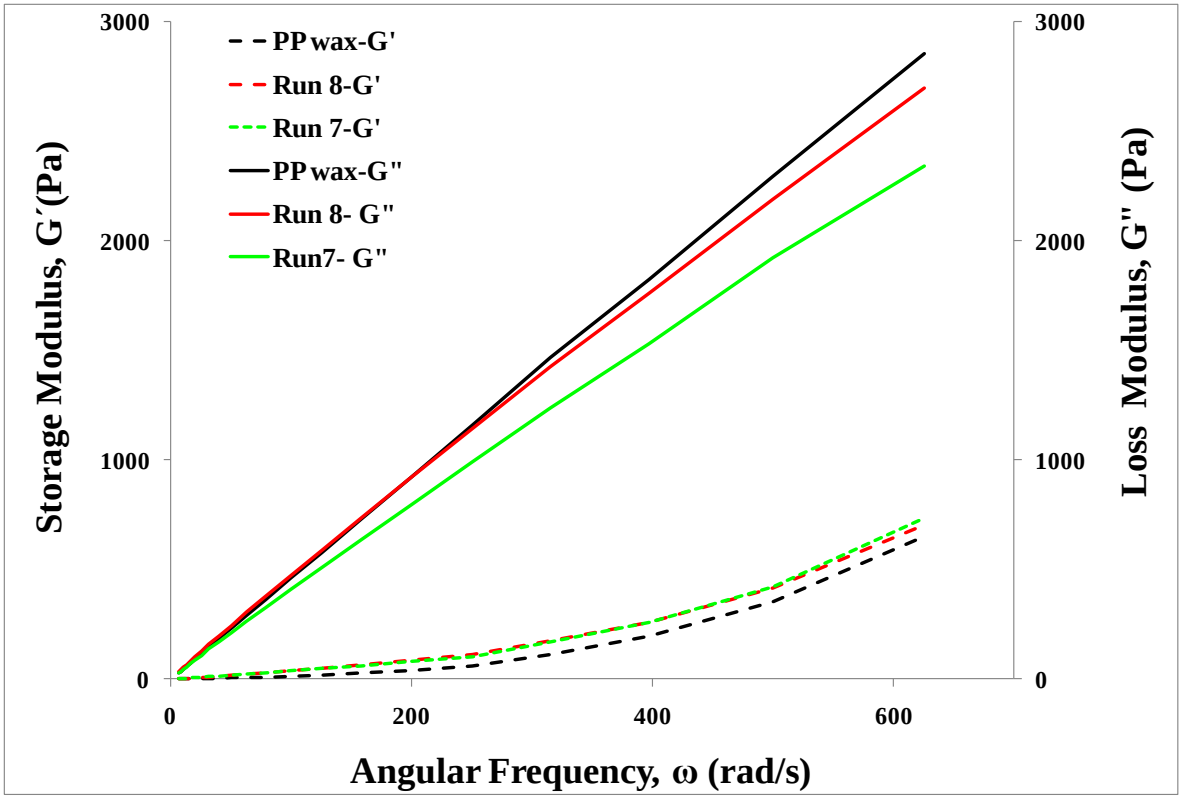

Figure 4-11: Frequency sweep for typical rheological response behavior of PP wax and PP-PDMS copolymer of Run 8 and 7 at 10% strain

Figure 4-12 and Figure 4-13 show the logarithms of frequency dependencies of G' and G" of PP wax and modified copolymer from Run 2 at 10% strain. G' values of copolymer increased as the frequency increased, which indicated that copolymer possesses higher melt elasticity, at higher frequency. It was also noted that G' values of copolymer were much higher than that of virgin PP at the lower frequency range, but very similar values were observed at higher frequency. This was because the copolymer consisted of two components: PP and PDMS, both of which can possess elasticity, and hence, they can store in more recoverable elastic energy than virgin PP. It may also be due to the formation of PP homodimers that have higher molecular weight than virgin PP wax and thus, resulted in greater elasticity in the final product. Similarly, Figure 4-13 illustrated that the loss modulus of copolymer increased with increasing frequency. Comparable trends were observed for all the other copolymers at both 10% and 15% strain (Figure 4-14 - Figure 4-15 and Figure A-0-6 - Figure A-0-7). In general, for all the copolymers, the low frequency range presented lower G' and G" values than the high frequency range. However, copolymers presented values of G' and G" that were similar to that of virgin PP at high frequency.

On the other hand, in relation to other copolymers, copolymer from Run 3 presented relatively smaller storage modulus than virgin PP wax at high frequency range. This may be the result of a poor mixing process during the reaction, and formation of higher amounts of side products such as PP homodimers, since higher temperature and lower catalyst concentration was used to carry out this experiment. Therefore, immiscible phases may

have been produced in this copolymer product and that was why its rheological properties behave distinctively from the rest of the copolymers.

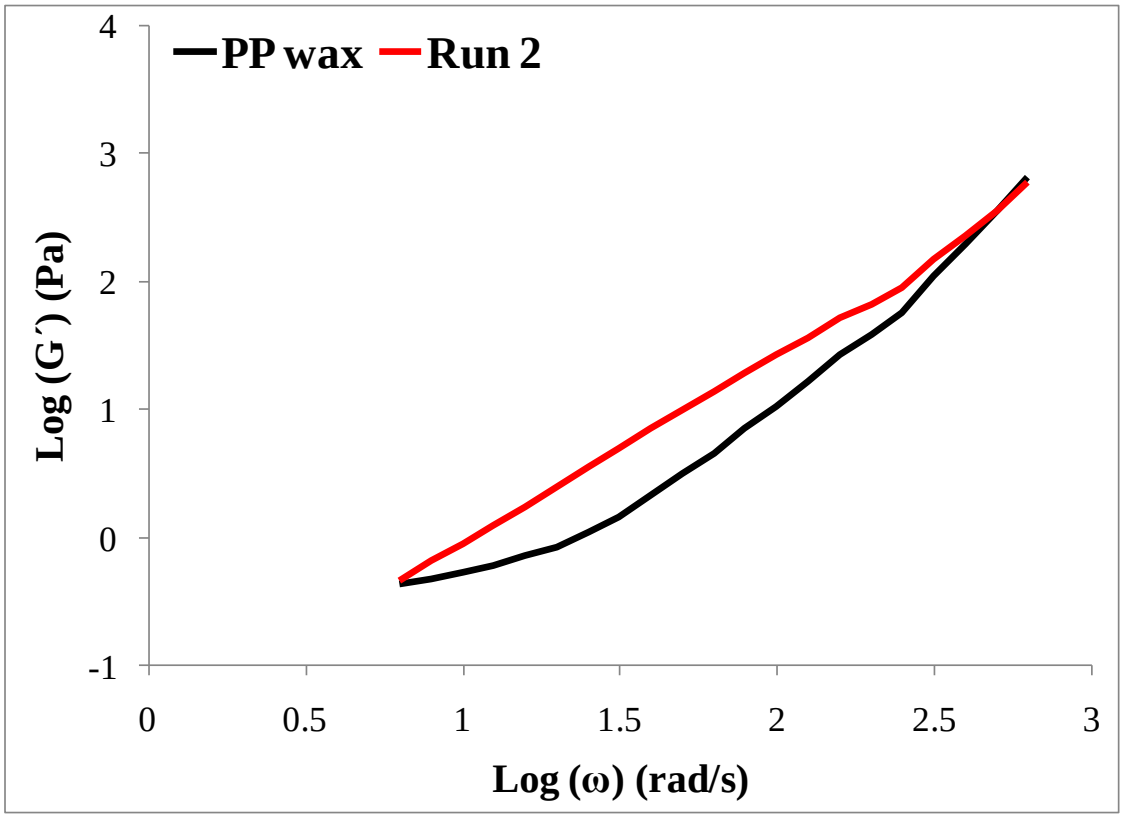

Figure 4-12: Frequency sweep for storage modulus (G′) of PP wax and purified copolymer Run 2 at 10% strain

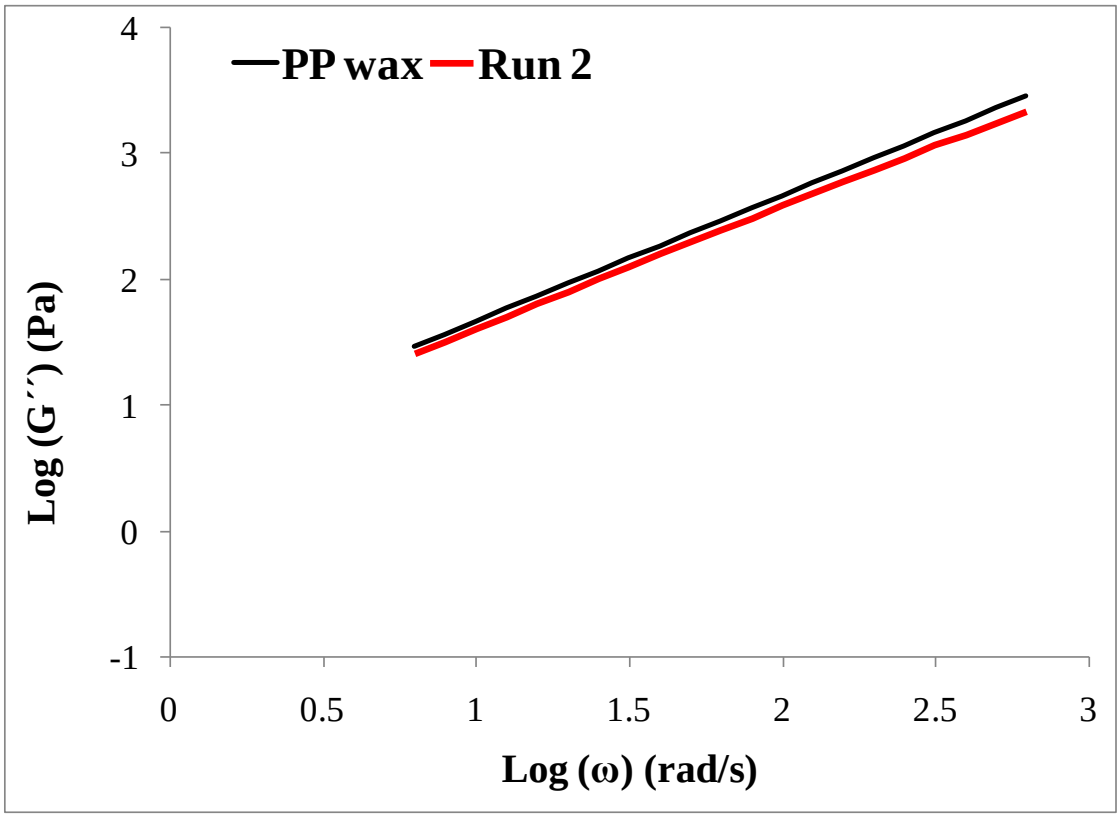

Figure 4-13: Frequency sweep of loss modulus (G″) of PP wax and purified copolymer Run 2 at 10% strain

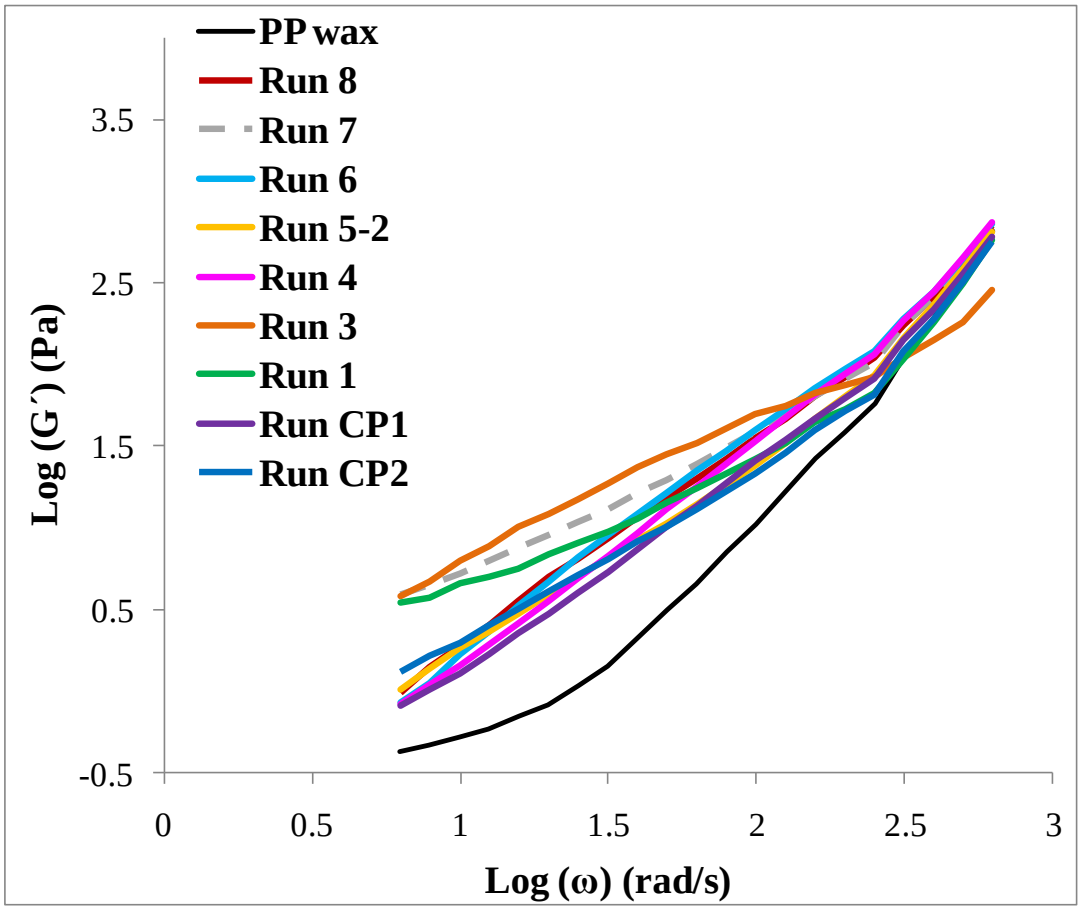

Figure 4-14: Comparison of frequency sweeps of storage moduli for PP wax and copolymers at 10% strain

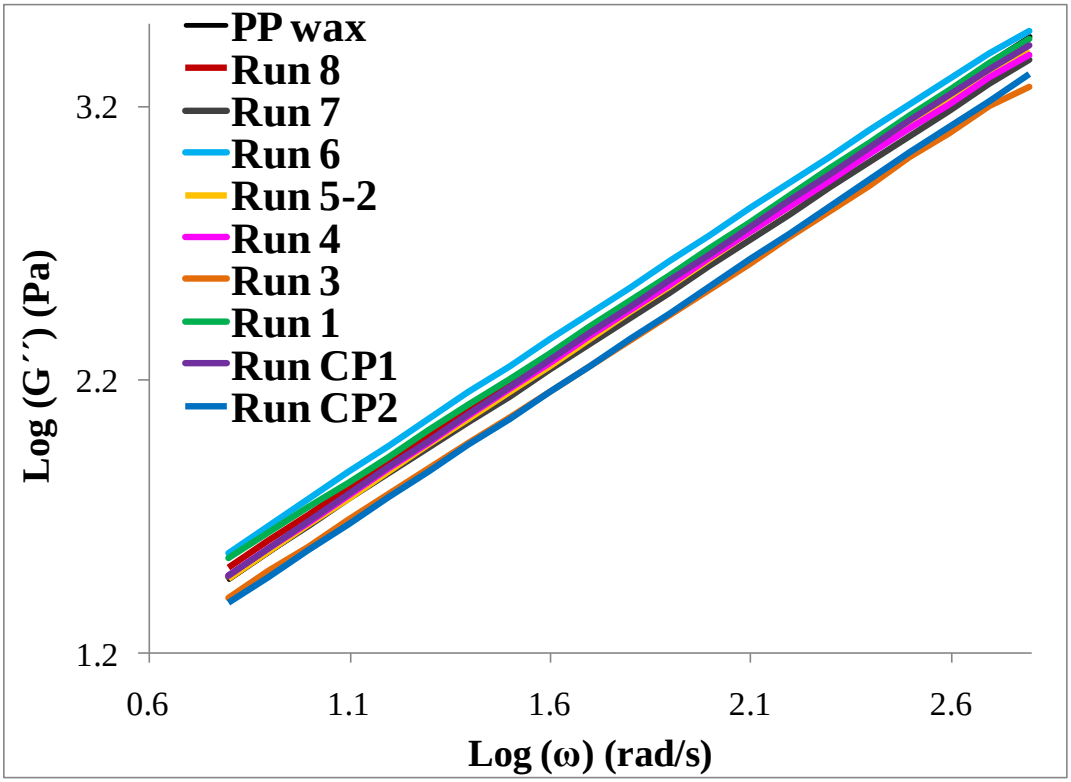

Figure 4-15: Loss moduli of PP wax and all copolymers at 10% strain

Moreover, the dependence of the logarithm of complex viscosity values (|ŋ*|) on the logarithm of frequencies, for virgin PP and all the copolymers is shown in Figure 4-16 and Figure 4-17. It was found that complex viscosity values of virgin PP were independent of frequency. In contrast, different viscosity behaviors, for the PP-PDMS copolymers at low and high frequency ranges, were observed. For example, at low frequency, the curve of log ((|ŋ*|) vs. log (ω) for copolymer from Run 2 exhibited a plateau, but its viscosity values decreased at the higher frequency range. Similar results were observed for other copolymers at both 10% and 15% strain frequency sweeps. All samples presented lower complex viscosity values at the higher frequency range than at lower frequency range (Figure 4-17 and Figure A-0-8). Although increasing in molecular weight due to the formation of copolymer and PP homodimers can lead to increase in viscosity, complex viscosities of most of the copolymers were smaller than that of virgin PP wax. This was because of the addition of the lubricating component PDMS into PP and this effect was more significant at high frequencies. Out of all the other copolymers, the sample from Run 3 displayed the lowest viscosity values. This may have resulted from a weak reaction between PP and PDMS during the polymerization, as discussed earlier. Consequently, the sample used here from Run 3 may contain unevenly distributed PDMS that causes very low viscosity.

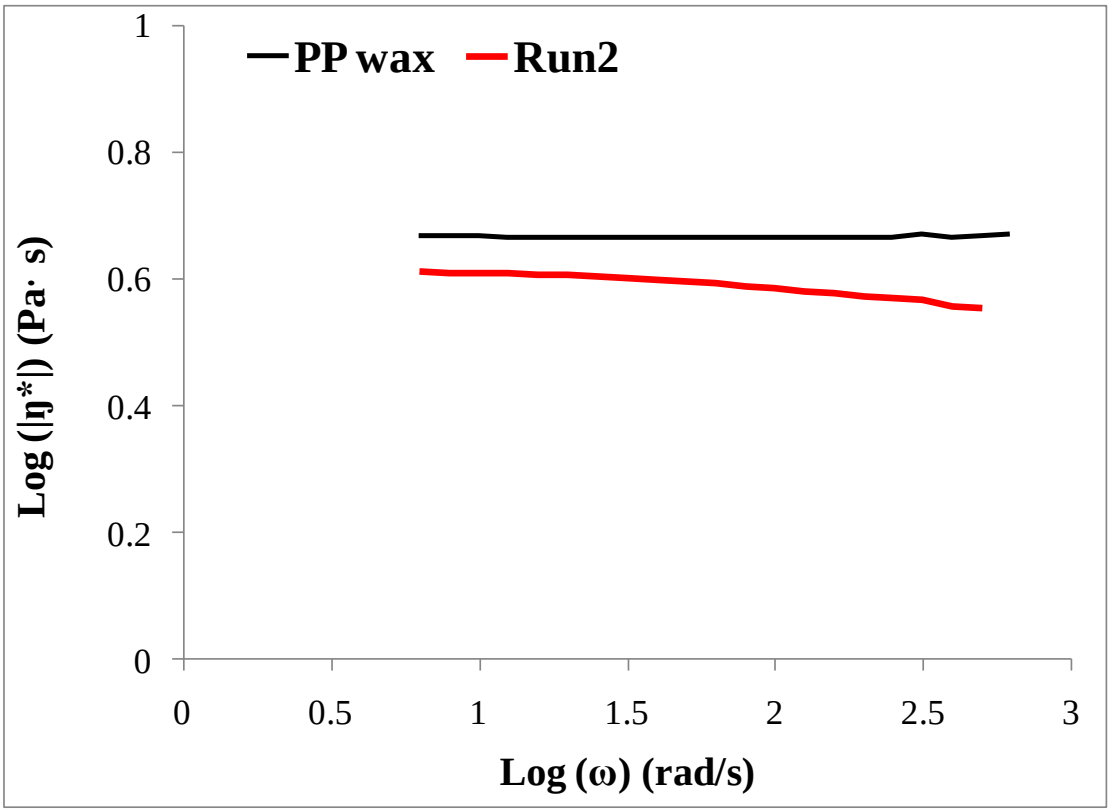

Figure 4-16: Frequency sweeps of Log ((|ŋ*|) vs. Log (ω) of product from Run 2 and PP wax at 10% strain

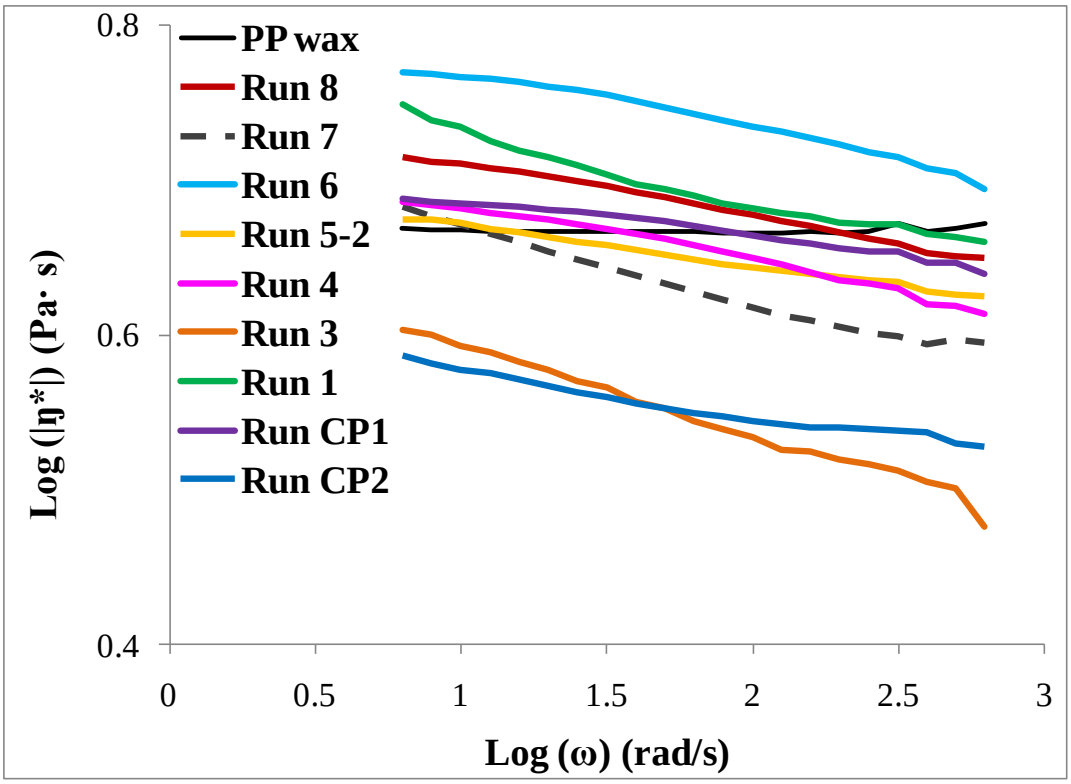

Figure 4-17: Complex viscosity of all copolymers and PP wax at 10% strain

4.2.4 SEM Studies

SEM studies were carried out to examine the morphology of virgin PP wax and copolymers. An EDX analyzer within the SEM was used to perform the estimates of elemental analysis. Figure 4-18 to Figure 4-20 show the scanning electron photomicrographs of virgin PP wax and copolymers obtained from Run 6 and Run 8. Both copolymers were synthesized at 165°C with the same PP to PDMS ratio ($\frac{PP}{PDMS} = 100$), but a higher catalyst concentration (140 mg) was used in the Run 6 experiment. Figure 4-18 displays the SEM micrograph of virgin PP wax scanned in 1000 magnification and distinct boundaries were observed. Those boundaries were the weak areas of PP and failure in polymers is normally initiated at these places [65]. The scanning electron micrographs of copolymers from Run 6 and 8 are displayed in Figure 4-19 and Figure 4-20, respectively. It is clear that PP was the discrete phase. It was apparent from the SEM-EDX analyses, that the stable droplet represents the PDMS component in the copolymers. Comparing Figure 4-19 and Figure 4-20, a finer and more homogeneous dispersion of PDMS phase was observed in the micrograph of the product from Run 6 (Figure 4-19). The observed results indicated that a more homogeneous copolymer product was synthesized in Run 6, presumably due to the addition of higher catalyst concentration. In addition, by choosing a random area of each copolymer, it was found that a similar weight amount of silicon atoms was present (Run 6: 5.5%; Run 8: 5.24%) in each sample. This result was expected since the same PP to PDMS molar ratio was applied into both experiments.

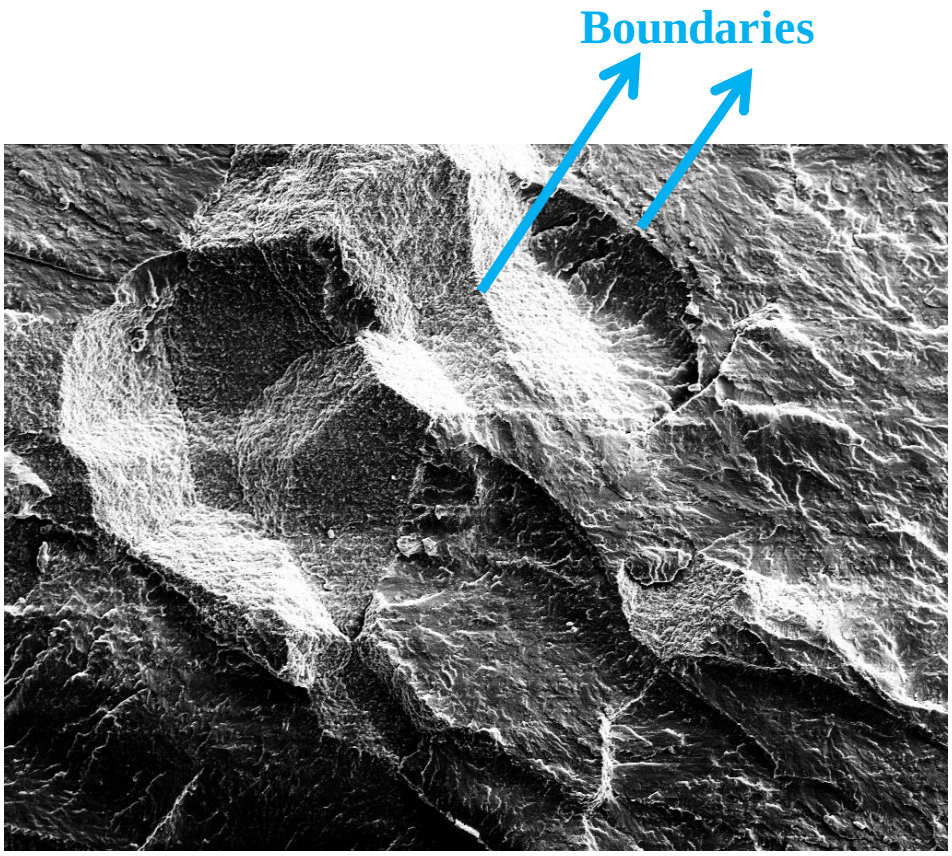

Mag = 1000, EHT =5 kV

Figure 4-18: SEM micrograph for virgin PP wax

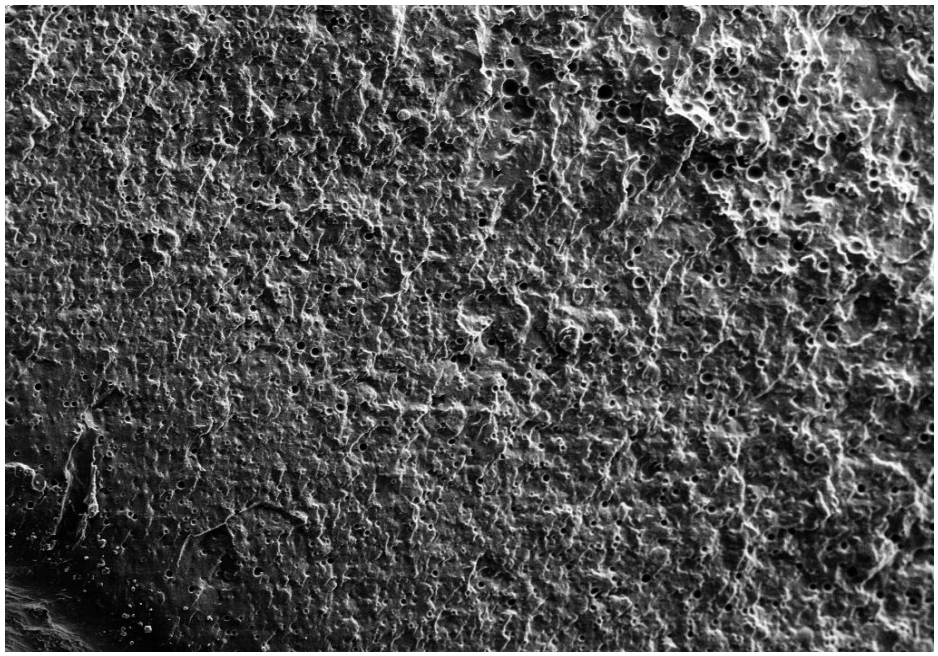

Mag = 1000, EHT =5 kV

Figure 4-19: SEM micrograph of copolymer from Run 6

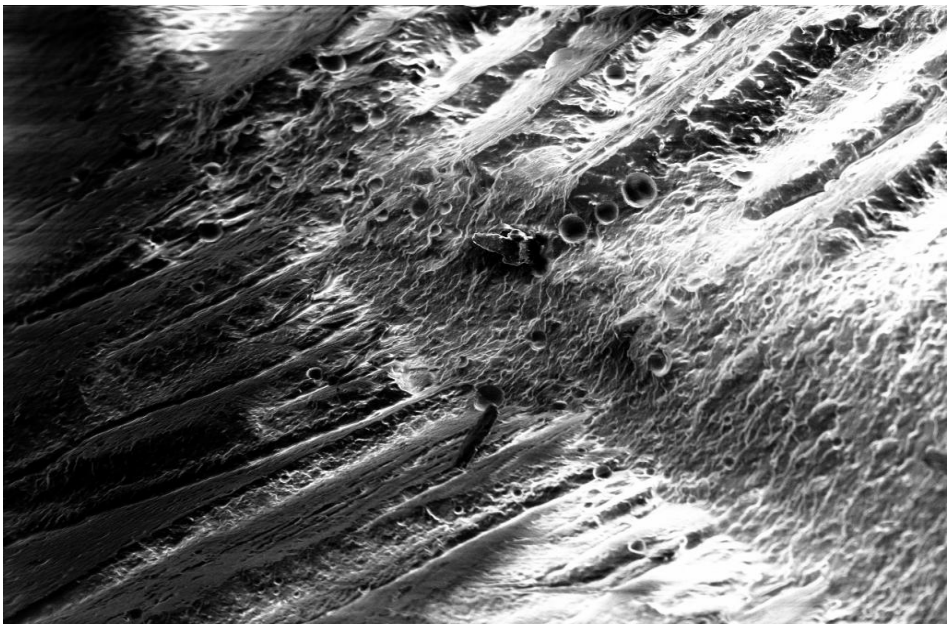

Mag = 1000, EHT =5 kV

Figure 4-20: SEM micrograph of copolymer from Run 8

4.2.5 Statistical Analysis

Analyses of variance (ANOVA) for two different responses are presented in this section. As mentioned in section 3.4.1, a 2^3 factorial design was conducted. Two physical responses, which are torque values obtained from the batch mixer and the remaining weight percentage at 350°C of each sample, were chosen for the statistical analyses and will be discussed.

4.2.5.1 Batch Mixer Torque Response

Among the most important measurements from the Haake mixer was the torque value recorded during the experiments. This value represented the instant torque of the rotors required for angular velocity to remain constant at 120 rpm. It provided information about the polymer melt inside the batch mixer chamber. Each PP-PDMS metathesis polymerization reaction was run for 30 minutes and the average torque value obtained at the last 5 minutes of every experiment was used for the ANOVA. The obtained data are tabulated in Table 4-6.

Table 4-6: Average last 5 minutes torque values in batch mixer

Factor	Temperature (°C)	PP/PDMS (mole ratio)	Torque (N·m)
Run 1	175	200	22.0
2	175	100	25.0
3	175	200	**45.6**
4	175	100	**51.4**
5	165	200	52.9
6	165	100	61.3
7	165	200	**24.5**
8	165	100	**32.0**

It is known that torque values are largely depended on temperature. In general, higher temperature should result in lower torque values since polymers melt and reach a steady state more quickly at higher temperature than at lower temperature. However, some of the torque values obtained from this study were unexpected. For instance, reaction temperatures in Runs 7 and 8 (165°C) were 10°C lower than the temperatures in Runs 3 and 4 (175°C), but lower torque values were observed from Runs 7 and 8, not 3 and 4. Furthermore, by looking at the torque profiles (Figure 4-21) of these four experiments, it was found that at the initial stage, torque values from Runs 3 and 4 were already higher than values from Runs 7 and 8. This was unreasonable since all the experiments started with the same amount of reagents; hence, the torque values at the earlier stage should only be dependent on the temperature level before addition of the catalyst. Consequently, there was little value in performing variance analysis on these torque values.

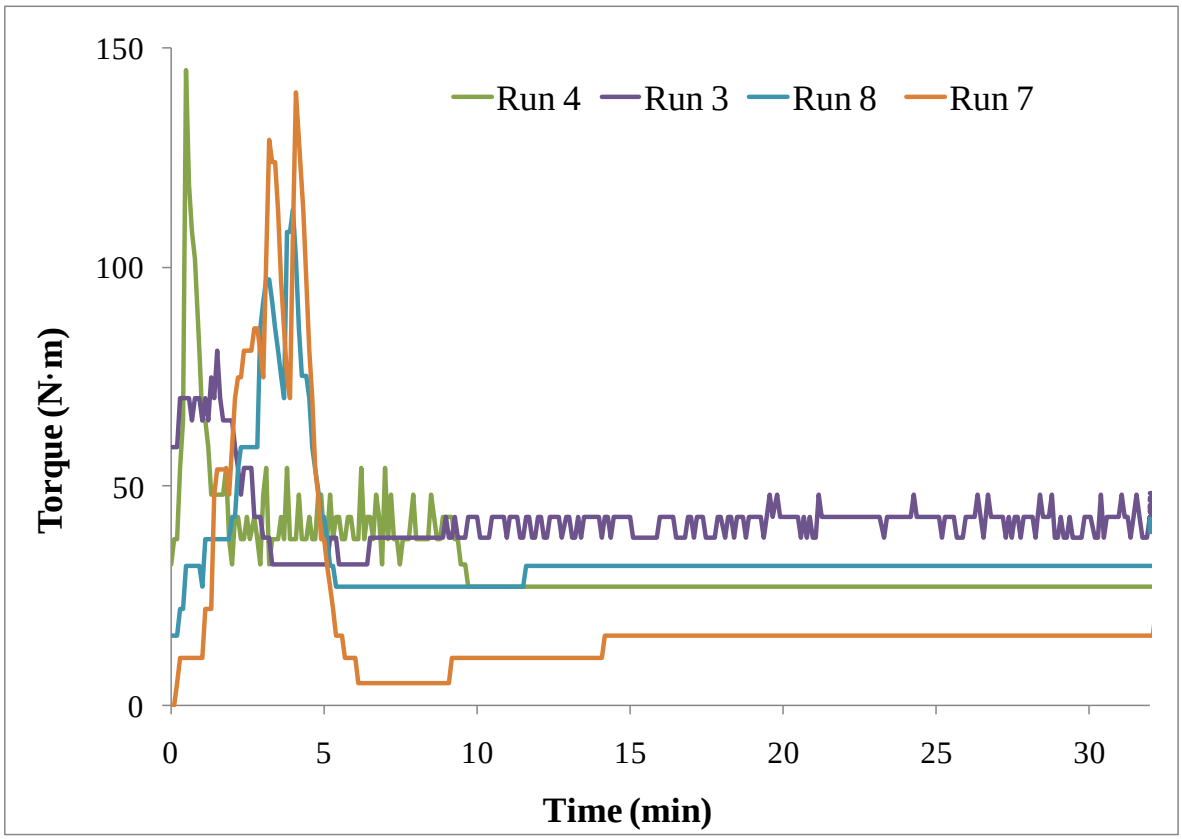

Figure 4-21: Torque response of copolymers from Run 3, 4, 7, and 8

Therefore, in order to investigate the effects of experimental factors on torque responses, variance analyses for differences in final average torque values and average torque values prior to catalyst addition were carried out. The calculated data from this analysis are summarized in the ANOVA table shown in Table 4-7. It can be seen that the calculated P-values for all the effects were larger than 0.01, which implies that none of the experimental factors played significant roles on the torque change responses. However, it was apparent that both temperature and molar ratios affected the final torque values based on the data from Table 4-6. Therefore, non-significant experimental effects observed in Table 4-7 may be due to the torque values which were too low and not sensitive enough to differentiate the effects between main experimental factors and their interactions.

Table 4-7: ANOVA table for differences in torque values

Source of Variance	Effect	SS	DF	MS	F	P-value
Main Effects						
Temperature (T)	-1.325	3.51125	1	3.51125	2.19	0.21340
Catalyst (C)	-1.925	7.41125	1	7.41125	4.61	0.09823
Mole Ratio (M)	0.975	1.90125	1	1.90125	1.18	0.33783
Interactions:						
TxC	3.425	23.4613	1	23.4613	14.60	0.01876
TxM	0.125	0.03125	1	0.03125	0.02	0.89582
CxM	0.625	0.78125	1	0.78125	0.49	0.52401
TxCxM	1.275	3.25125	1	3.25125	2.02	0.22795
Error				1.61		
Total		40.35				

Where SS = sum of squares, DF = degree of freedom, MS = mean squares, F = variance ratio, p = probability.

4.2.5.2 TGA Response

Thermal gravimetric analysis (TGA) was used to determine thermal stability for each copolymer and the data obtained was summarized in section 4.2.2.The tabulated data output from an ANOVA table is shown in Table 4-8, and from this, the effect of experimental factors, and interactions between experimental factors on the thermal stability of copolymers was determined.

Table 4-8: ANOVA table for TGA response of experimental factors on remaining weight % (RW%) at 350°C

Source of Variance	Effect	SS	DF	MS	F	p
Main Effects:						
Temperature (T)	-8.6025	148.0060	1	148.0060	16.4962	0.01533
Catalyst (C)	-4.3375	37.6278	1	37.6278	4.1939	0.10995
Mole Ratio (M)	-15.488	479.7250	1	479.7250	53.4685	0.00186
Interactions:						
TxC	13.0775	342.0420	1	342.0420	38.1228	0.00349
TxM	3.1975	20.4480	1	20.4480	2.27906	0.20564
CxM	1.0925	2.38711	1	2.38711	0.26606	0.26606
TxCxM	1.6775	5.62801	1	5.62801	0.62728	0.47268
Error			4	8.97212		
Total		1035.86	13			

Where SS = sum of squares, DF = degree of freedom, MS = mean squares, F = variance ratio, p = probability.

It was observed that the main factors that affected thermal stability of the modified PP were reaction temperature (T), PP to PDMS molar ratio (M) and interactions between temperature and catalyst (TxC). Using the calculated coefficients, the model used to describe the relationship between remaining weight percentage and significant main and interaction effects is shown in Equation (4-1)

$$\boldsymbol{RW\% = 57.1013 - 4.3013 \times T - 7.7438 \times M + 6.5388 \times T \times C} \quad (4\text{-}1)$$

However, since the interaction effect of TxC was included in this model, the main effect C needed to be taken into account in order to make this model hierarchical. The resulting model is thus:

$$\boldsymbol{RW\% = 57.1013 - 4.3013 \times T - 2.1687 \times C - 7.7438 \times M + 6.5388 \times T \times C} \quad (4\text{-}2)$$

This equation indicated that thermal stability of copolymers at 350°C increases with smaller PP to PDMS molar ratio and lower temperature. The effect of molar ratio was expected since the smaller the PP to PDMS molar ratio, more PDMS component can be incorporated onto PP during the polymerization; hence, greater thermal stability can be obtained. In addition, if the catalyst reactivity was greater at lower temperature than at higher temperature, it is reasonable to obtain better incorporation between PP and PDMS and get higher thermal stability for copolymers when a lower reaction temperature was used.

The main and interaction effects between experimental factors could also be interpreted from the graphs shown in Figure 4-22 to 4-27. It is known that non-significant main effects would plot as a nearly horizontal straight line, and non-significant interactions result as almost parallel plots. As seen in Figure 4-22 to Figure 4-24, it was found that plots for temperature and molar ratio main effects had much steeper slopes than the one in the catalyst main effect plot.

Similar conclusions can be drawn, with increasing temperature and molar ratio, as thermal stability at 350°C decreased significantly. It is known that at higher reaction temperature, some degradation of PP was possible; and so overall thermal stability of copolymers could be reduced because of that. Moreover, thermal stability of copolymers was also affected by the catalyst amount, which gives relatively lower thermal stability when higher amount of catalyst was used. This may be due to the presence of heavy metals that could lead to accelerated degradation of polymers; in this case, more catalyst could lead to lower thermal stability. On the other hand, significant interactions between temperature and catalyst were observed by the crossing of plots in Figure 4-25. When the reaction temperature was at 165°C, higher thermal stability was evidenced when 60 mg of catalyst was used. When reaction temperature was at 175°C, the reverse was true.

Furthermore, a normal probability plot (presented in Figure 4-28) of all 7 effects was generated to determine if the interaction effect between T and C was real. It was seen that the TxC interaction effect significantly deviates from the line seen in Figure 4-28; hence, the interaction effect between temperature and catalyst was confirmed to be true and significantly affecting the TGA responses.

Therefore, using a 2^3 factorial design coupled with statistical analysis of the main effects and interactions of experimental factors, the optimal experimental conditions for synthesizing PP-PDMS copolymers in melt phase could be determined for different desired responses.

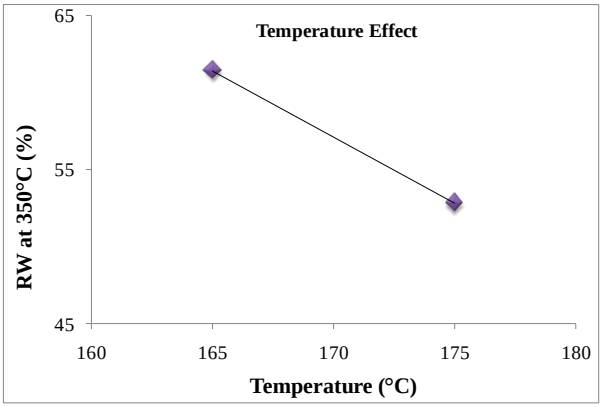

Figure 4-22: Effect of temperature on RW% at 350°C

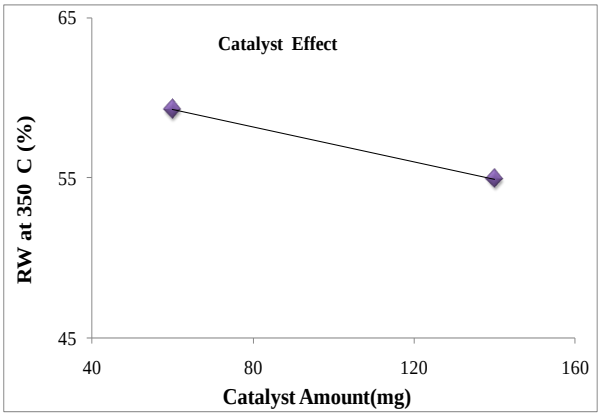

Figure 4-23: Effect of catalyst amount on RW% at 350°C

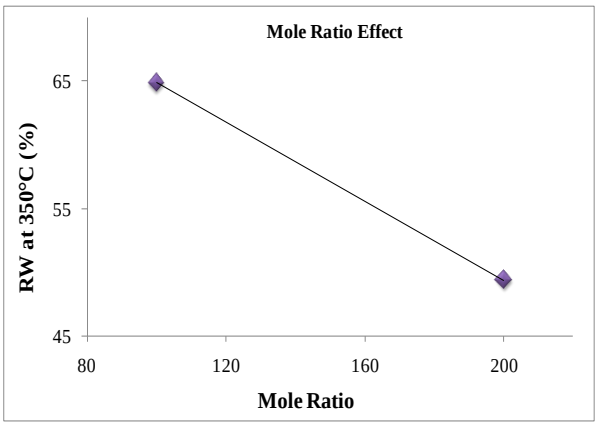

Figure 4-24: Mole ratio main effect on RW% at 350°C

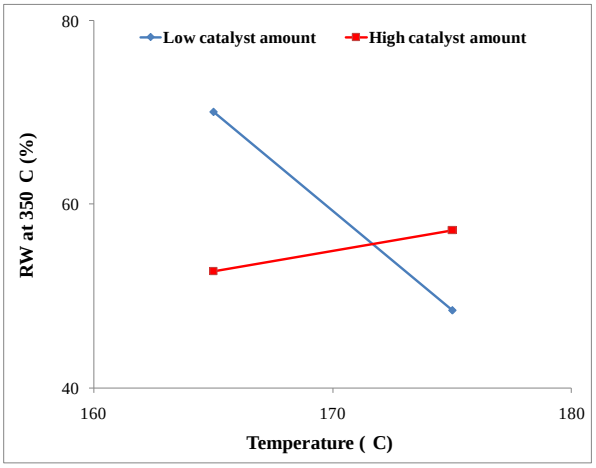

Figure 4-25: TxC interaction effect on RW% at 350°C

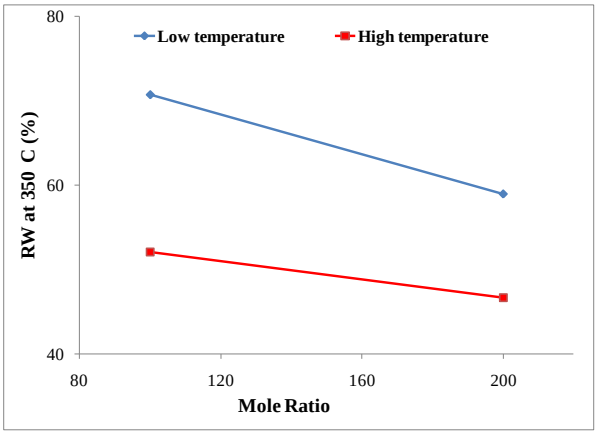

Figure 4-26: TxM interaction effect on RW% at 350°C

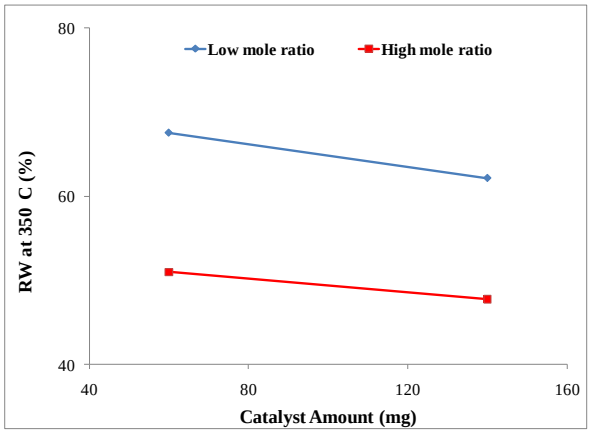

Figure 4-27: CxM interaction effect on RW at 350°C

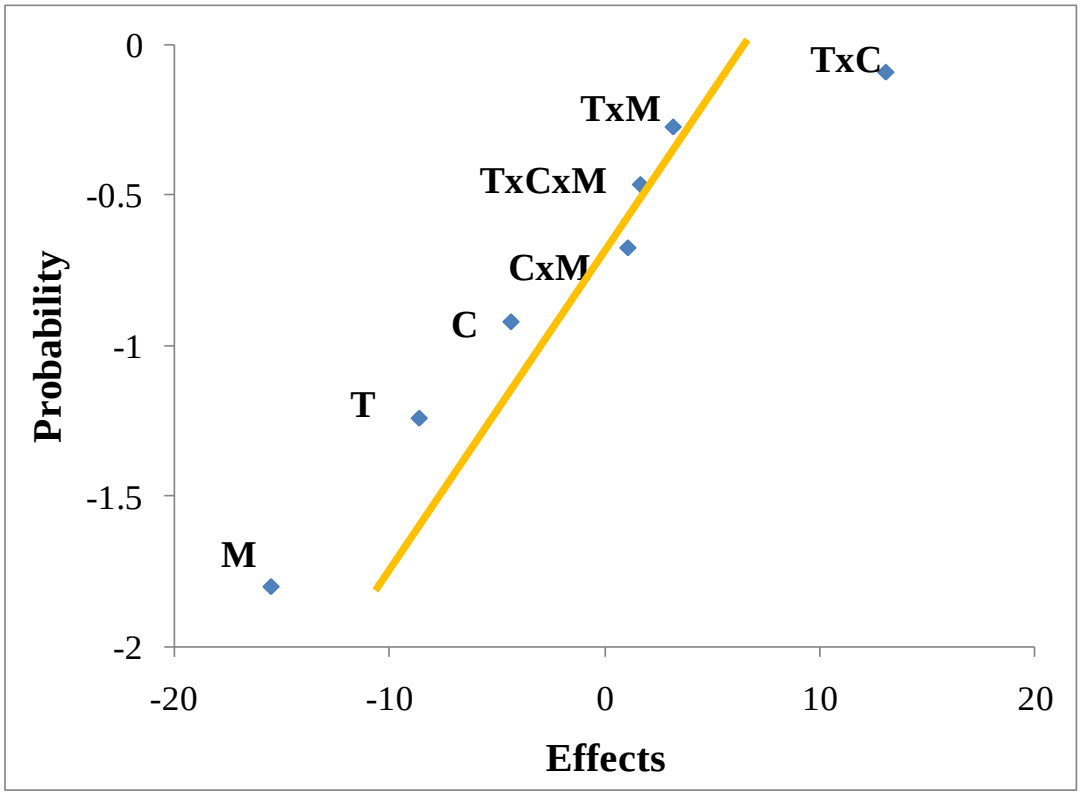

Figure 4-28: Normal probability plot for all effects on thermal stability

Chapter 5 Conclusions and Recommendations

5.1 Conclusions

The objective of this project was to show that PP could be modified by using cross metathesis in the melt phase. The modification was to incorporate PDMS units and this was done by cross metathesis using a vinyl terminated PDMS to react with vinylidene terminated PP. A 2^3 factorial design was conducted in a series of experiments to determine and quantify the relationship among experimental factors (temperature, catalyst concentration, $\frac{PP}{PDMS}$ mole ratio) and their main effects and interaction effects were also observed.

Chemical composition of purified copolymers was determined from high temperature NMR, which confirmed the presence of PDMS and the feasibility of CM reaction in the melt phase of high temperature. The analyses also showed that the initial and final $\frac{PP}{PDMS}$ ratio was quite similar, which indicated that both reagents PP and PMDS were almost exclusively reacted during the modification process.

Thermal and rheological properties of modified PP copolymers were also characterized. DSC analysis demonstrated that temperatures for the melting peaks of the copolymers in the range from 150°C to 160°C, were almost the same as the ones observed for virgin PP wax. However, addition of PDMS significantly influenced the crystalline PP phase in copolymers, and associated heating enthalpies of copolymers' melting points were smaller than those for virgin PP. In addition, DSC melting profiles also proved the presence of PDMS in copolymers by observing the glass transition at around -120°C and double melting peaks in the range from -50°C to -40°C.

Weight loss behavior of copolymers related to temperature was determined from TGA analysis in air and nitrogen. When TGA tests were carried out in air, large differences in thermal degradation temperatures between virgin PP and copolymers were observed. On the contrary, insignificant differences were found in thermal degradation temperatures of virgin PP and copolymers when tests were performed in nitrogen atmosphere. Furthermore, the determined weight loss of each sample at 350°C and 450°C showed that higher thermal stability was attained for the copolymers. It is expected that more PDMS content (or lower $\frac{PP}{PDMS}$ mole ratio) added into the reaction should give higher thermal stability of copolymers.

In rheometric studies, results obtained from frequency sweeps indicated that the viscous component of all copolymers and PP wax is dominant over the elastic component. It was observed that storage moduli (G') increased and loss moduli (G") decreased as frequency increased, for all materials studied. This result was expected since viscous PDMS was added into the copolymers, which reduced the G" and complex viscosity values. Furthermore, synthesis of block copolymers (PP-PDMS) allowed them to possess higher storage modulus than virgin PP wax because both PP and PDMS components can store elastic energy. Complex viscosities of copolymers were also determined. As with the loss moduli, the measured viscosities of copolymers decreased as frequency increased. Due to the lubricating properties of PDMS, copolymers had lower complex viscosity values than virgin PP at the high frequency range.

Dependence of average torque values on experimental factors and their interactions were studied through an analysis of variance (ANOVA). It was shown that temperature had the most significant main effect on torque and higher temperature resulted in lower torque

values. This was because PP can be easily melted at higher temperature; therefore, less energy was required to maintain a constant rotating speed of rotors. Moreover, variations of thermal stability of copolymers were also investigated. According to ANOVA results, it was found that when lower $\frac{PP}{PDMS}$ molar ratio was applied, thermal stability increased due to increase of PDMS content, which was to be expected because PDMS is widely known for its high stability at high temperature.

In summary, PP-PDMS copolymers were successfully synthesized by an olefin metathesis reaction using unconventional experimental condition, i.e., melt phase at elevated temperatures. In terms of the reaction products, polymers were made that had higher elasticity and lower viscosity than virgin PP wax.

5.2 Future Work Recommendations

The factorial design results showed some apparent anomalies in the values obtained for certain measurements with varying factors. The most notable was the torque values for runs 3 and 4 as compared to those for runs 7 and 8. These followed a trend that was opposite to what was expected by normal physical behavior of polymers with respect to temperature. For example, the torque values were lower for the runs of the lower temperature. Therefore, it is recommended that in the future studies, all the designed experiments should be replicated in order to generate a fully replicated 2^3 factorial design. The purpose of performing replications is to see if these torque values mentioned above were simply within the normal

range of uncertainty expected for these types of mixes at these temperatures or if they were indeed anomalous results that should be treated as outliers.

In addition, NMR results also showed a degree of variation that was unreasonably high with respect to the determination of the amounts of remaining double bonds in PP. For instance, the results obtained from run 7 (see Table 4-2) showed that after 5 min there was a considerable reduction in vinylidene content. Yet the result for the product at 30 min showed very little drop in residual vinylidene content. Given the mechanism of metathesis, this result could not be possible. It could however, be explained if the PP to PDMS reaction mixture was not homogeneous. In the current work, PP to vinylidene group molar ratio obtained from NMR results was comparable to that of previous studies using FTIR technique. Hence, one can also apply FTIR calibration method in the future to determine the amount of vinylidene group that has been consumed in the polymerization process, by relating its concentration to the absorbance at 888 cm^{-1}.

In this study, only one type of PP and one type of PDMS was considered, as a screening study. There are many types of these materials (i.e., with different MW) and so the study should be extended to see how general good the process is for a range of different PP resins and PDMS fluids. In addition to the above, since we have proved the effectiveness of the metathesis reactions at these harsh experimental conditions, we can extend these studies to look at the same reaction for other polyolefins with terminated vinyl groups such as polyethylene (PE) and polybutadiene (PB). Elastic materials such as EPDM (ethylene-propylene-diene copolymer) and SBR (styrene-butadiene rubber), which contain double

bonds, can also be used to react with PP, PB or PE to provide compatabilizers and process additives for plastic or rubber blends.

Synthesis of copolymers in this project was carried out in a batch mixer. Since PP and PDMS are highly incompatible, the reaction time for each CM polymerization in a batch mixer was set at 30 minutes to obtain a better mixing. However, at such long experimental reaction time, it was likely that the catalyst degraded under the conditions chosen. This is indicated by certain NMR and torque results. Therefore, in order to achieve optimal reaction of compounds, superior mixing is required. This could be achieved by synthesizing copolymers in an extruder, which can not only give better mixing, but also take less reaction time (around 10 min) compared to the reaction time in the batch mixer (30 min).

Appendix

Calculations for $\frac{PP}{PDMS}$ and $\frac{PP}{Vinylidene}$ from 1H-NMR spectra

Example: use copolymer from Run 6, final product obtained after 30 minutes of reaction

- Both PP wax and PDMS have 6 protons on their repeating units. PP has two vinylidene protons.
- Molecular weight of PP repeating unit = 42 g/mol,
- Molecular weight of PDMS repeating unit = 72 g/mol
- Figure A-0-1 is the MR spectrum of purified copolymer Run 6, the product obtained after 30 mins reaction in batch mixer.
- The sharp peak near 0.0 ppm represents the methyl protons attached to silicon atoms
- The multiple peaks from 0.5 to 1.9 ppm indicate protons in PP repeating units
- The presence of vinylidene protons was confirmed by the observation of double peaks at 4.6 and 4.7 ppm.

$$\frac{\boldsymbol{PP}}{\boldsymbol{PDMS}} = \frac{Integral\ of\ PP\ repeating\ unit \times MW\ of\ PP\ repeating\ unit \times 6\ protons}{Integral\ of\ PDMS\ repeating \times MW\ of\ PDMS\ repeating\ unit \times 6\ protons}$$

$$= \frac{1667.39\ \times 42 \times 6}{124.44 \times 72 \times 6} = \ 7.8$$

$$\frac{\boldsymbol{PP}}{\boldsymbol{Vinylidene}} = \frac{Integral\ of\ PP\ repeating\ unit \times 2protons}{Integral\ of\ vinylidene\ protons \times 6\ protons}$$

$$= \frac{1667.39\ \times 2}{(0.99 + 0.67) \times 6} = \ \ 334.82$$

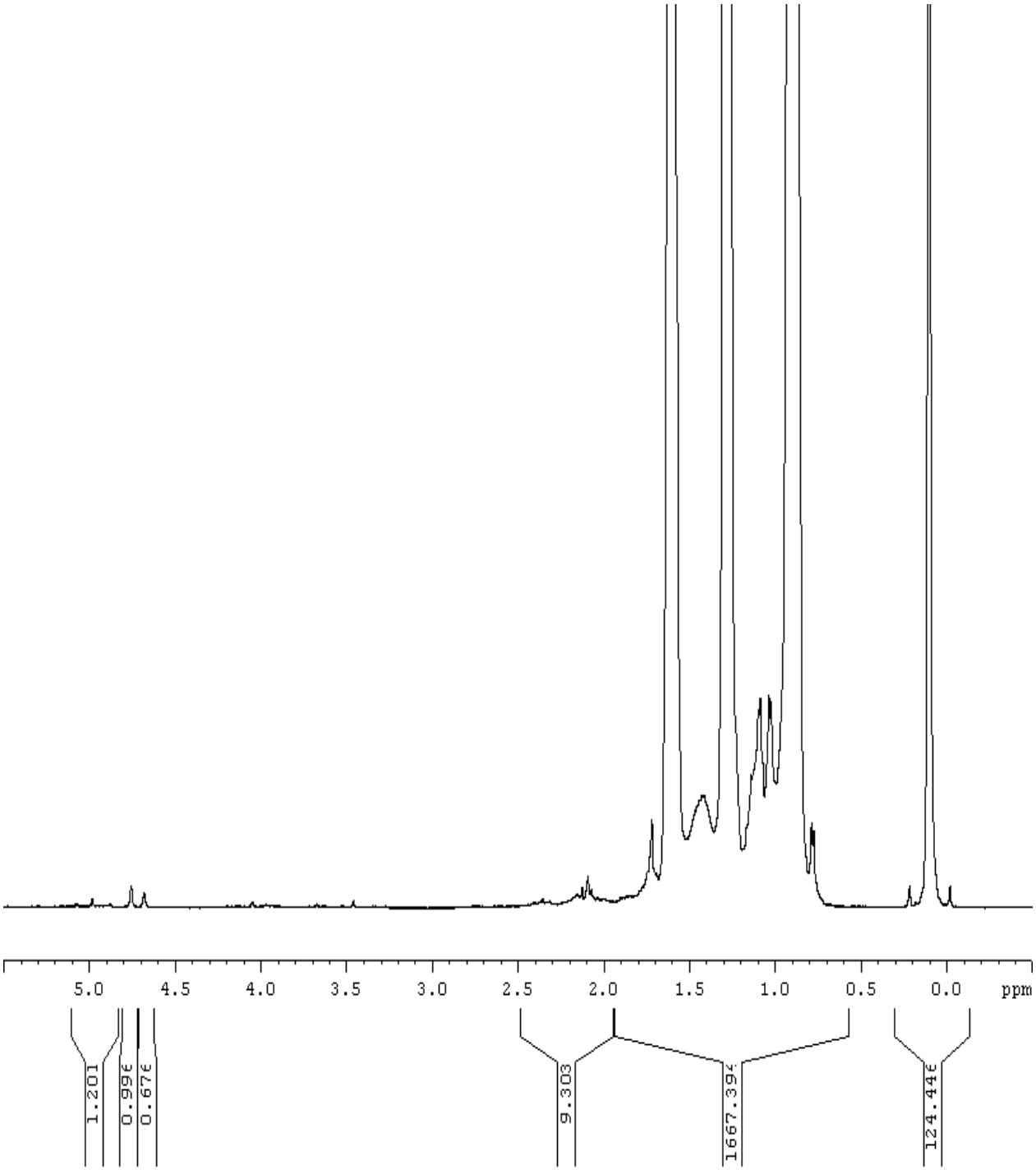

Figure A-0-1: NMR spectrum of copolymer Run 6 at 30 mins, TCE solvent, 120°C

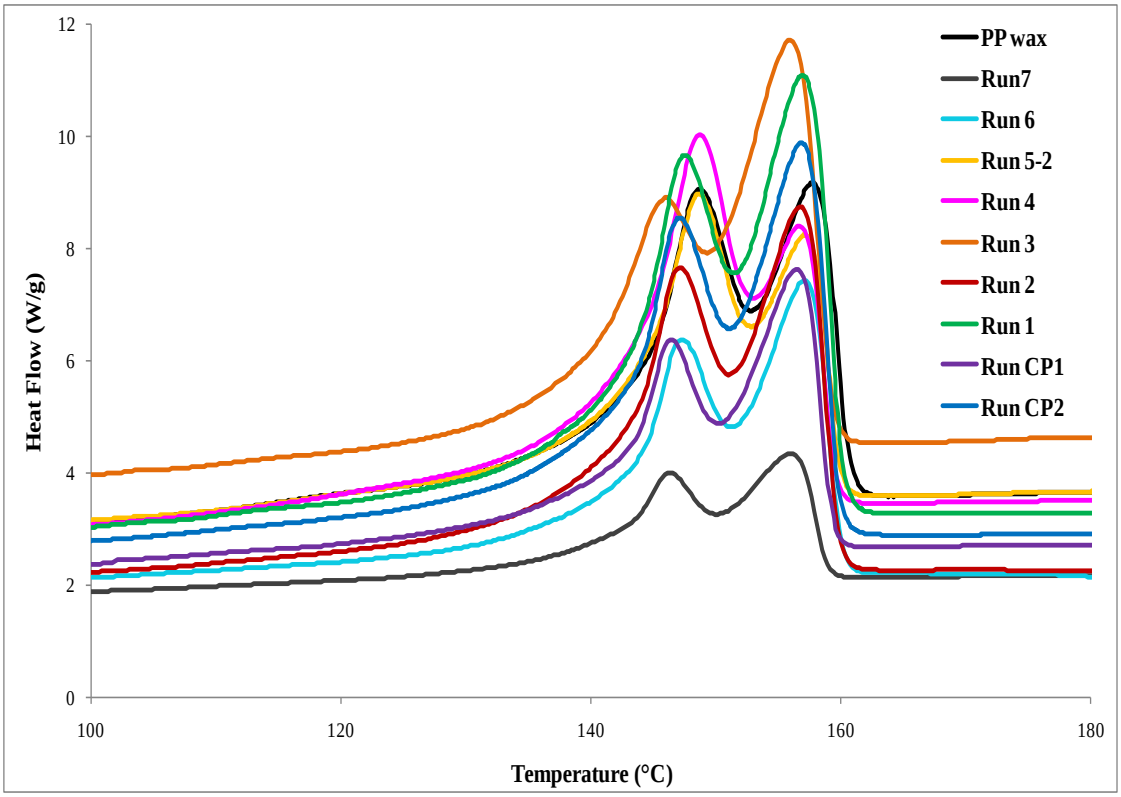

Figure A-0-2: DSC thermograms of PP wax and copolymers from 100°C to 180°C

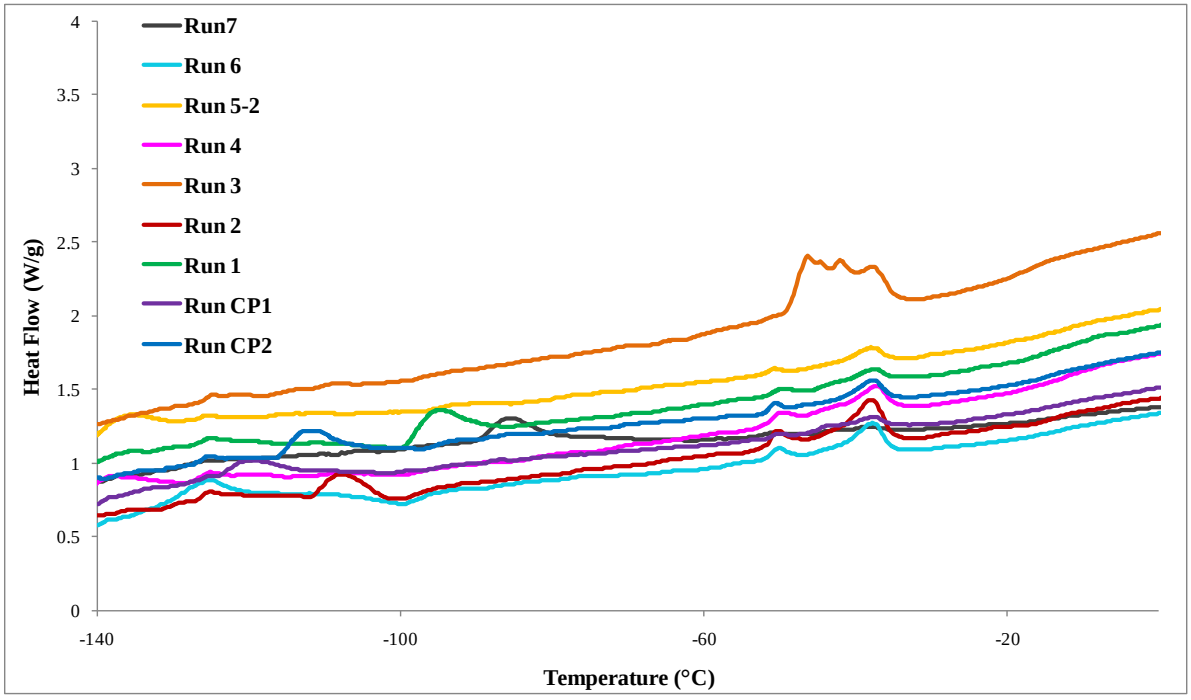

Figure A-0-3: DSC thermograms of copolymers from -140°C to 0°C

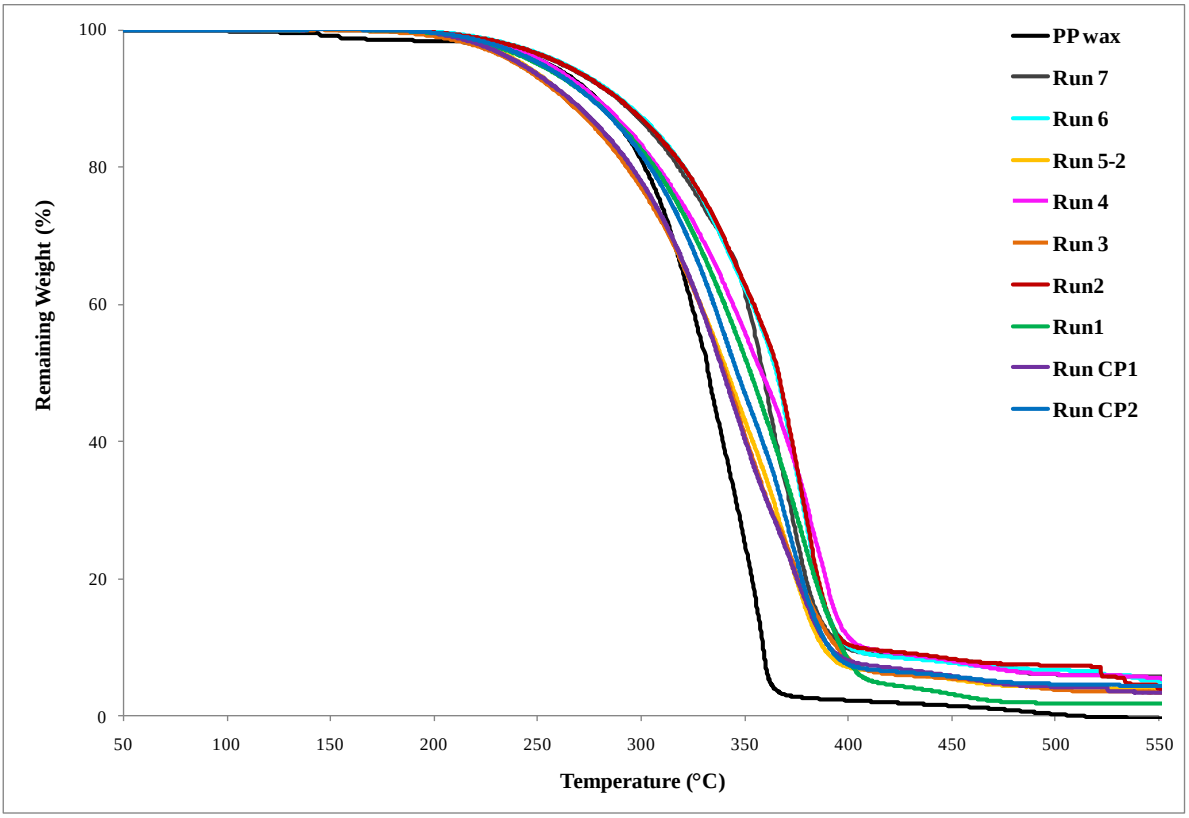

Figure A-0-4: TGA curves of copolymers from 50°C to 550°C in air

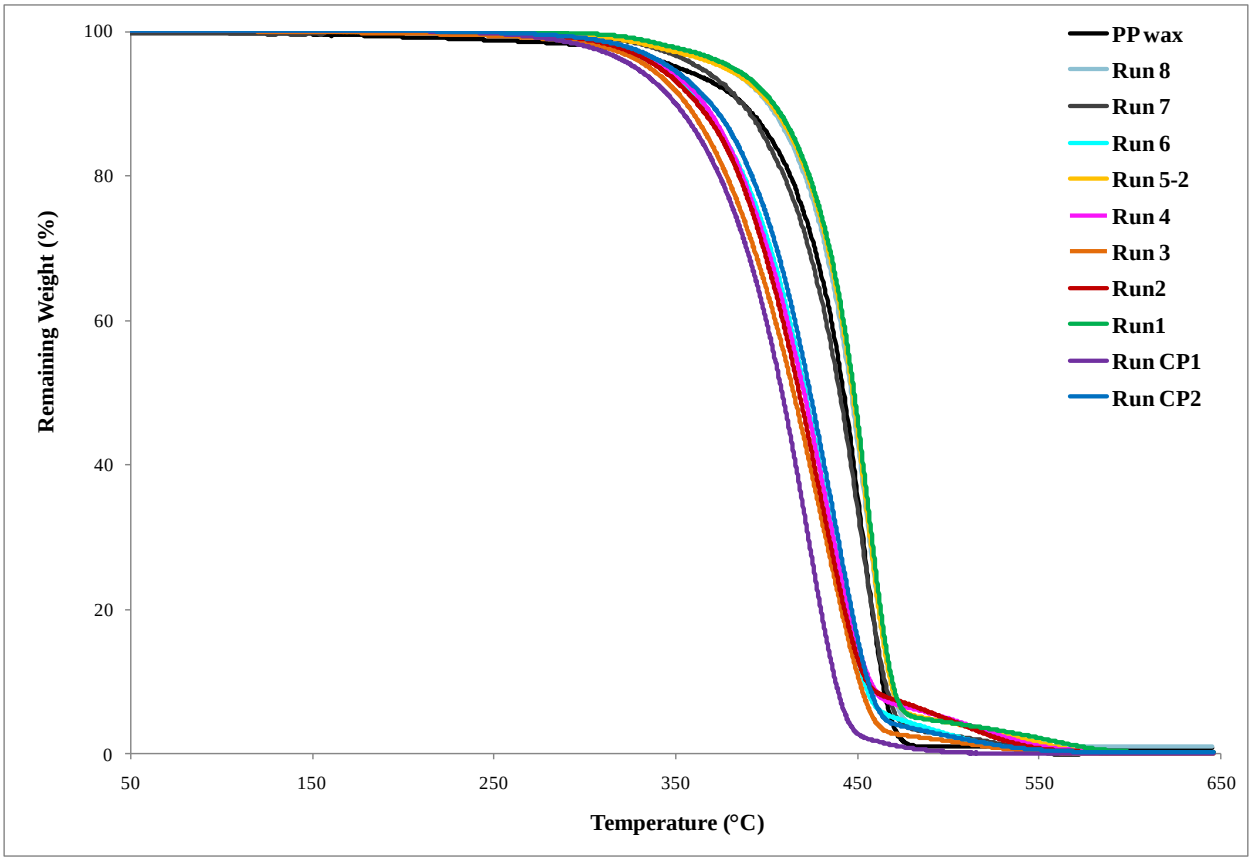

Figure A-0-5: TGA curves of copolymers from 50°C to 550°C in N_2

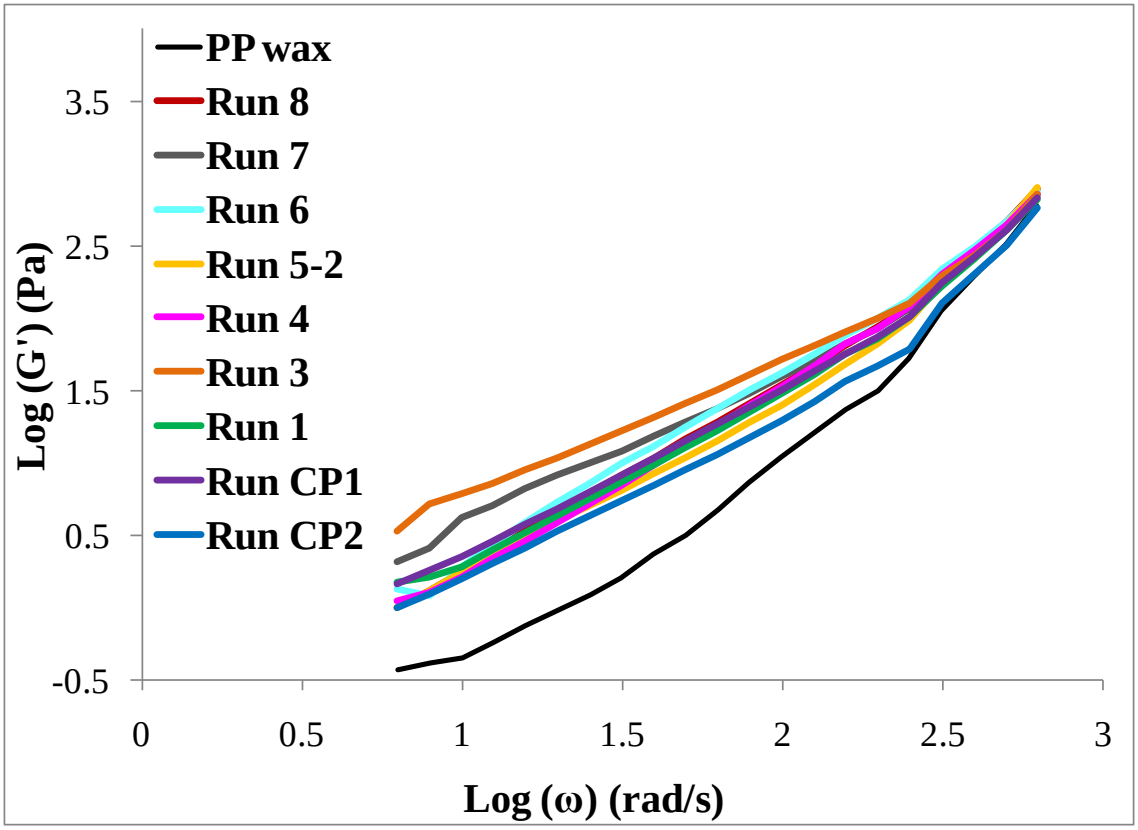

Figure A-0-6: Elastic modulus of PP wax and copolymers at 15% strain

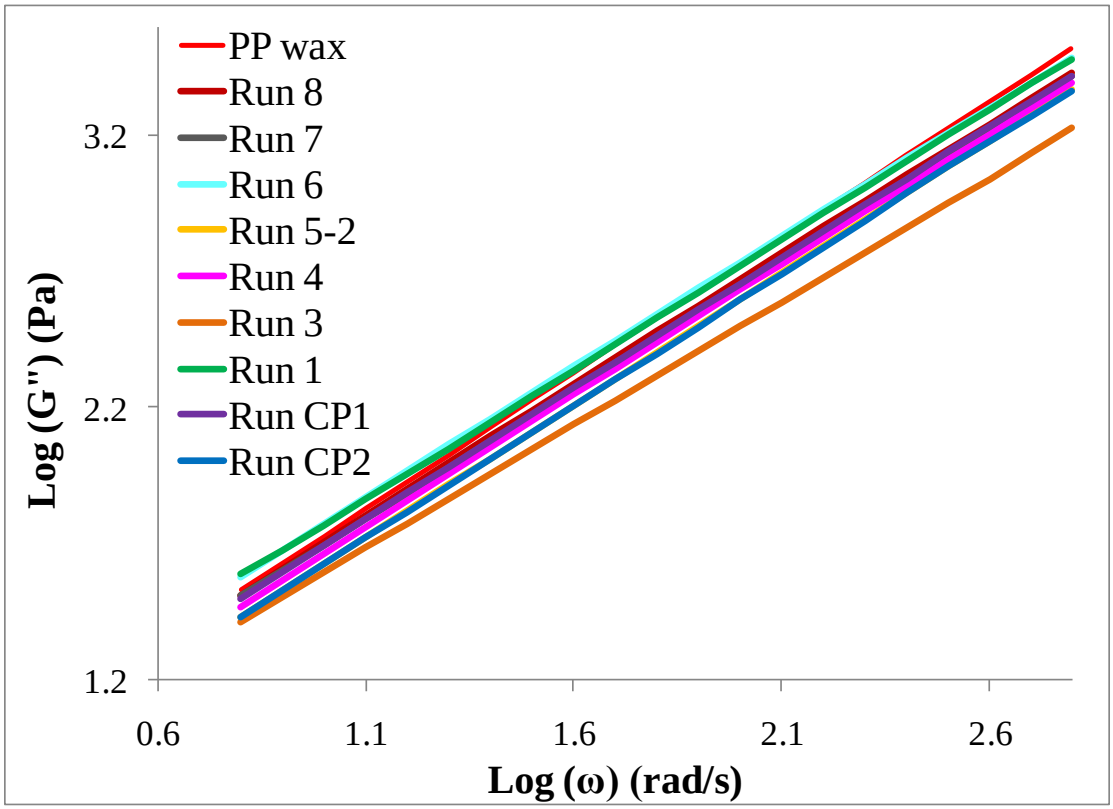

Figure A-0-7: Viscous modulus of PP wax and copolymers at 15% strain

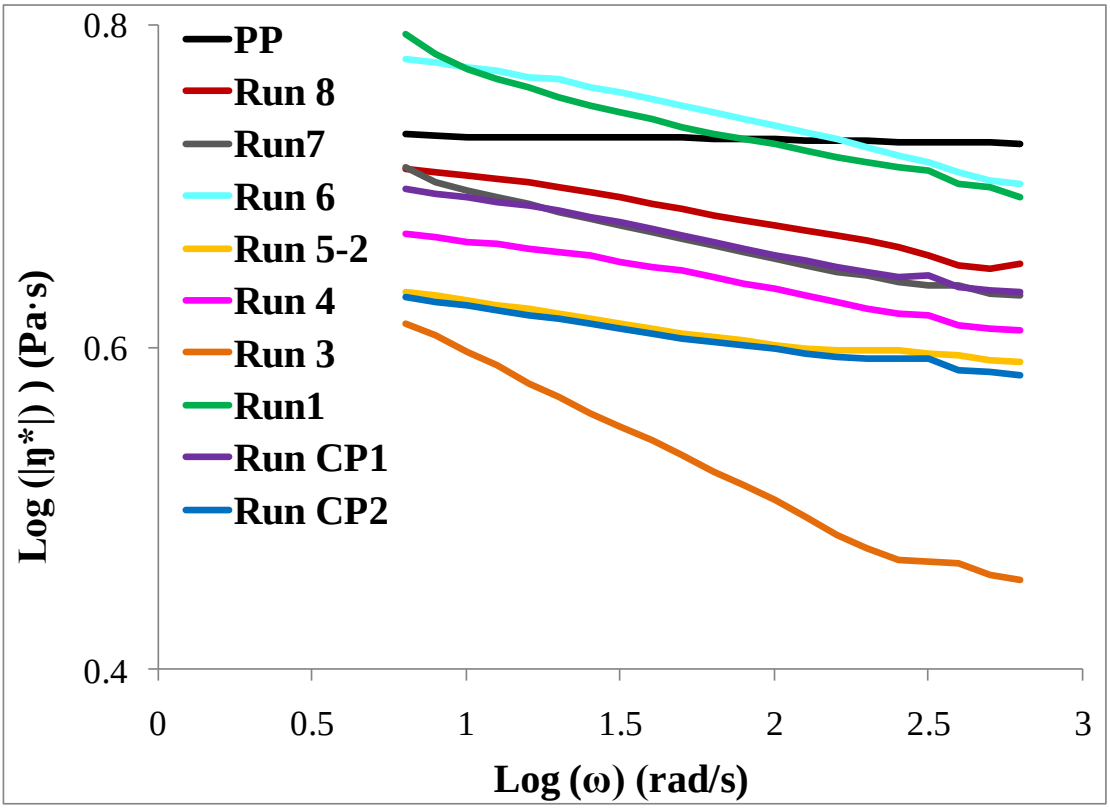

Figure A-0-8: Complex viscosity of PP wax and copolymers at 15% strain

References

1. Tzoganakis, C.; Tang, Y.; Vlachopoulos, J.; Hamielec, A. E. *Polym. Plast. Technol. Eng.* **1989**, *3*, 319-350.

2. Xu, G.; Lin, S. *J. Macromol. Sci. Rev. Macromol. Chem. Phys.* **1994**, *34 (4)*, 555-606.

3. Kim, B. K.; Kim, K. J. *Adv. Polym. Technol.* **1993**, *3*, 263-269.

4. Scheve, B. J.; Mayfield, J. W.; DeNicola, J.; Anthony, J. *US Patent* 4, 916, 198, 1990.

5. Andriot, M.; DeGroot Jr., J. V.; Meeks, R.; et al Chapter 2 - Silicones in Industrial Applications. In *Inorganic Polymers;* De Jaeger, R., Gleria, M., Eds.; Nova Science Publishers: 2007.

6. McManus, N. T.; Zhu, S. H.; Tzoganakis, C.; Penlidis, A. *J. Appl. Polym. Sci.* **2006**, *6*, 4230-4237.

7. Patricia MuÑoz P, M.; Werlang, M. M.; Yoshida, I. V. P.; Mauler, R. S. *J Appl Polym Sci* **2002**, *83*, 2347.

8. Yilgor, E.; Sinmazcelik, T.; Yilgor, I. *J. Appl. Polym. Sci.* **2002**, *3*, 535-40.

9. Yilgor, I.; Yilgor, E.; Suzer, S. *J. Appl. Polym. Sci.* **2002**, *8*, 1625-1634.

10. Smith, S. D.; Wnuk, A. J.; Gerber, M. S. *US Patent* 5,476,901, 1995.

11. Long, J.; Tzoganakis, C.; Chen, P. *J. Appl. Polym. Sci.* **2003**, *14*, 3117-3131.

12. Malz, H.; Tzoganakis, C. *Polym. Eng. Sci.* **1998**, *12*, 1976-1984.

13. Graves, V. *Polypropylene: A commodity Plastic Reaches Record Highes in 1994 Production;* Modern Plastics Encyclopedia 1996, McGraw-Hill: 1995.

14. Frank, H. P. *Polypropylene;* Gordon and Breach Science Publishers: New York, 1968; Vol. 2.

15. Maier, C.; Calafut, T. *Polypropylene: The Definitve User's Guide and Databook;* Plastics Design Library: New York, 199.

16. Azizi, H.; Ghasemi, I. *Polym. Test.* **2004**, *2*, 137-143.

17. Blancas, C.; Vargas, L. *J. Macromol. Sci, Phys* **2001**, *40 (3&4),* 315-326.

18. Tzoganakis, C.; Vlachopoulos, J.; Hamielec, A. E. *Chem. Eng. Prog.* **1988**, *11,* 47-49.

19. Tzoganakis, C. *Can. J. Chem. Eng.* **1994**, *4,* 749-754.

20. Psarreas, A.; Tzoganakis, C.; McManus, N.; Penlidis, A. *Polym. Eng. Sci.* **2007**, *12,* 2118-23.

21. Schrock, R. R. Olefin metathesis by Well-Defined Complexes Molybdenum and Tungsten. In *Alkene Metathesis in Organic Synthesis;* Füstner, A., Ed.; Springer: Berlin, 1999; Vol. 1.

22. Scorah, M. J.; Zhu, S.; Psarreas, A.; McManus, N. T.; Dhib, R.; Tzoganakis, C.; Penlidis, A. *Polym. Eng. Sci.* **2009**, *9*, 1760-1766.

23. Sommer, L. H.; Pierusza, E. W.; Whitmore, F. C. *J. Am. Chem. Soc.* **1947**, *69*, 188-189.

24. Marciniec, B. In *Hydrosilylation: A Comprehensive Review on Recent Advances.* Matisons, J., Ed.; Advances in Silicon Science; Springer: Germany, 2009; Vol. 1.

25. Hayashi, T. Chapter 7: Hydrosilylation of Carbon Carbon Double Bonds. In *Comprehensive Asymmetric Catalysis: Supplement;* Jacobsen, E. N., Pfaltz, A. and Yamamoto, H., Eds.; Springer: Germany, 2004; Vol. 1, pp 319.

26. Marciniec, B.; Gulinski, J.; Urbaniac, W.; Kornetka, Z. W. *Comprehensive Handbook of Hydrosilylation.* Pregamon Press: Oxford, England, 1992.

27. Lewis, L. N.; Stein, J.; Gao, Y.; Colborn, R. E.; Hutchins, G. *Platinum Metals Rev.* **1997**, *41 (2)*, 66-75.

28. Lewis, L. N.; Lewis, N. *J. Am. Chem. Soc.* **1986**, *108*, 7228-7231.

29. Lewis, L. N. *J. Am. Chem. Soc.* **1990**, *112*, 5998-6004.

30. Malz, H.; Tzoganakis, C. *Polym. Eng. Sci.* **1998**, *12*, 1976-1984.

31. Bank, H. M. *US Patent* 5359113, 1994.

32. Ojima, I. *The Chemistry f Organic Silicon Compounds;* John Wiley and Sons Ltd.: New York, 1989.

33. Ojima, I.; Li, Z.; Zhu, J. In *Recent Advances in Hydrosilylation and Related Reactions.* Rappoport, Z., Apeloig, Y., Eds.; The Chemistry of Organic Silicon Compounds; 1998; Vol. 2, Chap. 29.

34. Guo, X.; Farwaha, R.; Rempel, G. L. *Macromolecules* **1990**, *24*, 5047-5054.

35. Tzoganakis, C.; Hauke, M. *US Patent* 6,114,445, 1997.

36. Romero, P. E.; Piers, W. E.; McDonald, R. *Angew. Chem. Int. Ed.* **2004**, *45*, 6161-6165.

37. Trnka, T. M.; Grubbs, R. H. *Acc. Chem. Res.* **2001**, *34 (1)*, 18-29.

38. Hérisson, P. J.; Chauvin, Y. *Die Makcromolekular Chemie* **1971**, *141*, 161-176.

39. Casey, C. P. *J. Chem. Educ.* **2006**, *2*, 192-195.

40. Chatterjee, A. K.; Choi, T.; Sanders, D. P.; Grubbs, R. H. *J. Am. Chem. Soc.* **2003**, *37*, 11360-11370.

41. Schrock, R. R. *Angew. Chem. Int. Ed.* **2006**, *23*, 3748-3759.

42. Schrock, R. R. *Tetrahedron* **1999**, *55 (27)*, 8141-8153.

43. Schrock, R. R. *Acc. Chem. Res.* **1990**, *23*, 158-165.

44. Nizovtsev, A. V.; Afanasiev, V. V.; Shutko, E. V.; Bespalova, N. B. Metathesis Catalysts Stability and Decomposition Pathway. In *Metathesis Chemistry: Nanostructure Design to Synthesis of Advanced Materials;* Imamoğlu, Y., Dragutan, V. and Karabulut, S., Eds.; Springer: The Netherlands, 2007; Vol. 243 (PART I), pp 125.

45. Kirkland, T. A.; Grubbs, R. H. *J. Org. Chem.* **1997**, *62*, 7310-7318.

46. Grubbs, R. H. *Tetrahedron* **2004**, *60 (34),* 7117-7140.

47. Obrecht, W.; Muller, J. M.; Nuyken, O.; Meca, L.; Triscikova, L. *US Patent* 0049700 A1, 2007.

48. Fuerstner, A.; Thiel, O. R. *J. Org. Chem.* **2000**, *6*, 1738-1742.

49. Huang, J.; Stevens, E. D.; Nolan, S. P.; Petersen, J. L. *J. Am. Chem. Soc.* **1999**, *12*, 2674-2678.

50. Simal, F.; Delfosse, S.; Demonceau, A.; Noels, A. F.; Denk, K.; Kohl, F. J.; Weskamp, T.; Herrmann, W. A. *Chem. Eur. J.* **2002**, *13*, 3047-3052.

51. Sandford, M. S.; Love, J. A.; Grubbs, R. H. *J. Am. Chem. Soc.* **2001**, *27*, 6543-6554.

52. Pietraszuk, C.; Fischer, H.; Marciniec, B. Cross-Metathesis of Vinyl-substituted Organosilicon Derivatives with Olefins and Dienes in the Presence of Grubbs Catalysts. In *Metathesis Chemistry: Nanostructure Design to Synthesis of Advanced Materials;*

Imamoğlu, Y., Dragutan, V., Eds.; Springer: The Netherlands, 2007; Vol. 243 (Part II), pp 265.

53. Zhang, Y. P. Mixing Studies in Twin Screw Extruders Using Functionalized Polypropylenes as Reactive Tracers, Chemical Engineering Program, University of Waterloo, Waterloo, Ontario, Canada, 2004.

54. Bousmina, M.; Ait-Kadi, A.; Faisant, J. B. *J. Rheol.* **1999**, *43 (2)*, 415-433.

55. Mark, J.; Ngai, K.; Graessley, W.; Mandekem, L.; Samulski, E.; Koenig, J.; Wignall, G. *Physical Properties of Polymers;* The Press Syndicate of the University of Cambridge: Cambridge, 2003.

56. Macosko, C. W. *Rheology: Principles, Measurements and Applications;* VCH Publisher Inc.: New York, 1994.

57. Kroschwitz, J. I. In *Polymers: Polymer Characterization and Analysis.* Wiley: New York, 1990.

58. Nielsen, L. E. *Polymer Rheology;* Marcel Dekker Inc.: New York, 1977.

59. Malkin, A. Y.; Isayev, A. I. *Rheology: Concepts, Methods and Applications;* Chem Tec Publishing: Toronto, 1994.

60. Weitz, D.; Wyss, H.; Larsen, R. *G. I. T. Laboratory Journal* **2007**, *3-4*, 68-70.

61. Goodwin, J. W.; Hughes, R. W. *Rheology for Chemists;* RSC Publishing: Cambridge, 2008.

62. Crompton, T. R. *Polymer Reference Book;* Rapra Technology Limited: UK, 2006.

63. Billmeyer, F. W. *Textbook of Polymer Science;* John Wiley & Sons: New York, 1984.

64. Zanetti, M.; Camino, G.; Reichert, P.; Mulahupt, R. *Macromol. Rapid Commun* **2001**, *22*, 176-180.

65. Tjong, S. C.; Shen, J. S.; Li, R. K. Y. *Polymer* **1996**, *12,* 2309-2316.